

THE EFFECTS OF FAULT-GENERATED  
TRANSIENTS ON OPERATION OF  
A STATIC DISTANCE RELAY

*A Thesis*

*Submitted to*

*The Faculty of Graduate Studies and Research*

*The University of Manitoba*

*In Partial Fulfillment*

*of the Requirements*

*for the Degree of*

*Master of Science*

by

YOUSSEF LOTFY ABDEL-MAGID

October 1972



## ABSTRACT

The object of this thesis was to investigate the effects of fault-generated transmission line transients on the operation of a MHO static relay as nearly as possible similar to one built by Ontario Hydro. The transmission line was modelled as a single nominal-T section. A mathematical analysis of the post fault relaying quantities was made. The experimental relay and the transmission line were simulated on an analog computer. Tests on the relay indicate clearly that excessive high frequency noise contained in the information given to the relay causes its misoperation.

## ACKNOWLEDGEMENTS

The author wishes to express his deep gratitude to Professor G.W. Swift for suggesting the thesis topic as well as for his valuable guidance and encouragement during the course of this work, and to the National Research Council for financially supporting this work under Grant No. A2780 through Professor G.W. Swift.

## TABLE OF CONTENTS

		<u>Page</u>
CHAPTER 1	INTRODUCTION	1
CHAPTER 2	MHO DISTANCE RELAY	4
	2.1 Theory of Operation of MHO Relay	4
	2.2 Conventional (Electromagnetic) Structure	8
	2.3 Static Protective Relays	8
	2.3.1. Principles	8
	2.3.2 Principles of Static MHO Relays	11
	2.4 The Experimental MHO Electronic Relay	13
	2.4.1 Theory of the Experimental Relay	13
CHAPTER 3	TRANSIENTS IN A POWER NETWORK DURING FAULTS	17
	3.1 Transients in Relaying Currents and Voltages	17
	3.2 Disregarding Shunt Capacitance	18
	3.3 Considering Shunt Capacitance	20
	3.3.1 Effect of Source Impedance on Relaying Quantities	27
	3.3.2 Effect of Using a Multisection Transmission Line Model on Relaying Quantities	28

	<u>Page</u>
CHAPTER 4 TRANSMISSION LINE AND RELAY ANALOG COMPUTER SIMULATION	29
4.1 Description of Transmission Line Model	29
4.2 Analog Computer Simulation	29
4.2.1 Disregarding Capacitance of the Faulted Line	31
4.2.2 Faulted Line Represented by a Nominal-T Section	35
4.3 Filters for the High Frequency Transients	37
CHAPTER 5 TESTING AND RESULTS	38
5.1 Description of Transmission Line Model	38
5.2 Discussion of Cases	39
5.2.1 Case One	39
5.2.2 Case Two	40
5.2.3 Case Three	40
5.2.4 Case Four	40
5.2.5 Case Five	40
5.2.6 Case Six	41
5.2.7 Case Seven	41
5.2.8 Case Eight	41
5.2.9 Case Nine	42
5.2.10 Case Ten	42
5.3 Filters for Relaying Quantities	42

	<u>Page</u>
CHAPTER 6	
ANALOG REALIZATION OF THE EXPERIMENTAL RELAY USING INTEGRATORS	110
6.1 Theory	110
6.2 Analog Computer Simulation	111
6.3 Results	111
CHAPTER 7	
CONCLUSIONS	117
7.1 Shunt Capacitance Neglected	117
7.2 Shunt Capacitance Considered	118
7.3 Realization Using Integrators	118
7.4 Suggestions for Future Work	119
BIBLIOGRAPHY	120
APPENDIX A Current Expression Derivations	123
APPENDIX B Design of Differentiators	128
APPENDIX C Filter Description	132

## TABLE OF SYMBOLS

$i$	= instantaneous value of relay current
$I$	= RMS value of relay current
$v$	= instantaneous value of relay voltage
$V$	= RMS value of relay voltage
$\omega$	= system frequency in radians/sec
$v_s$	= instantaneous value of generator voltage
$\hat{V}_s$	= generator voltage amplitude
$\delta$	= phase of incidence of the fault with respect to the voltage wave form
$L$	= line plus source inductance
$R$	= line plus source resistance
$Z \angle \phi$	= line plus source impedance
$Z_s \angle \phi_s$	= source impedance
$Z_L \angle \phi_L$	= impedance of system between relay point and fault
$C_L$	= line capacitance
$L_L$	= inductance of system between relay point and fault
$R_L$	= resistance of system between relay point and fault
$L_s$	= source inductance
$R_s$	= source resistance
$s$	= Laplace operator
$S_1, S_2$	= input signals to the comparator

$S_3 = S_2$  shifted by  $90^\circ$   
 $R_e$  = load resistance  
 $T$  = actuating quantity  
R.S. = relay signal to circuit breaker  
 $\dot{S}_1, \dot{S}_2$  = derivative of input signals to the comparator  
 $\dot{S}_3$  = derivative of  $S_2$  shifted by  $90^\circ$   
 $L_r$  = replica inductance  
 $R_r$  = replica resistance  
 $Z_r, \phi_r$  = replica impedance  
 $h$  = scale factor (=3)  
 $k_1, k_2$  = constant of proportionality



## CHAPTER 1

### INTRODUCTION

The function of protective relays is to cause the prompt removal from service of any element of a power system when it suffers a short circuit, or when it starts to operate in any abnormal manner that might cause damage or otherwise interfere with the effective operation of the rest of the system. Protective relays must, however, not operate - to keep the system intact - when the fault is not within the relay's jurisdiction. These two functions are usually referred to as reliability and security, respectively.

In the continued development of improved relaying, static relays are being actively considered because they give promise of one cycle operation for all types of faults at all points on the protected circuit, in addition to the possible reduction of maintenance and the very much lower VA burden. Fortunately, static relays can be designed to obtain operation characteristics<sup>21,8</sup> similar to those now available in electromechanical relays. However, before static relays can be accepted in the protective relay field, they must be at least as good as electromagnetic

relays in all respects.

One possible difficulty with high speed relays (which compare instantaneous voltage and current) lies in the fact that input wave forms to the relay may be distorted, or transients may appear under fault conditions. The results of such distortion may then be such as to cause operation different from that predicted by the theory based upon sine waves of relay voltage and current. It is the purpose of this thesis to study the behaviour of an experimental MHO static relay (as nearly as possible, a duplicate of one designed and built by Ontario Hydro) with distorted or transient affected input waveforms. The theory of the experimental relay is given in detail in Chapter 2. The resulting characteristic is found to be the familiar mho circle.

In many earlier publications<sup>1,2</sup>, fault-generated transmission line transients were analyzed in a simplified manner without taking into consideration the effect of line capacitance on the transient relaying quantities and by assumption of damping of transient currents according to single exponential functions. In Chapter 3, fault-generated transients are analyzed for a transmission line modelled as a single nominal-T. The wave forms of the relaying current and voltage are shown to contain high frequency noise together with d.c. offset.

A detailed simulation of the transmission line and the experimental relay on an analog computer is given in

Chapter 4, while Chapter 5 is devoted to the results of tests performed on the relay.

In Chapter 6, a different way of realizing the experimental relay is introduced.

The experimental results obtained indicate that the relay misoperates when there is excessive high-frequency content.

## CHAPTER 2

### MHO DISTANCE RELAY

The need for more adequate discrimination by means of distance relays between fault conditions and power swings has been heightened in recent years by the construction of longer transmission lines and by the transmission of larger amounts of energy over existing lines.

Several papers<sup>7</sup>, have described the inadequacy of the impedance and reactance type directional distance relays to fulfil this need without the addition of auxiliary operating units. Auxiliary units always introduce trouble, increase the need for maintenance and make the maintenance more difficult.

In 1944, Warrington<sup>7</sup> described the use of a relay which measures a constant component of admittance for providing this discrimination, in addition to providing correct directional action and accurate distance measurement, all in one unit. This characteristic has been named a MHO characteristic.

#### 2.1 Theory of Operation of MHO Relay

In a MHO relay, the torque produced by a current-

voltage directional element is balanced against the torque of a voltage element. In other words, a MHO relay is a voltage-restraining element that opposes a directional element. If the control-spring constant is  $-K_s$ , the torque equation of such a relay is

$$T = K_1 VI \cos(\theta - \tau) - K_2 V^2 - K_s$$

where  $I, V$  are the rms values of the current and voltage, respectively,  $\theta$  and  $\tau$  are the phase angle between  $I$  and  $V$  and the angle of maximum torque, respectively. At the balance point when the relay is on the verge of operating, the net torque is zero, and hence

$$K_2 V^2 = K_1 VI \cos(\theta - \tau) - K_s$$

Dividing both sides by  $K_2 VI$ , we get

$$\frac{V}{I} = Z = \frac{K_1}{K_2} \cos(\theta - \tau) - \frac{K_s}{K_2 VI}$$

If the control-spring constant is neglected, we have

$$Z = \frac{K_1}{K_2} \cos(\theta - \tau)$$

On an R-X diagram, the operating characteristic represented

by this equation is a circle of diameter  $\frac{K_1}{K_2}$  practically independent of voltage or current, except at very low magnitudes of current and voltage when the control spring effect is taken into account, which causes the diameter to decrease. The MHO relay characteristic is shown in Fig. 2.1.

The fact that the characteristic passes through the origin means that the unit is inherently directional. By taking  $\tau$  equal to, or a little less lagging than  $\theta$ , the circle is made to fit very closely around the fault area so that the relay is less sensitive to power swings and hence valuable for the protection of long or heavily loaded lines.

The complete distance relay for transmission line protection is composed of three high-speed MHO units ( $M_1, M_2, M_3$ ) and a timing unit (Fig. 2.2). The first zone gives instantaneous operation while the second and third zones complete the trip circuit only through the contacts of the timer to give time delay tripping. In the practical relay, the third zone element may be used as shown in Fig. 2.3 or with a reversed third zone as shown in Fig. 2.4.

By means of current biasing, a MHO relay characteristic circle can be offset so that either it encircles the origin of the R-X diagram or the origin is outside the circle depending upon the application requirements.

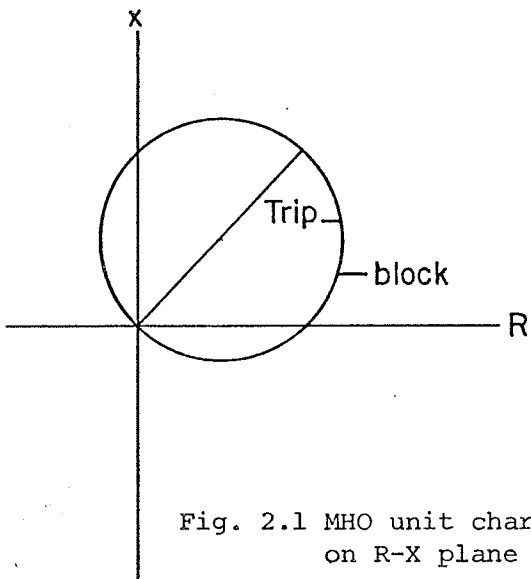


Fig. 2.1 MHO unit char. on R-X plane

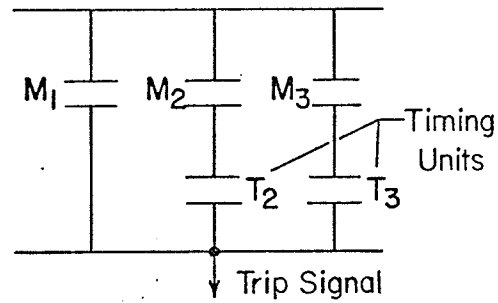


Fig. 2.2 Contact-circuit connections of a MHO distance relay

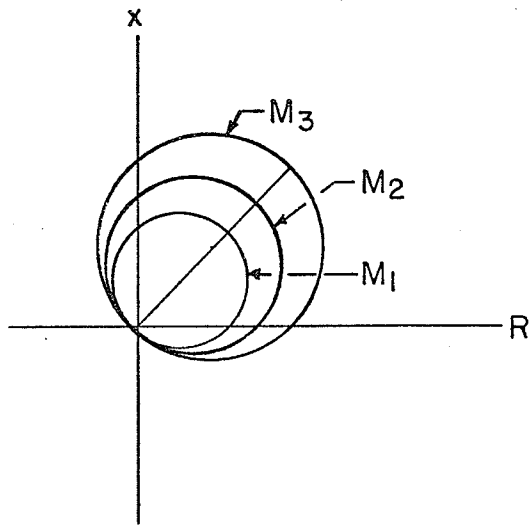


Fig. 2.3 Three-step MHO relay characteristic

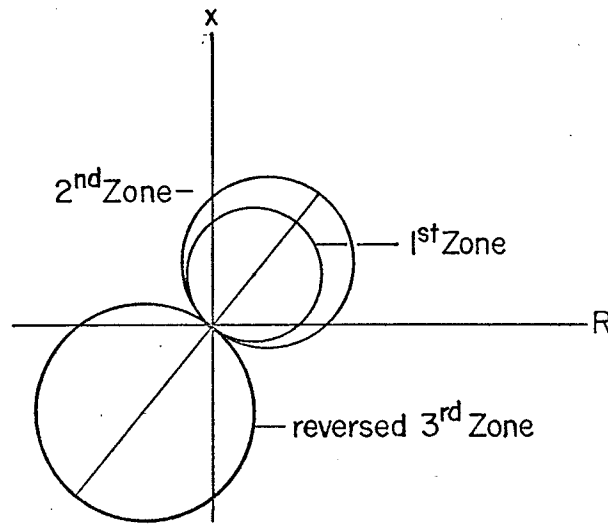


Fig. 2.4 Three-step MHO relay characteristic (showing reversed 3rd zone)

## 2.2 Conventional (Electromagnetic) Structures

The induction cup and double-induction loop are the type of structures used for high-speed MHO distance relays. They are efficient torque producers. These two structures are shown in Fig. 2.5 and Fig. 2.6, respectively. They most closely resemble an induction motor, except that the rotor iron is stationary, only the rotor-conductor portion being free to rotate. The cup structure employs a hollow cylindrical rotor, whereas the double-loop structure employs two loops at right angles to one another. Functionally, both structures are practically identical. A complete description of the operation is given in references 10 and 11.

## 2.3 Static Protective Relays

Static protective relays are now coming into prominence because of their promise of better performance, lower input power (burdens), smaller size and freedom from maintenance. Detailed accounts of the work on static relays up to the present time may be found in references 8, 6, 21 and 15.

### 2.3.1 Principles

It is well known that the characteristic of all distance relay functions may be obtained by the comparison of two different input combinations of current



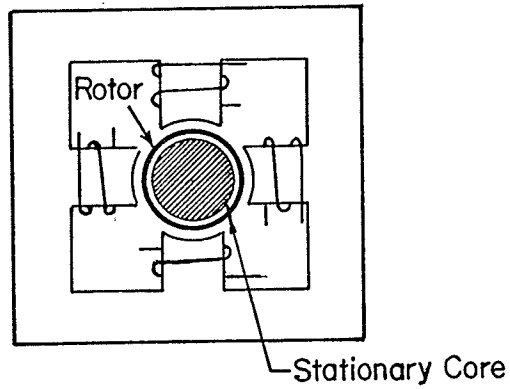


Fig. 2.5 Induction-cup structure

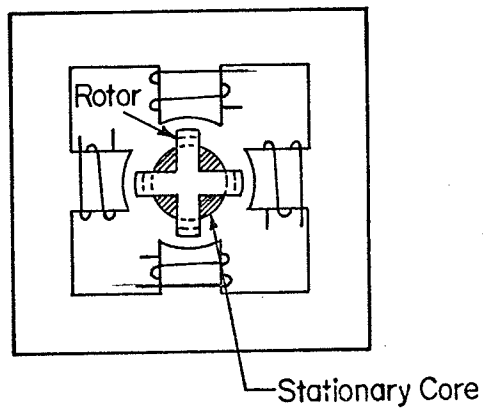


Fig. 2.6 Double-induction-loop structure

and voltage. This is usually done using either an amplitude or phase-comparing measuring element. An amplitude comparator compares only the magnitude of the input signals and ignores their phase angle, while a phase comparator responds only to the phase relation between the two input quantities, irrespective of their magnitudes.

Since the two inputs to a static relay are not electrically separate as they are in a conventional electromagnetic relay, they must be similar, e.g. two currents or two voltages. In a voltage comparator, the current is turned into a voltage by passing it through an impedance,  $Z_r \angle \phi_r$ , which is a replica of the impedance of the protected section on a secondary basis. In a current comparator a current is derived from the voltage by connecting the replica impedances in series with it.

When single-term quantities are compared, the resulting characteristic is either a straight line through the origin or a circle with its center at the origin (depending upon whether a phase or an amplitude comparison is made, and whether the characteristic is plotted upon an impedance or an admittance diagram). If one quantity is compared with the sum or difference of the two quantities the circle passes through the origin and the straight line does not.

### 2.3.2 Principles of Static MHO Relays

The MHO characteristic is obtained equally from phase or amplitude comparators, but because the directional function is inherently a phase-angle measurement, the phase comparator is the more convenient construction.

Figure 2.7 shows the basic input arrangement for a MHO connected phase comparator. The two quantities which are compared in phase are

$$S_1 = V = V_s \frac{Z_L}{Z_s + Z_L}$$

$$\begin{aligned} S_2 &= IZ_r - V \\ &= \frac{V_s}{Z_s + Z_L} (Z_r - Z_L) \end{aligned}$$

where  $V_s$  is the source voltage,  $V$  and  $I$  are the voltages and currents at the relay point. Other quantities are defined in the figure. The criterion for operation is that

$$-\frac{\pi}{2} \leq \psi \leq \frac{\pi}{2}$$

where  $\psi = \text{angle of } S_1 - \text{angle of } S_2$ . The relative phase angle between  $S_1$  and  $S_2$  is not disturbed if they are multiplied by the same quantity, that is,  $\frac{Z_s + Z_L}{V_s}$ .

The two vectors to be compared in phase are therefore

\* In the remainder of the thesis, a symbol may represent a phasor quantity or an instantaneous quantity depending on the context.

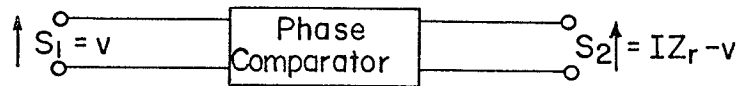
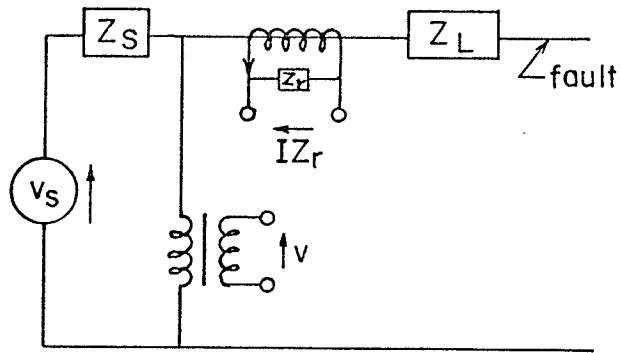


Fig. 2.7 Basic connection for MHO relay

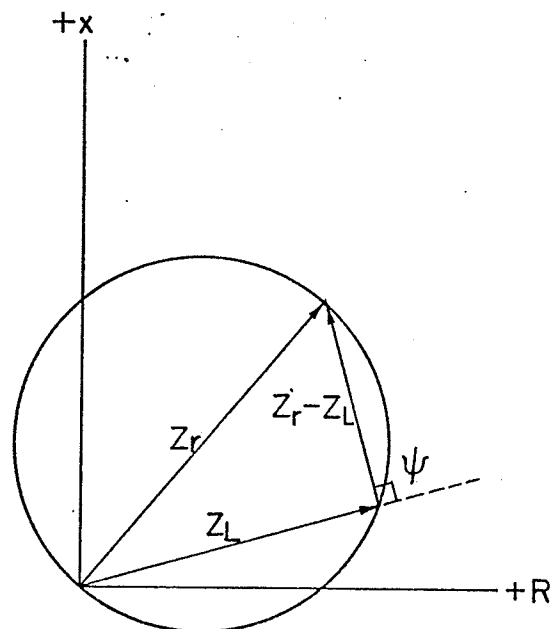


Fig. 2.8 MHO relay characteristic

$$S_1' = Z_L$$

$$S_2' = Z_r - Z_L$$

The vector diagram is shown in Fig. 2.8, and it is clear that the locus of the  $Z_L$  is a circle with  $Z_r$  as diameter.

#### 2.4 The Experimental MHO Electronic Relay

In this relay, phase comparison is achieved through differentiators and multipliers. The relay has the feature of simplicity in its theory and realization.

##### 2.4.1 Theory of the Experimental Relay

In the steady-state, the input signals to the comparator,  $S_1$  and  $S_2$ , are sine waves. If each signal is differentiated with respect to time, multiplied by the other signal, and the two resulting products are subtracted, the sign of the resultant quantity will be found to depend on the phase-angle between the two signals (Fig. 2.9).

Let  $S_1 = A \sin \omega t$

$$S_2 = B \sin(\omega t + \psi)$$

Hence  $\dot{S}_1 = A\omega \cos \omega t$

$$\dot{S}_2 = B\omega \cos(\omega t + \psi)$$

Multiplying  $\dot{S}_2$  by  $S_1$ , and  $\dot{S}_1$  by  $S_2$  we get

$$\dot{S}_2 S_1 = AB\omega \sin \omega t \cos(\omega t + \psi)$$

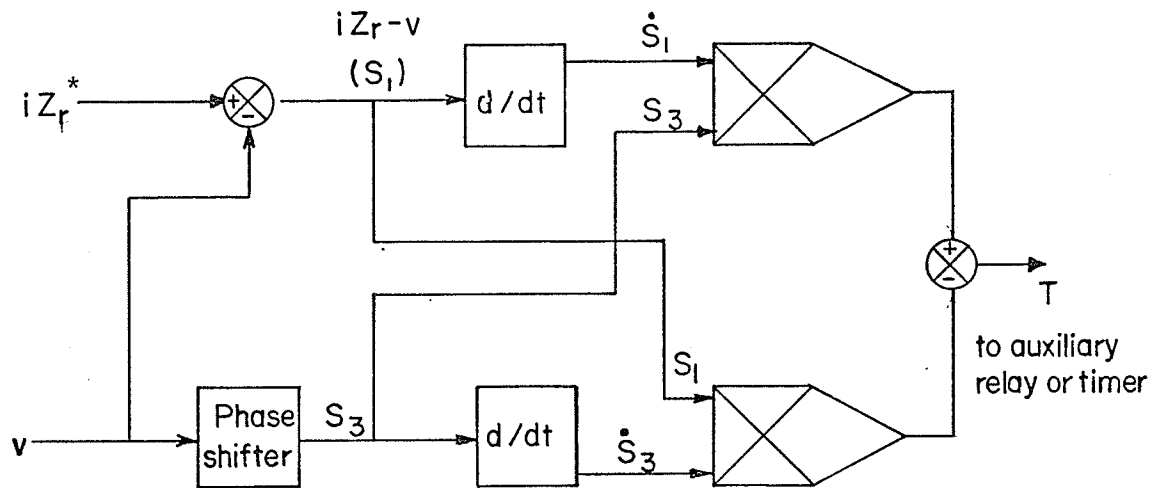


Fig. 2.9 Block diagram of the experimental relay

\* in this context  $Z_r$  is the operator  $R_r + L_r \frac{d}{dt}$

and

$$\dot{S}_1 S_2 = AB\omega \sin(\omega t + \psi) \cos \omega t$$

$$\text{Let } T = \dot{S}_1 S_2 - \dot{S}_2 S_1$$

Hence

$$T = AB\omega [\sin(\omega t + \psi) \cos \omega t - \sin \omega t \cos(\omega t + \psi)]$$

$$T = AB\omega \cdot \sin \psi$$

It is clear that  $T$  is positive for values of  $\psi$  ranging between zero and  $180^\circ$ .

However, if one of the two signals is phase-shifted by  $\frac{\pi}{2}$  before differentiation takes place, the range of  $\psi$  for which  $T$  is positive will be shifted by  $90^\circ$ . Accordingly if we let

$$S_1 = A \sin \omega t$$

$$S_3 = S_2 (\text{shifted}) = B \cos(\omega t + \psi)$$

hence

$$\dot{S}_1 = A\omega \cos \omega t$$

$$\dot{S}_3 = -B\omega \sin(\omega t + \psi)$$

$$T = S_3 \dot{S}_1 - \dot{S}_3 S_1$$

$$T = AB\omega [\cos(\omega t + \psi) \cos \omega t + \sin(\omega t + \psi) \sin \omega t]$$

$$T = AB\omega \cos \psi$$

which means that  $T$  is positive for values of  $\psi$  ranging from

$-\frac{\pi}{2}$  to  $+\frac{\pi}{2}$ , i.e.  $(-\frac{\pi}{2} \leq \psi \leq \frac{\pi}{2})$ . Hence, this principle can be used to perform the phase angle comparison required to obtain a MHO characteristic.

In a relay using this principle, the signal  $T$  is fed into an electronic circuit which gives a logic 1, or a trip signal to the breaker when  $T$  is positive, and logic 0 or block signal when  $T$  is negative. The moment  $T$  becomes positive a signal is transferred to an auxiliary relay which trips the breaker, or breakers, to isolate the faulty section.

Figure 2.9 shows a simplified block diagram of the experimental relay.



## CHAPTER 3

### TRANSIENTS IN A POWER NETWORK DURING FAULTS

The behaviour of distance relays under transient conditions has recently attracted attention with the demand for reduction in relaying time. Full account must be taken not only of the d.c. offset, but also of the effect of high frequency transients on the relay operation. A detailed study of the post fault conditions is important.

#### 3.1 Transients in Relaying Currents and Voltages

During normal conditions, the line voltage is the rated value and the phase current is between zero and a full load value, depending upon the load. When a fault occurs, both the current and voltages suddenly change in amplitude and/or angle, and because of the reactive components of the system impedances, the current and voltage go through some transient values before settling down to the values corresponding to the short-circuited condition of the system.

In many former publications<sup>1,2</sup> concerning short-circuits and network protection, the transients were mathematically analyzed in a simplified manner without taking

into account the influence of line capacitance on the transient currents and voltages as well as by the assumption of damping of transient currents according to the single exponential function. Expressions for relaying current and voltage in the case where the capacitance is neglected and the case where it is taken into consideration are derived.

### 3.2 Disregarding Shunt Capacitance

Figure 3.1 indicates the simplification employed, which is to regard the fault as due to a sine wave of voltage  $\hat{V}_s \sin(\omega t + \delta)$  suddenly applied to the circuit  $R + j\omega L = Z \angle \phi$  at the instant  $t=0$ , where

$$R = R_s + R_L$$

$$L = L_s + L_L$$

The instantaneous values of current and voltage at the relaying point after the fault are given by

$$i = \frac{\hat{V}_s}{Z} [\sin(\omega t + \delta - \phi) - \exp(-\frac{R}{L}t) \sin(\delta - \phi)]$$

and

$$v = \frac{\hat{V}_s}{Z} Z_L [\sin(\omega t + \delta - \phi + \phi_L) - \frac{\sin(\phi - \phi_L) \sin(\delta - \phi) \exp(-\frac{R}{L}t)}{\sin \phi}]$$

The left hand terms represent the steady-state fault condition and the right-hand terms the transient components which

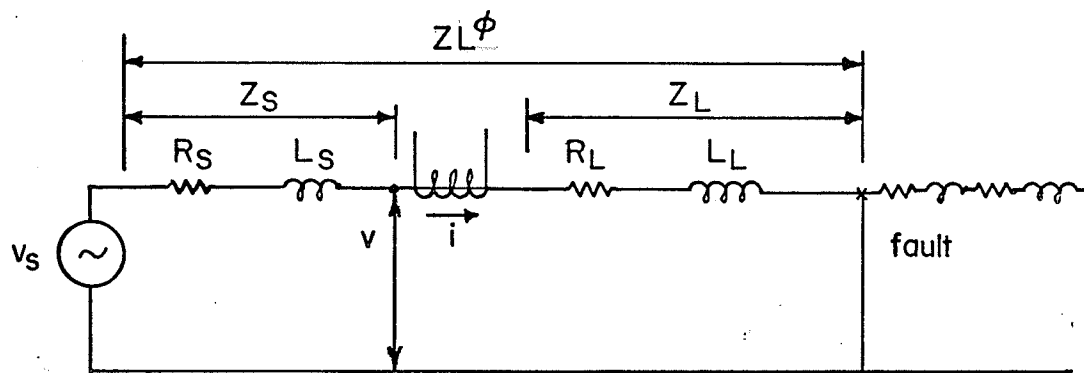


Fig. 3.1 Equivalent circuit of faulted system (disregarding shunt capacitance)

exist during the transition from normal to fault conditions.

Inspection of the right-hand terms of the expression for current will show that it is a d.c. offset which decays exponentially (Fig. 3.2). Its size depends upon the moment the fault strikes and the duration increases with the reactance to resistance ratio of the system. Load flow before fault occurrence tends to decrease the amount of offset<sup>10</sup>. The second term in the voltage equation, which is the transient voltage at the relaying point, vanishes if  $\phi = \phi_L$ , i.e. a uniform angle throughout the system (usually referred to as a homogeneous system).

### 3.3 Considering Shunt Capacitance

In an accurate analysis of transient behaviour of transmission lines, it would be desirable to represent each transmission line by its distributed parameter model. The solution of the resultant partial differential equations is simple only in single mode propagation, and then only with simple initial and boundary conditions<sup>19</sup>. It is, however, quite complex in any typical faulted system.

On the other hand, it has been shown<sup>4</sup> that a nominal-T representation of a long transmission line is adequate for the study of transient effects on high speed relays, and that such a model leads to straight-forward simulation on an analog computer.

Consider the circuit of Fig. 3.3. The transmission line is represented by a nominal-T section and the source

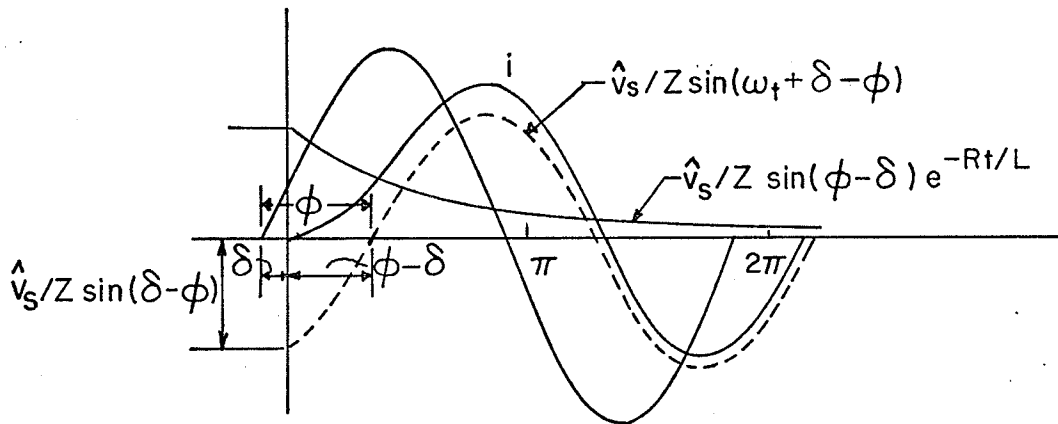
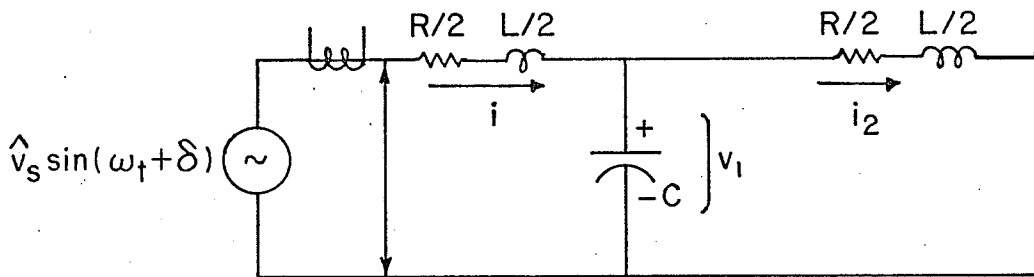


Fig. 3.2 Fault current transient

Fig. 3.3 Equivalent circuit of faulted system  
(capacitance considered)

impedance is neglected for simplicity.

The instantaneous values of current and voltage at the relaying point are given by:

$$i = \frac{\hat{V}_s}{2L[a^2+(\omega-b)^2][a^2+(\omega+b)^2]} \left[ \cos \delta \left\{ \begin{aligned} &(2a+4a\omega^2) \sin \omega t \\ &+ 2\omega(\omega^2-b^2-a^2) \cos \omega t e^{-at} \\ &+ 2 \frac{a}{b} \omega(\omega^2+b^2+a^2) \sin \omega t e^{-at} \\ &- 2\omega(\omega^2-b^2-a^2) \cos \omega t \\ &- 2\omega(\cos \omega t - e^{-2at}) \left[ \frac{(a^2+\omega^2+b^2)^2-4a^2b^2}{4a^2+\omega^2} \right] \end{aligned} \right\} \right. \\ \left. + \sin \delta \left\{ \begin{aligned} &2\omega(\omega^2-a^2-b^2) \sin \omega t - 4a\omega^2 \cos \omega t e^{-at} \\ &+ [2b(a^2+b^2-\omega^2) + 2 \frac{a^2}{b}(a^2+b^2+\omega^2)] \sin \omega t e^{-at} + 4a\omega^2 \cos \omega t \\ &+ 2 \left[ \frac{(a^2+b^2+\omega^2)^2 - 4\omega^2b^2}{4a^2+b^2} \right] [2a(\cos \omega t - e^{-2at}) + \omega \sin \omega t] \end{aligned} \right\} \right]$$

where  $\delta$  is the fault incidence angle

$$a = \frac{R}{2L} \text{ secs}$$

$$b = \left( \frac{4}{LC} - \frac{R^2}{4L^2} \right)^{\frac{1}{2}} \text{ rads/sec}$$

$L$ ,  $R$ ,  $C$  are the inductance, resistance and capacitance of the faulted section of the line.

On the assumption of one to one ideal current and potential transformers, the voltage across the replica impedance is given by

$$v_R = iR_r + L_r \frac{di}{dt}$$

where

$$\frac{di}{dt} = \frac{\hat{V}_s}{2L[a^2 + (\omega - b)^2][a^2 + (\omega + b)^2]} \left[ \begin{array}{l} \cos \delta \left\{ \begin{array}{l} (2a + 4a\omega^2)\omega \cos \omega t \\ + 2\omega(\omega^2 - b^2 - a^2)(-b \sin bt - a \cos bt)e^{-at} \\ + 2\omega \frac{a}{b}(\omega^2 + b^2 + a^2)(b \cos bt - a \sin bt)e^{-at} \\ + 2\omega^2(\omega^2 - b^2 - a^2) \sin \omega t \\ - \frac{2\omega}{4a^2 + \omega^2}[(a^2 + b^2 + \omega^2)^2 - 4\omega^2 b^2](2ae^{-2at} \\ - \omega \sin \omega t) \end{array} \right. \\ \\ + \sin \delta \left\{ \begin{array}{l} 2\omega^2(\omega^2 - a^2 - b^2) \cos \omega t \\ + 4a\omega^2(b \sin bt + a \cos bt)e^{-at} \\ + [2b(a^2 + b^2 - \omega^2) + \frac{2a^2}{b}(a^2 + b^2 + \omega^2)][b \cos bt - a \sin bt]e^{-at} \\ - 4a\omega^3 \sin \omega t \\ + 2\left[\frac{(a^2 + b^2 + \omega^2)^2 - 4\omega^2 b^2}{4a^2 + b^2}\right][2a(2ae^{-2at} - \omega \sin \omega t) + \omega^2 \cos \omega t] \end{array} \right. \end{array} \right]$$

Details concerning the derivation of the above expressions are contained in Appendix A.

Computer plots for current expressions with different switching angles are given in Fig. 3.4 to Fig. 3.6 for the transmission line described in Chapter 5. Investigation of these and other plots shows that:

- (1) high frequency noise can be present
- (2) the transient frequency gets larger the smaller

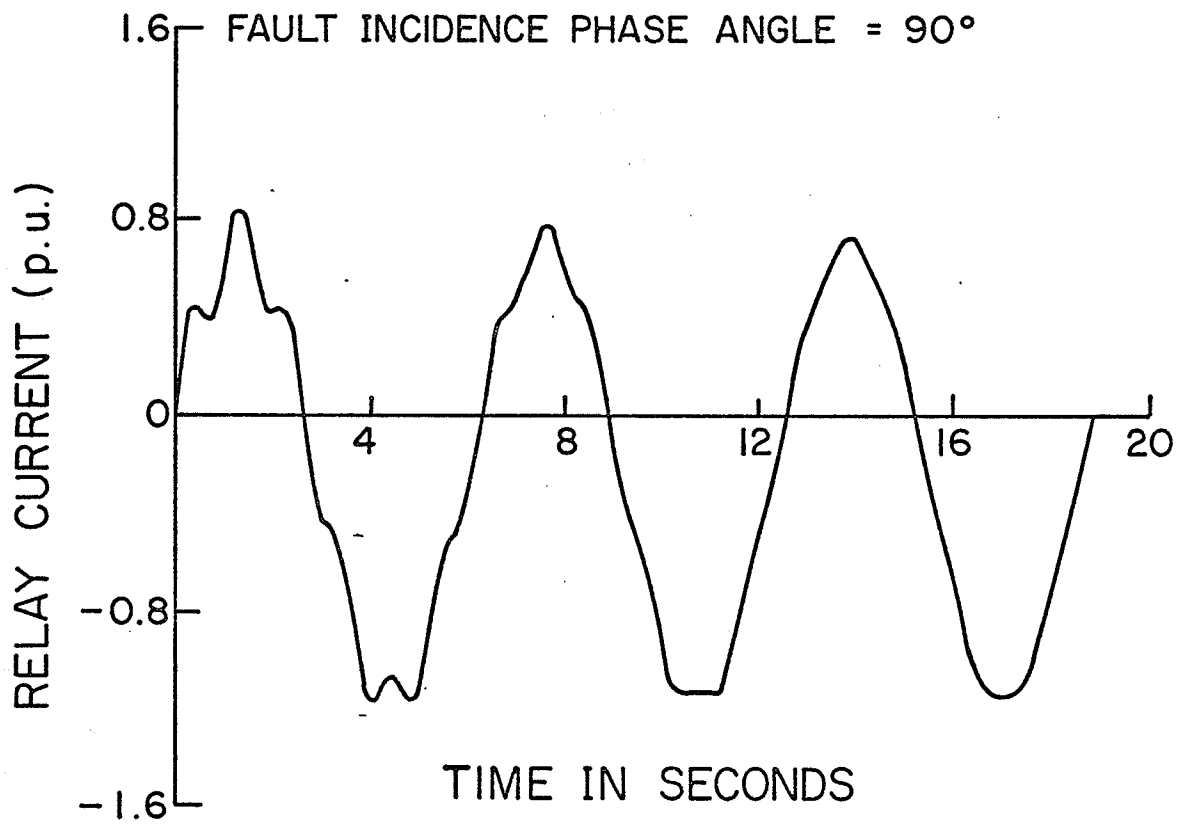


Fig. 3.4 Base frequency for these plots  
is  $\frac{1}{2\pi}$  Hz



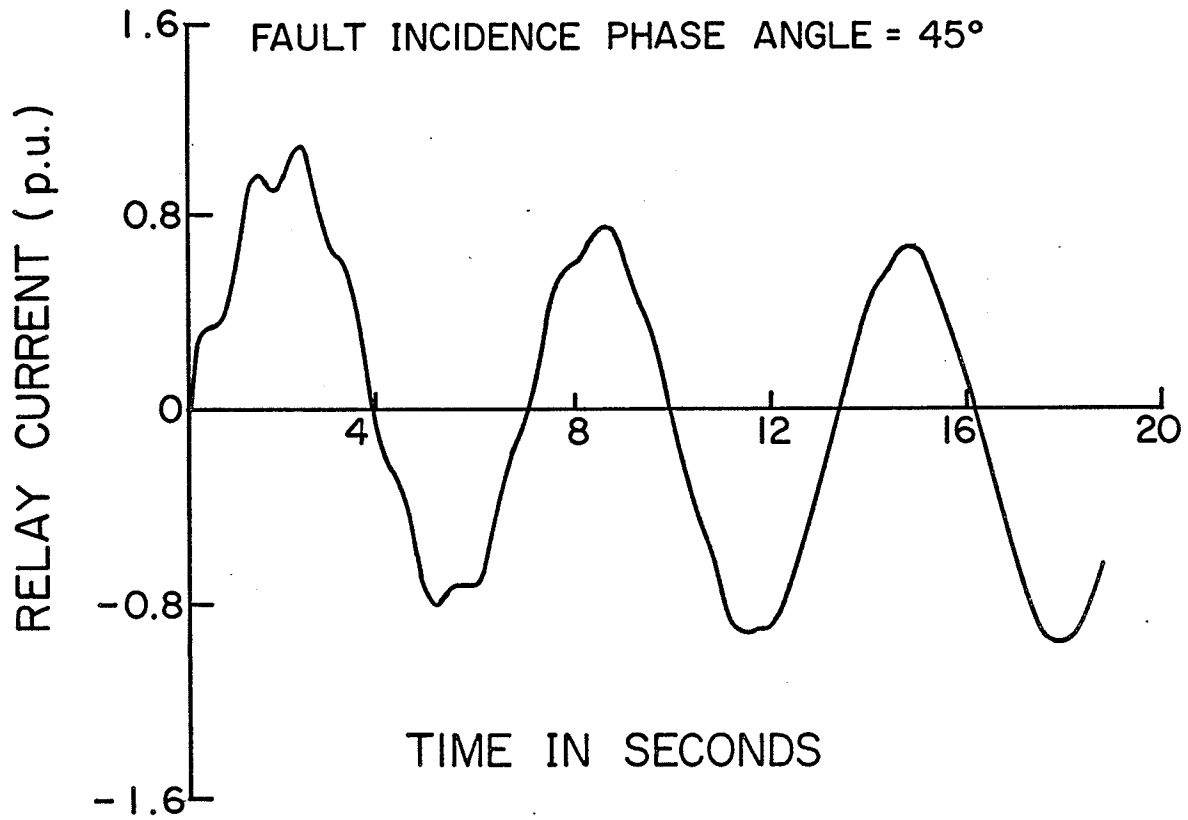


Fig. 3.5

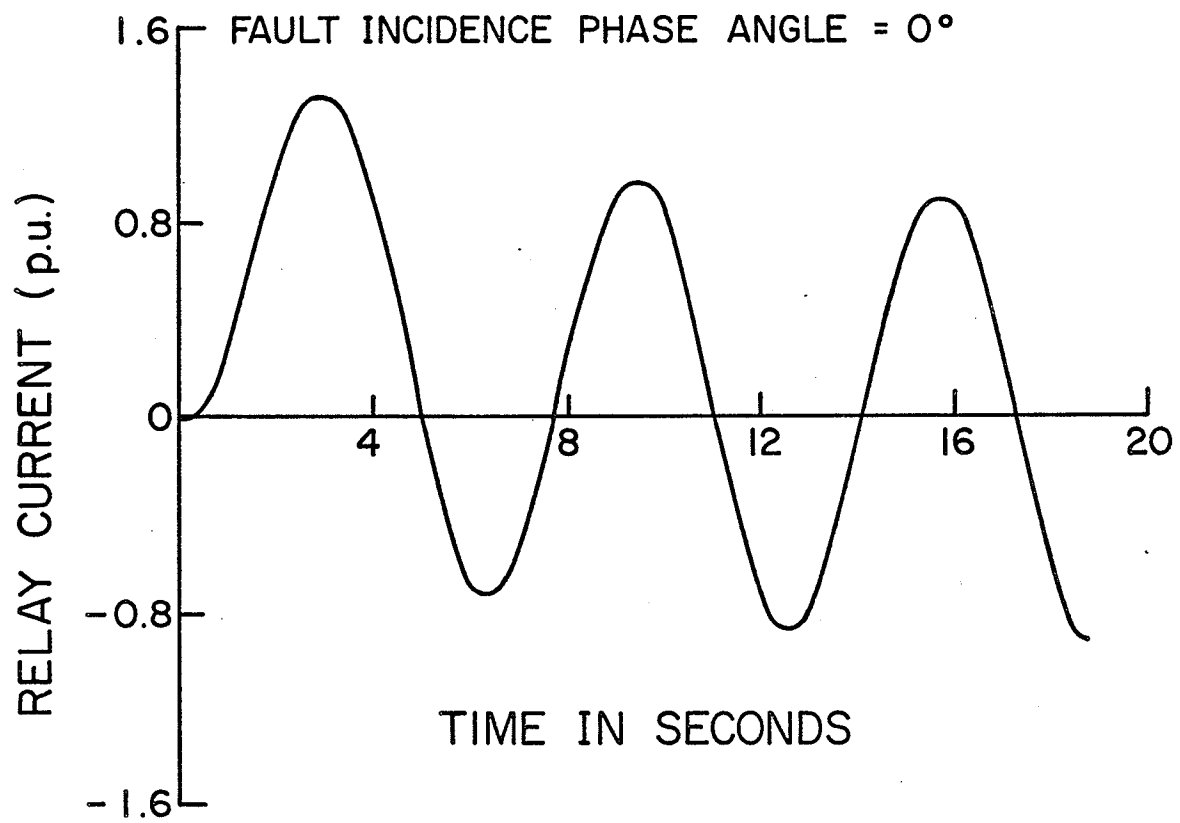


Fig. 3.6

- the source to fault impedance
- (3) maximum high frequency noise results if the fault incidence angle  $\delta = 90^\circ$
  - (4) maximum low frequency noise (d.c. offset) results if  $\delta = 0^\circ$
  - (5) the instant of maximum low frequency noise corresponds to minimum high frequency noise and vice versa.

In single phase systems, high frequency transients are zero for two particular points-on-wave, but in a three phase system the situation is different and high frequency transients always show up on at least two phases<sup>4,9</sup>. Accordingly, the high frequency transients influence to a high degree the accuracy of distance measurement by high-speed relays which often operate on information derived during the first or second half cycle following a disturbance.

### 3.3.1 Effect of Source Impedance on Relaying Quantities

Derivation of similar expressions for relaying voltages and currents with the source impedance taken into consideration involves considerable labor. For this reason transients on complicated power systems are most conveniently determined by transient network analyzer or by electronic

analog computer whenever possible.

### 3.3.2 Effect of Using a Multisection Transmission Line Model on Relaying Quantities

If  $n$  T-sections are used, there are  $n$  modes of oscillations<sup>9</sup> at  $n$  frequencies. The lowest of these frequencies is more nearly equal to the lowest frequency present when the distributed model is used<sup>4</sup>. If the lowest mode is filtered out as much as possible with a low pass filter, the even higher frequencies of the higher modes are effectively eliminated. Accordingly, it is argued<sup>4</sup> that a one-section model is quite sufficient for the study of transient effects on high-speed relays.

## CHAPTER 4

### TRANSMISSION LINE AND RELAY ANALOG

#### COMPUTER SIMULATION

##### 4.1 Description of Transmission Line Model

Figure 4.1 shows a simplified circuit diagram of the transmission line and the experimental relay to be simulated on an analog computer. For simplicity the circuit is shown on a single-phase basis, although a three-phase relay would use three such units. For purposes of the following analysis, the transformer ratios may be considered to be one to one. The closing of switch  $s_f$  is controlled by an electronic circuit so that there is phase control over the incidence of the fault. A control circuit readily allows for various fault locations. A high performance X,Y recorder is used to record current and voltage wave forms.

##### 4.2 Analog Computer Simulation

The transmission line and the relay are simulated on a TR-48<sup>†</sup> Analog Computer for two cases:

---

<sup>†</sup> Electronic Associates, Incorporated.

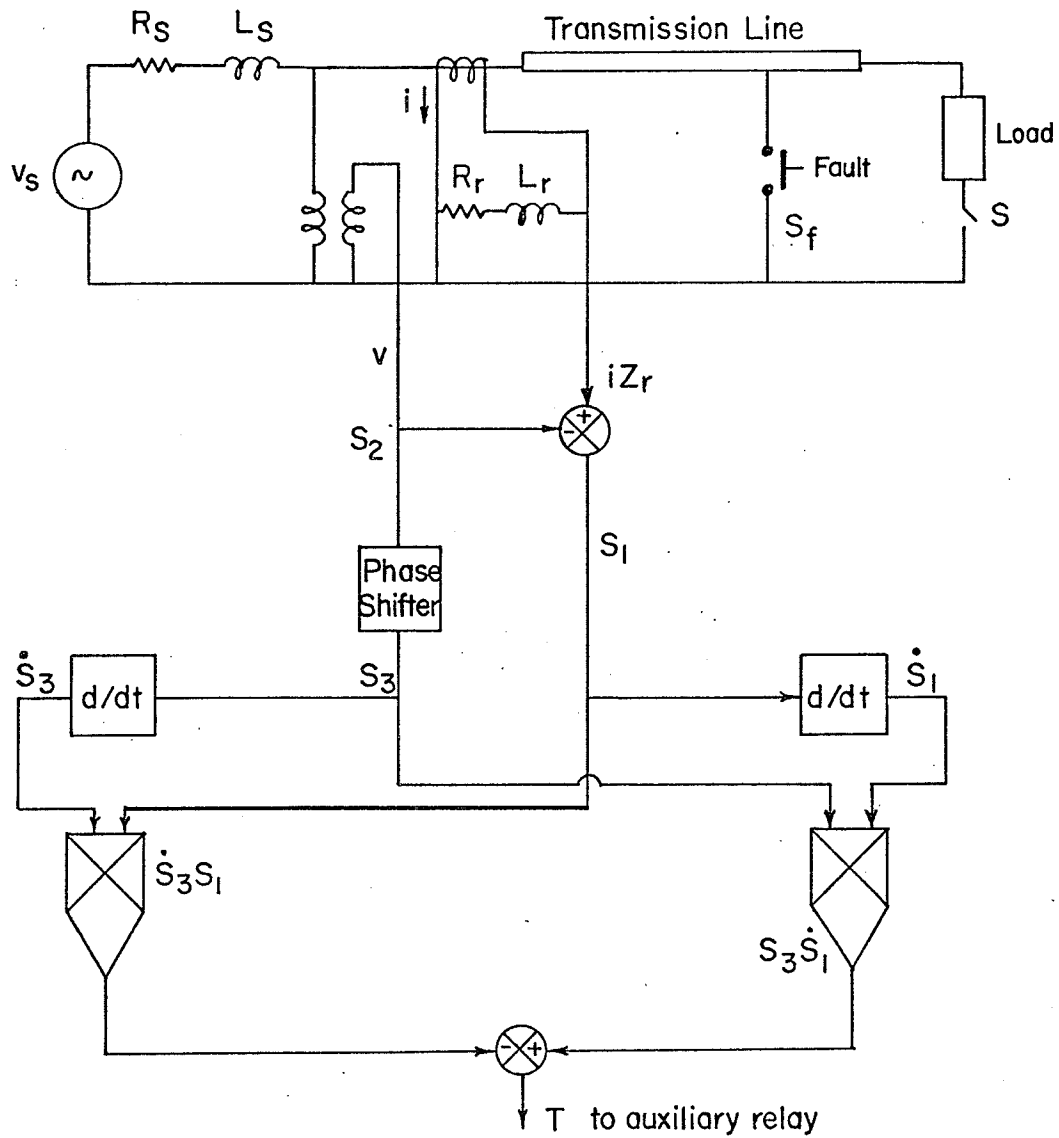


Fig. 4.1 Single phase representation of transmission line of relay

- (1) the faulted line is represented by an impedance  
 $R + j\omega L$
- (2) the faulted line is represented by a nominal-T  
 section.

In both cases, faults of different phase incidence and different parameter values are applied by appropriate control circuit and potentiometer settings.

#### 4.2.1 Disregarding Capacitance of the Faulted Line

The simulation is made on the assumption that a resistive load  $R_e$  is connected at the end of the line, i.e. switch  $s$  is closed. For a fault  $KZ_r$  miles out on the line, the differential equations relating current and voltage are given by

$$v_s = \hat{V}_s \sin(\omega t + \delta)$$

where  $v_s$  is the source voltage and  $\omega$  is the source radian frequency

$$v = v_s - iR_s - L_s \frac{di}{dt}$$

#### Before the Fault

$$v = iR + L \frac{di}{dt} + R_e i$$

where  $v$ ,  $i$  are the relaying voltage and current and  $R_e$  is

the load resistance.

After the Fault

The load is shorted and we have

$$v = (iR)K + (L \frac{di}{dt})K$$

where K is the ratio of the faulted section length to the complete line length. By changing K different fault locations can be simulated.

Figure 4.2 shows the complete analog computer simulation, as well as the equivalent circuit of the transmission line. Details concerning differentiators are given in Appendix B.

A simple mathematical analysis may be made in this case to clarify the fact that the experimental relay has a distance relay characteristic.

At the moment of the fault, the relay current is

$$i = \frac{\hat{V}_S}{Z} [\sin(\omega t + \delta - \phi) - e^{-\frac{R}{L}t} \sin(\delta - \phi)]$$

and the relay voltage is

$$v = \frac{\hat{V}_S}{Z} Z_L [\sin(\omega t + \delta - \phi + \phi_L) - \frac{\sin(\phi - \phi_L) \cdot \sin(\delta - \phi)}{\sin \phi} e^{-t \frac{R}{L}}]$$

The voltage on the replica impedance is:



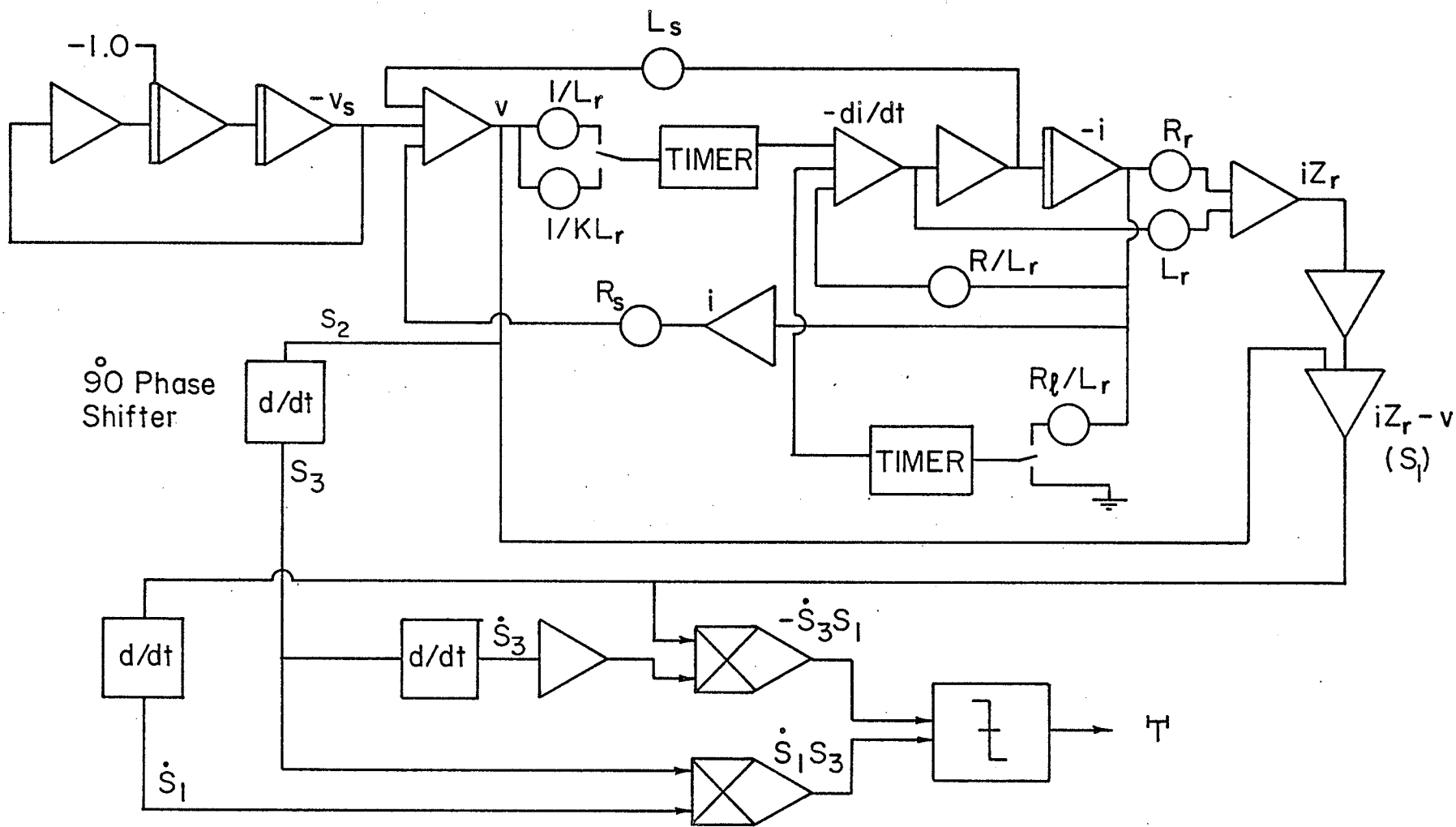


Fig. 4.2. Analog Computer Simulation. (Capacitance Not Considered)

$$iZ_r = \frac{V}{Z} Z_r \left[ \sin(\omega t + \delta - \phi + \phi_r) - \frac{\sin(\phi - \phi_r) \sin(\delta - \phi)}{\sin \phi} e^{-t \left( \frac{R}{L} \right)} \right]$$

For a Homogeneous System

$$\phi = \phi_L = \phi_r$$

and hence

$$S_2 = v = \frac{\hat{V}_s}{Z} Z_L \sin(\omega t + \delta)$$

$$iZ_r = \frac{\hat{V}_s}{Z} Z_r \sin(\omega t + \delta)$$

$$S_1 = iZ_r - v = \frac{\hat{V}_s}{Z} (Z_r - Z_L) \sin(\omega t + \delta)$$

$$\dot{S}_1 = \omega \frac{\hat{V}_s}{Z} (Z_r - Z_L) \cos(\omega t + \delta)$$

$$S_3 = \frac{\hat{V}_s}{Z} Z_L \cos(\omega t + \delta)$$

$$\dot{S}_3 = -\omega \frac{\hat{V}_s}{Z} Z_L \sin(\omega t + \delta)$$

$$T = S_3 \dot{S}_1 - \dot{S}_3 S_1$$

$$T = \omega \frac{\hat{V}_s^2}{Z^2} Z_L (Z_r - Z_L) [\cos^2(\omega t + \delta) + \sin^2(\omega t + \delta)]$$

$$T = \omega \frac{\hat{V}_s^2}{Z^2} Z_L (Z_r - Z_L)$$

but

$$Z_L = K Z_r$$

therefore

$$T = \frac{\hat{V}_S}{Z} Z_L Z_R (1-K)$$

$$\text{sgn}(T) = \text{sgn}(1-K)$$

which prove that for a homogeneous system, the relay will trip for  $K < 1$ , i.e. for a fault inside the protected section, while for  $K > 1$ ,  $T$  is negative and the relay will not trip.

The result is expected, since all the compared terms  $iZ_R - v$  and  $v$  contain the primary current transient reproduced. It cancels out in the measurement of impedance on a homogeneous system. This is actually one of the main advantages of using a replica impedance in the C.T. circuit.

The above analysis, however becomes tedious if the system is not homogeneous, or if the capacitance is included. In these cases, the analog computer use is justified.

#### 4.2.2 Faulted Line Represented by a Nominal-T Section

Simulation is done with the line originally open-circuited. Figure 4.3 shows the complete analog computer simulation. The differential equation relating current and voltage are:

Before the Fault:

$$v_s = v + iR_s + L_s \frac{di}{dt}$$

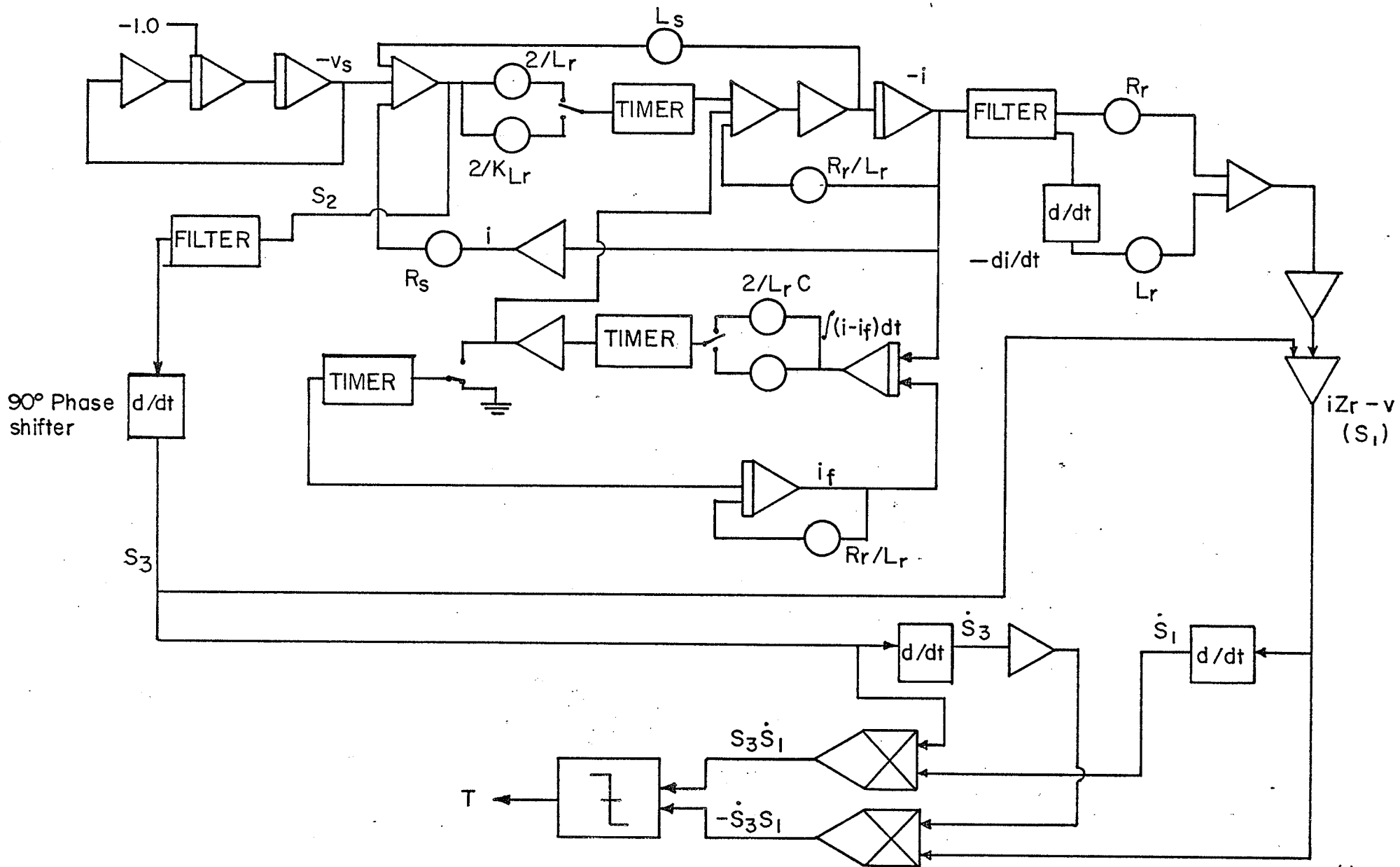


Fig. 4.3 Analog Computer Simulation. (Capacitance Considered)

$$\frac{2}{L} v = i \frac{R}{L} + \frac{di}{dt} + \frac{2}{LC} \int i dt$$

After the Fault

$$\frac{2}{KL} v = i \frac{R}{L} + \frac{di}{dt} + \frac{2}{K^2 LC} \int (i - i_f) dt$$

where K depends on fault locations and is unity for faults at the end of the line.

#### 4.3 Filters for the High Frequency Transients

The possibility of using filters to get rid of high frequency noise and the effect of this noise on the operation of the experimental relay was also investigated. For this, two low pass fourth order filters with adjustable cut-off frequencies were simulated on two (TR-20)<sup>†</sup> analog computers. Analog simulation diagrams together with the amplitude frequency response curves are given in Appendix C.

---

<sup>†</sup>Electronic Associates, Incorporated.

## CHAPTER 5

### TESTING AND RESULTS

#### 5.1 Description of Transmission Line Model

The model line used for acquisition of data is described as follows.

(1) the voltage applied is 1.0 p.u. (volt), with a frequency of  $\frac{1}{2\pi}$  p.u.

(2) the transmission line impedance consists of a resistance of 0.25 p.u. (ohm) in series with an inductance of 1.0 p.u. A smaller coil of resistance 0.05 p.u. (ohm) and inductance 0.2 p.u. (henry) simulate the source impedance. In this case the system is homogeneous (i.e. uniform phase angle along the system).

(3) the system can be made non-homogeneous by making the source impedance more lagging than that of the line.

(4) in the case where the line is represented by a nominal-T a capacitance is chosen such that the single T-circuit will have a six-to-one ratio of HF transient frequency to fundamental frequency. The length of the

line which will have this six-to-one ratio is found to be 258 miles.

(5) a 6 p.u. resistance is connected to the line through a switch so that faults on loaded or on open-circuit line can be obtained.

(6) the replica impedance connected in the current transformer circuit is equal to that of the line, i.e. a resistance of 0.25 p.u. in series with an inductance of 1.0 p.u.

(7) the C.T. and P.T. turns ratios are assumed to be one-to-one.

## 5.2 Discussion of Cases

Testing of the experimental relay includes a detailed study of its behaviour immediately after the fault inception for different fault locations and for different phase of incidence with respect to the voltage wave form. In each case, output from the analog computer is recorded on a high performance X-Y recorder.

### 5.2.1 Case One (Figs. 5.2.1.1 to 5.2.1.3)

The shunt capacitance is disconnected. The fault occurs at maximum source voltage. The system is homogeneous. Different fault locations within and outside the protected section are considered. Notice that the relay operates correctly and with zero time delay for

faults within its setting.

#### 5.2.2 Case Two (Figs. 5.2.2.1 to 5.2.2.3)

This case is identical to case one except that the fault occurs near a voltage zero. Notice that the relay trips when it should and does not trip when it should not.

#### 5.2.3 Case Three (Figs. 5.2.3.1 to 5.2.3.3)

The effect of angular mismatch\* between source impedance and line impedance is considered in this case. Faults occur at maximum source voltage. The relay still operates correctly and with zero time delay for faults within its setting.

#### 5.2.4 Case Four (Figs. 5.2.4.1 to 5.2.4.3)

The above case was reconsidered again but with faults occurring near voltage zero. Notice fast operation of the relay.

From the foregoing cases, the relay seems to respond perfectly and instantaneously to faults within its setting, no matter whether the system is homogeneous or not. A wrong trip signal is noticed when the fault occurs outside the protected region and at source voltage zero.

---

\* 8 degrees



#### 5.2.5 Case Five (Figs. 5.2.5.1 to 5.2.5.5)

This case is identical to that of case one except that the line is modelled as a single nominal-T section. Considerable amounts of high frequency transients show up together with a small amount of d.c. offset. Notice that the frequency of the transients gets larger as the distance from the source to the fault becomes smaller. It is clear that the relay trips whether the faults are within its setting or not.

#### 5.2.6 Case Six (Figs. 5.2.6.1 to 5.2.6.5)

This case is similar to the previous case except that faults occur near zero source voltage. A large d.c. offset in the current waveform is noticed. The relay still trips for faults away from the protected section.

#### 5.2.7 Case Seven (Figs. 5.2.7.1 to 5.2.7.4)

The line is modelled as a single nominal-T section and the source impedance is more lagging than the line impedance. Fault occurs near zero source voltage. Notice that the relay misoperates for faults outside the protected region.

#### 5.2.8 Case Eight (Figs. 5.2.8.1 to 5.2.8.4)

This case is identical with case seven

except that the fault inception is at source voltage maximum. It would appear that the angular mismatch between the source impedance and the line impedance does not have any effect on the relay response to unhealthy conditions.

#### 5.2.9 Case Nine (Figs. 5.2.9.1 to 5.2.9.3)

In this case, the source impedance is neglected and the single nominal-T section is used to represent the line. Fault occurs at maximum source voltage. Notice the trip signal for faults outside the protected zone.

#### 5.2.10 Case Ten (Figs. 5.2.10.1 to 5.2.10.3)

This case is identical to case nine, but with fault inception near zero voltage.

Cases five to ten show that the experimental relay due to fault generated high frequency transients tends to operate for a larger value of impedance than that for which it is adjusted to operate under steady-state conditions.

### 5.3 Filters for Relaying Quantities

Two low pass filters were used for filtering both current and voltage signals before they are fed to the relay. Cases 5.3.1 to 5.3.5 are identical to cases 5.2.5

to 5.2.10 but with the filters inserted into the circuit. The cut-off radian frequency for both filters is adjusted to 1.0 p.u. (Appendix C). Notice that the filters do not better the performance of the relay in addition to introducing time delay.

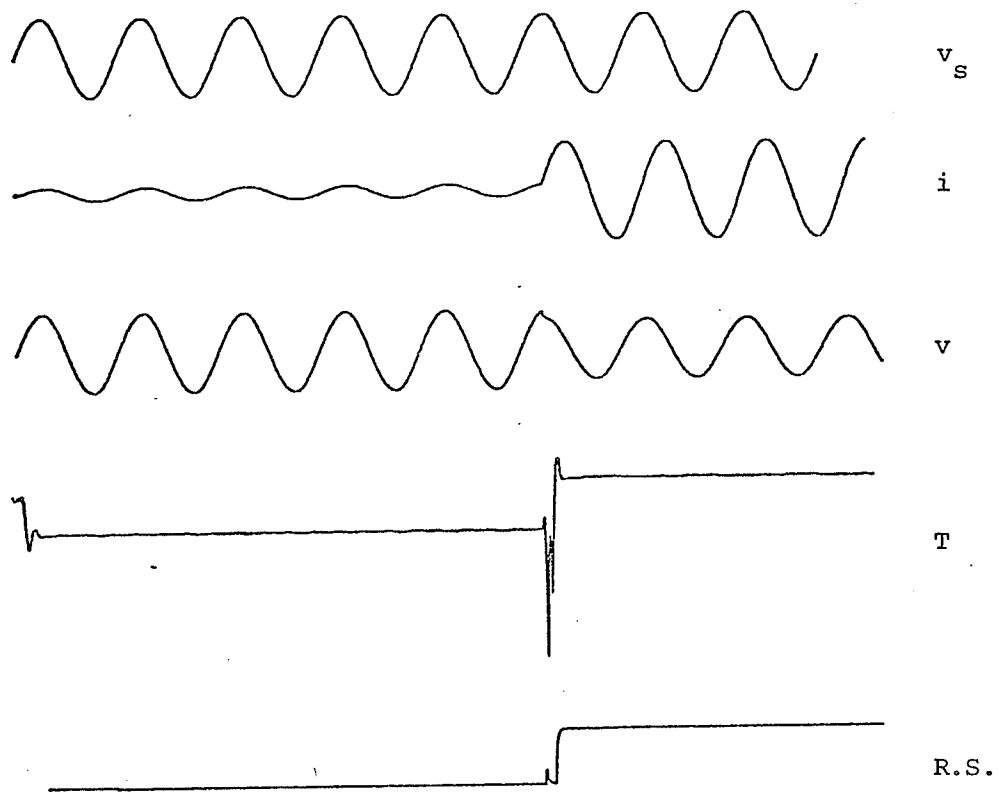


Fig. 5.2.1.1 Line capacitance neglected.  
 Fault incidence angle =  $90^\circ$   
 Relay-to-fault impedance = 0.5 line impedance  
 $\phi_s = \phi_r$

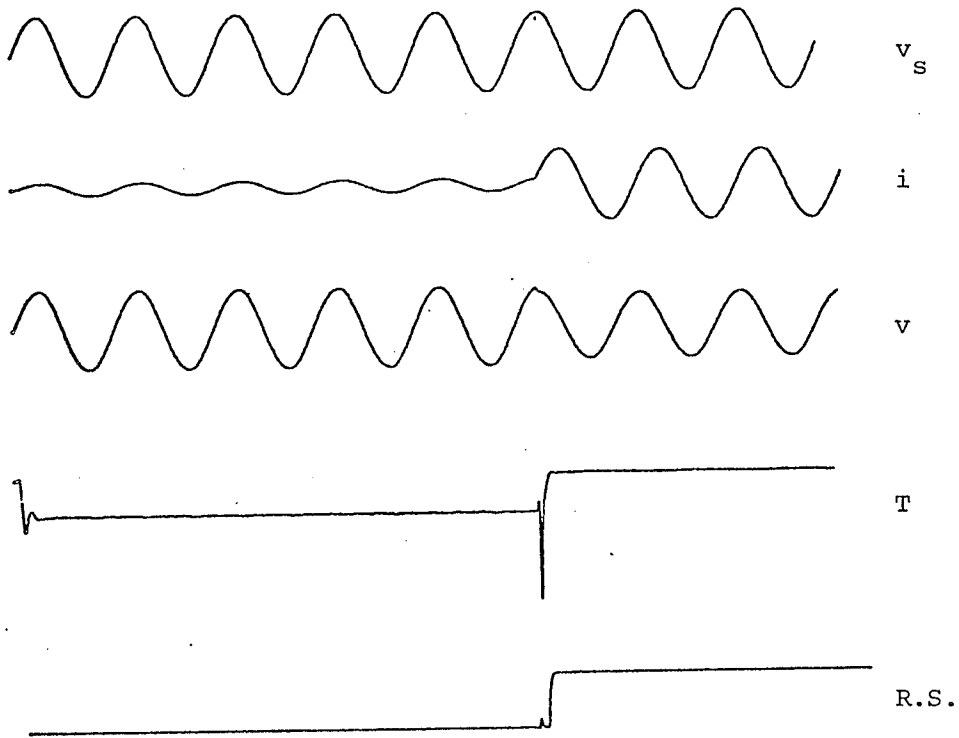


Fig. 5.2.1.2 Line capacitance neglected  
Fault incidence angle =  $90^\circ$   
Relay-to-fault impedance = 0.8 line impedance  
 $\phi_s = \phi_r$

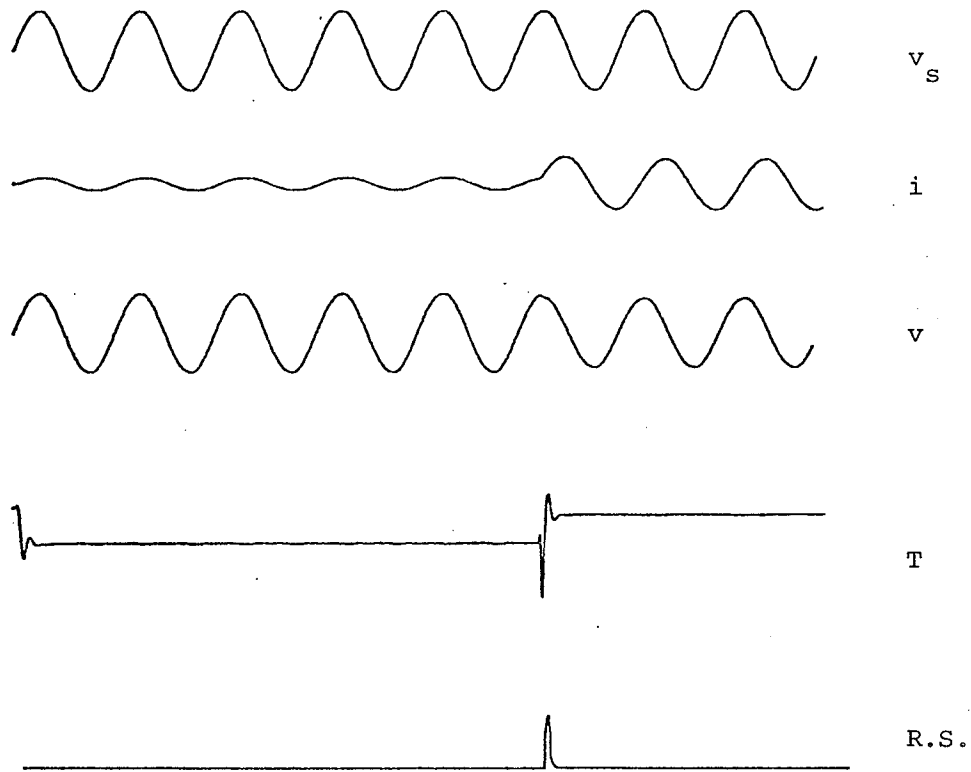


Fig. 5.2.1.3 Line capacitance neglected  
Fault incidence angle =  $90^\circ$   
Relay-to-fault impedance = 1.2 line impedance  
 $\phi_s = \phi_r$

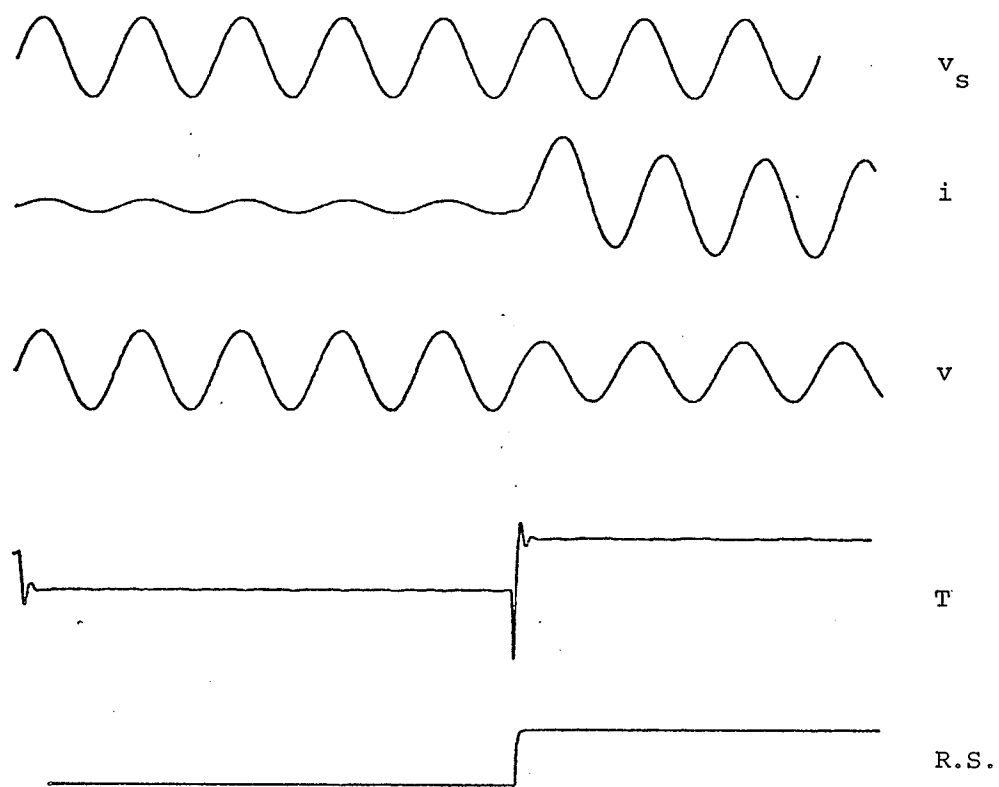


Fig. 5.2.2.1 Line capacitance neglected  
Fault incidence angle =  $0^\circ$   
Relay-to-fault impedance = 0.5 line impedance  
 $\phi_s = \phi_r$

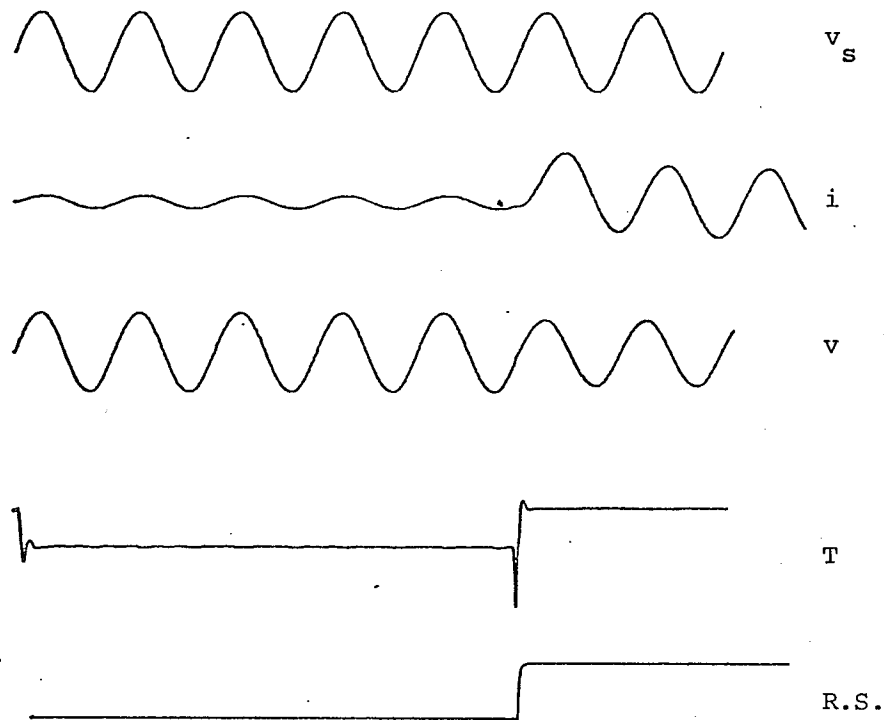


Fig. 5.2.2.2 Line capacitance neglected  
Fault incidence angle =  $0^\circ$   
Relay-to fault impedance = 0.8 line impedance  
 $\phi_s = \phi_r$



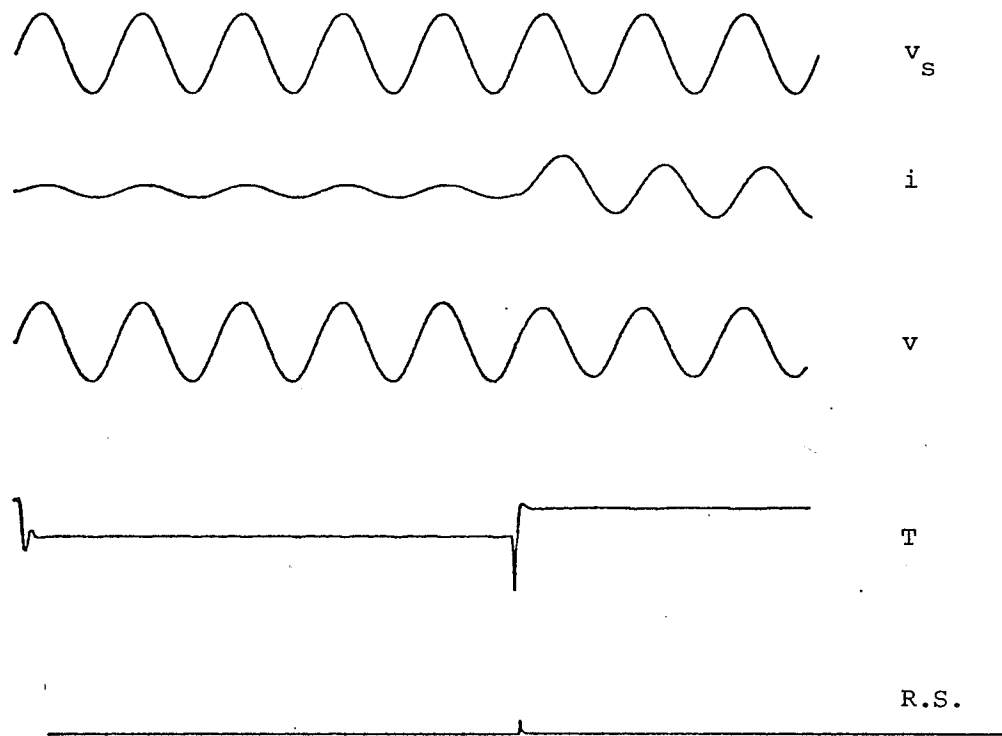


Fig. 5.2.2.3 Line capacitance neglected  
Fault incidence angle =  $0^\circ$   
Relay-to-fault impedance = 1.2 line impedance  
 $\phi_s = \phi_r$

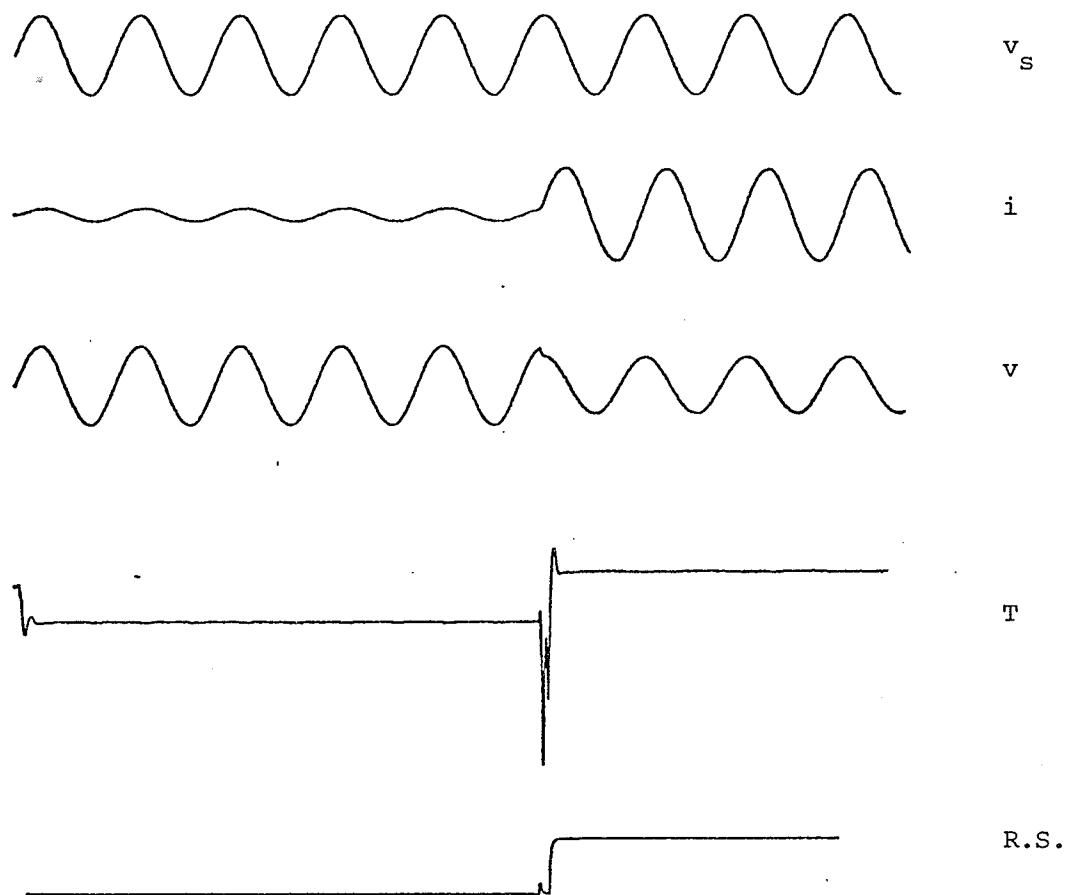


Fig. 5.2.3.1 Line capacitance neglected  
 Fault incidence angle =  $90^\circ$   
 Relay-to-fault impedance = 0.5 line impedance  
 $\phi_s \neq \phi_r$

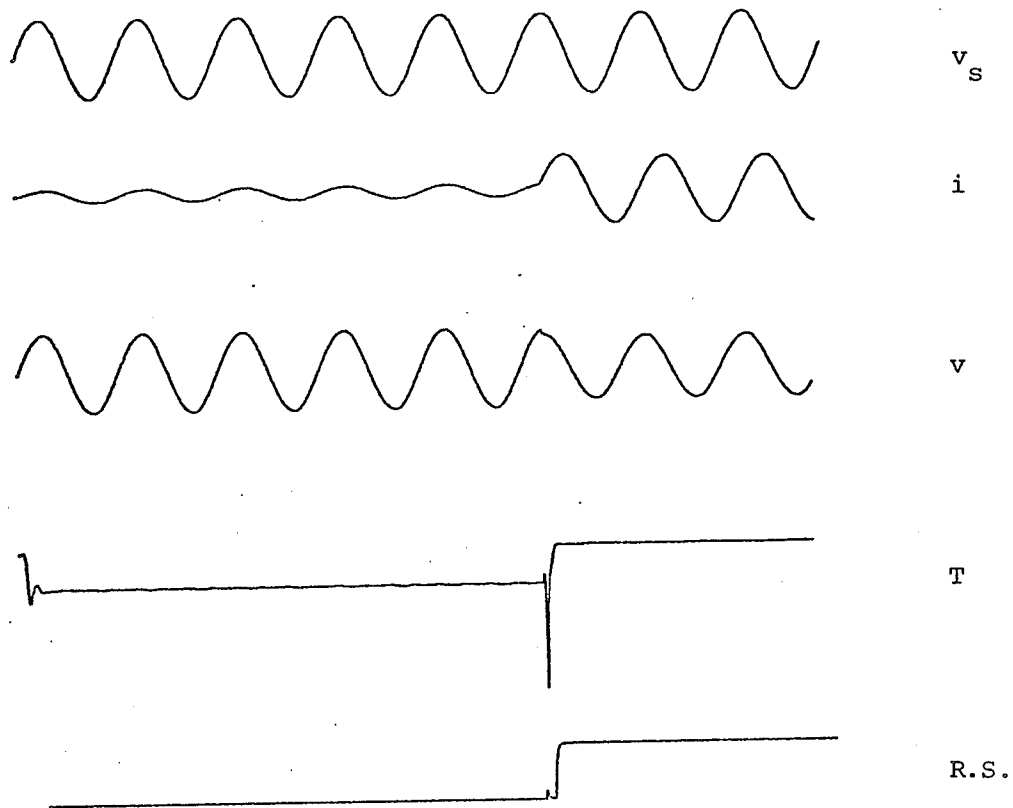


Fig. 5.2.3.2 Line capacitance neglected  
Fault incidence angle =  $90^\circ$   
Relay-to fault impedance = 0.8 line impedance  
 $\phi_s \neq \phi_r$

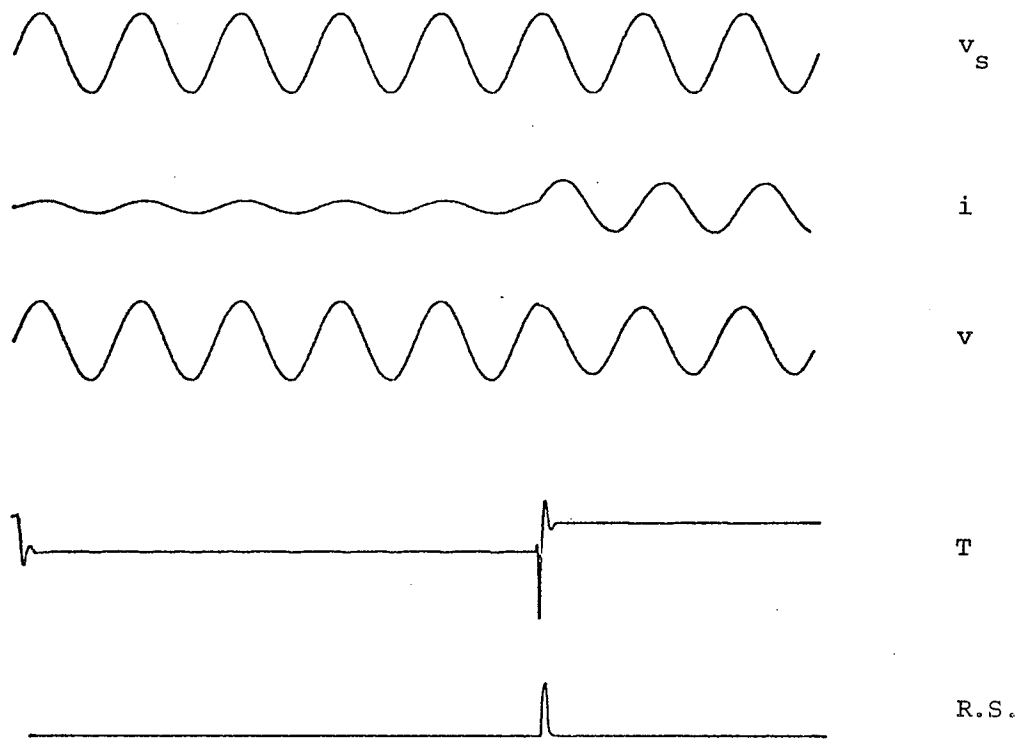


Fig. 5.2.3.3 Line capacitance neglected  
Fault incidence angle =  $90^\circ$   
Relay-to-fault impedance = 1.2 line impedance  
 $\phi_s \neq \phi_r$

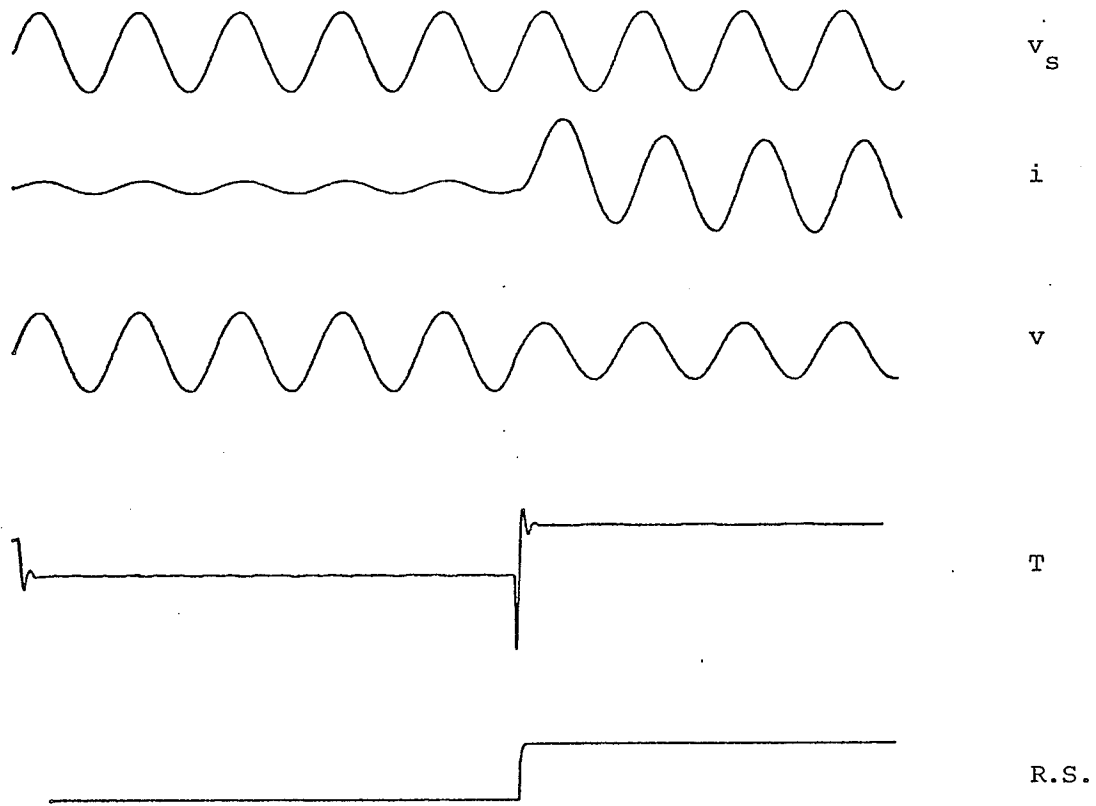


Fig. 5.2.4.1 Line capacitance neglected  
Fault incidence angle =  $0^\circ$   
Relay-to-fault impedance = 0.5 line impedance  
 $\phi_s \neq \phi_r$

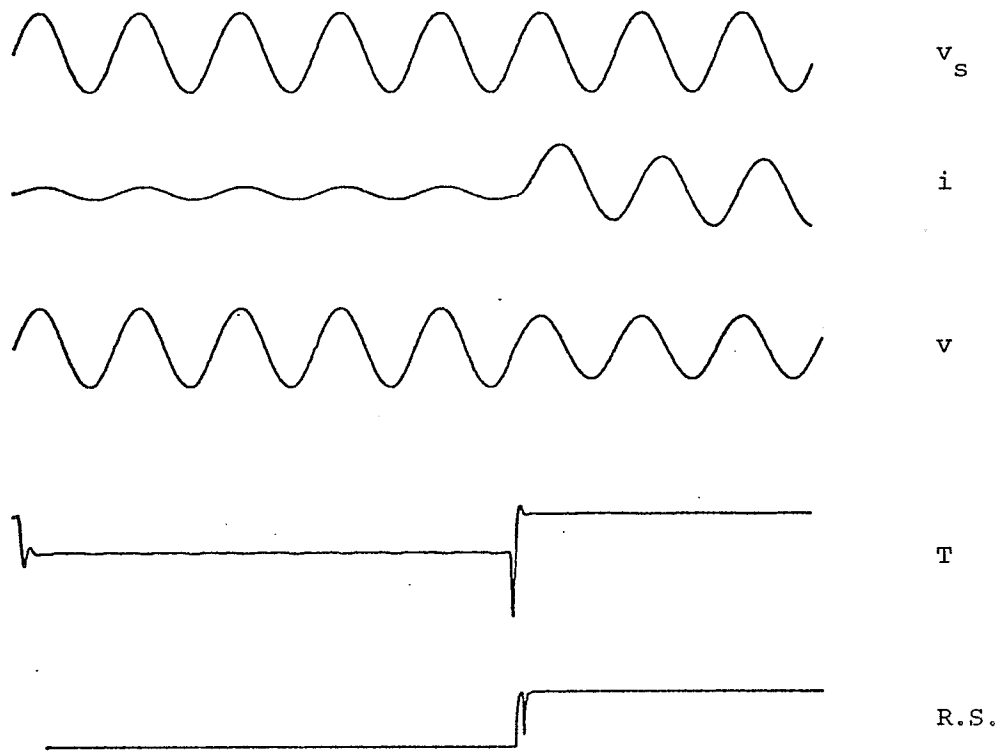


Fig. 5.2.4.2 Line capacitance neglected  
Fault incidence angle =  $0^\circ$   
Relay-to-fault impedance = 0.8 line impedance  
 $\phi_s \neq \phi_r$

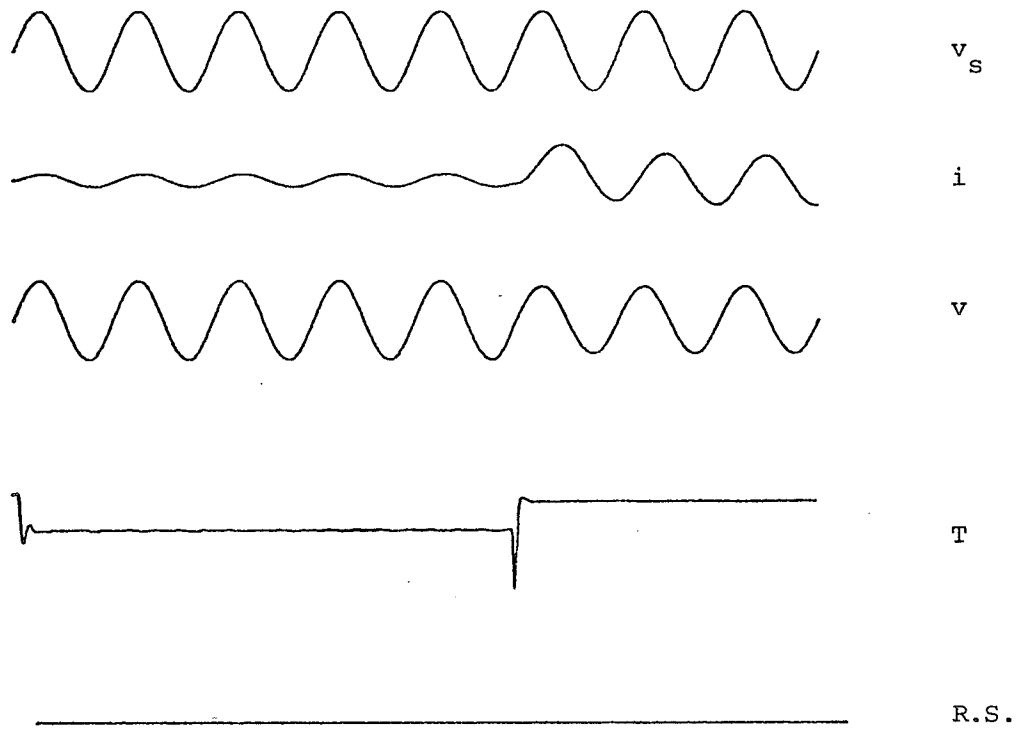


Fig. 5.2.4.3 Line capacitance neglected  
Fault incidence angle =  $0^\circ$   
Relay-to-fault impedance = 1.2 line impedance  
 $\phi_s \neq \phi_r$

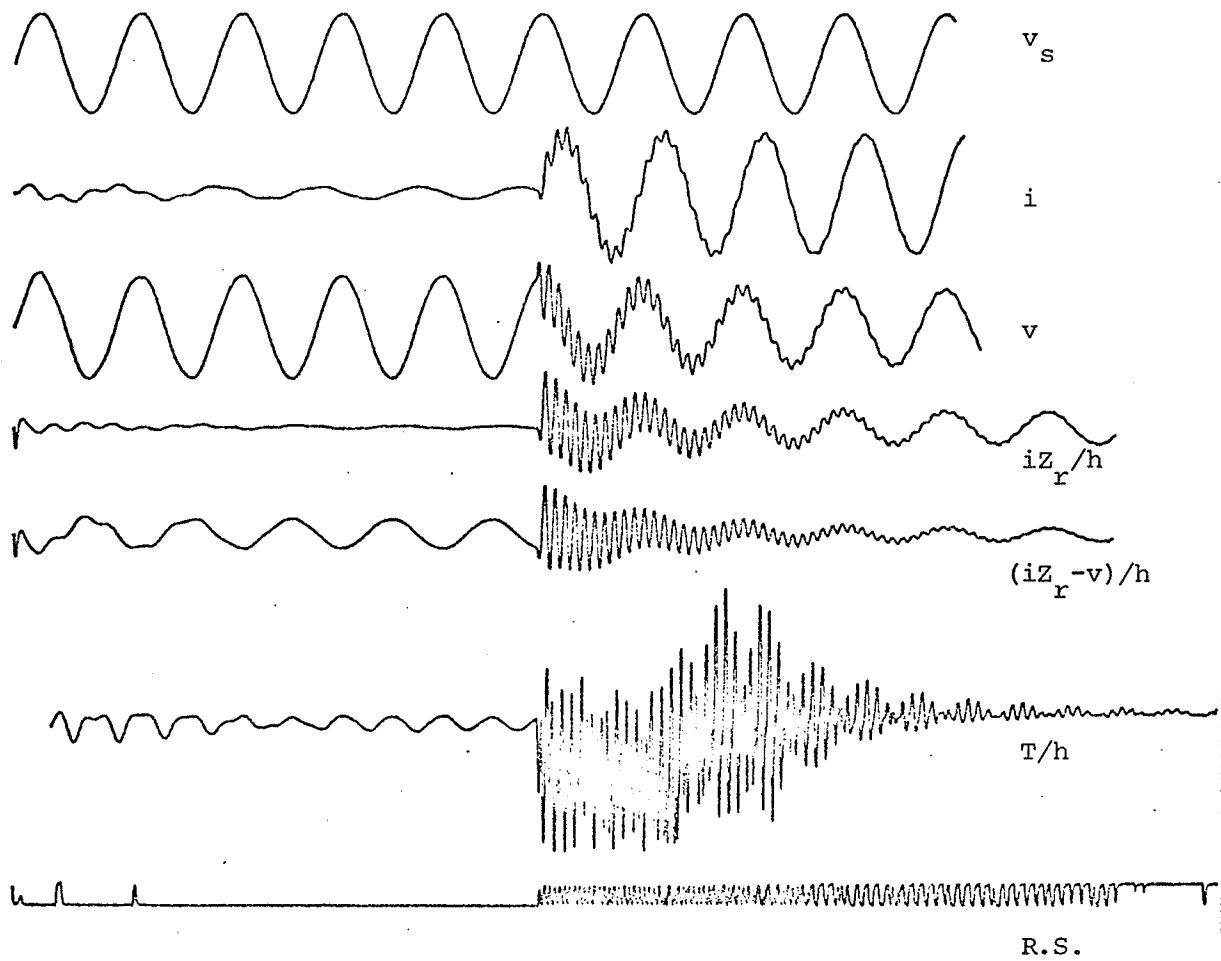


Fig. 5.2.5.1 Line capacitance considered  
 Fault incidence angle =  $90^\circ$   
 $\phi_s = \phi_r$   
 Relay-to-fault impedance = 0.5 line impedance



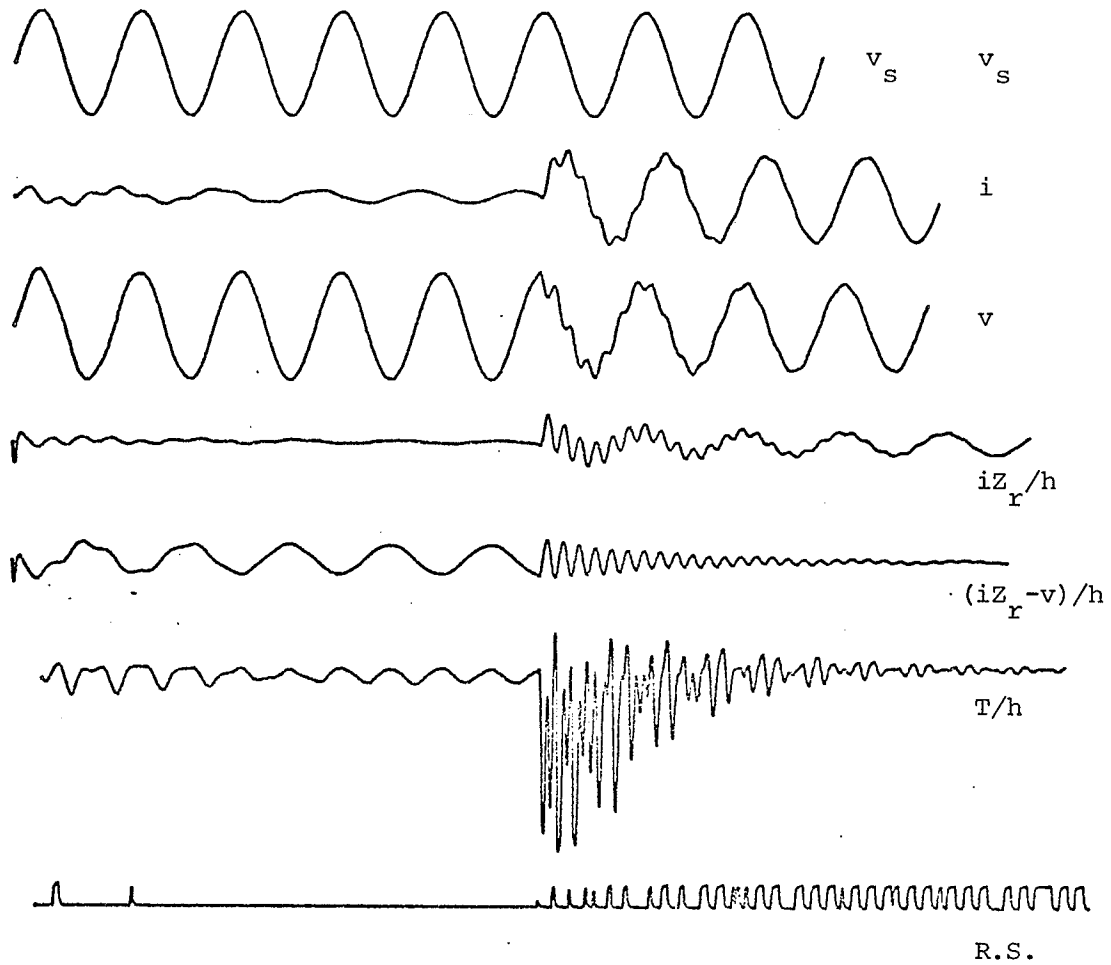


Fig. 5.2.5.2 Line capacitance considered  
 Fault incidence angle =  $90^\circ$   
 $\phi_s = \phi_r$   
 Relay-to-fault impedance = 0.8 line impedance

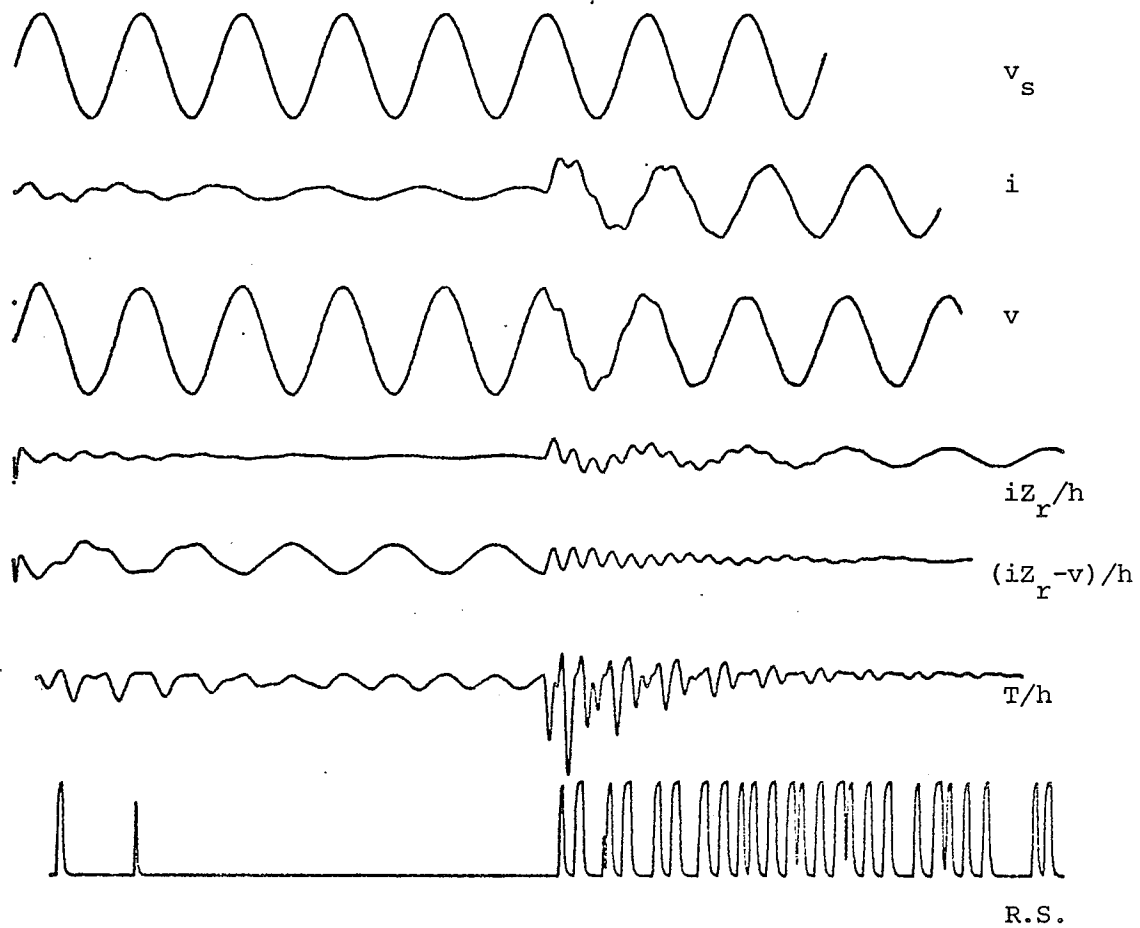


Fig. 5.2.5.3 Line capacitance considered  
 Fault incidence angle =  $90^\circ$   
 $\phi_s = \phi_r$   
 Relay-to-fault impedance = 1.0 line impedance

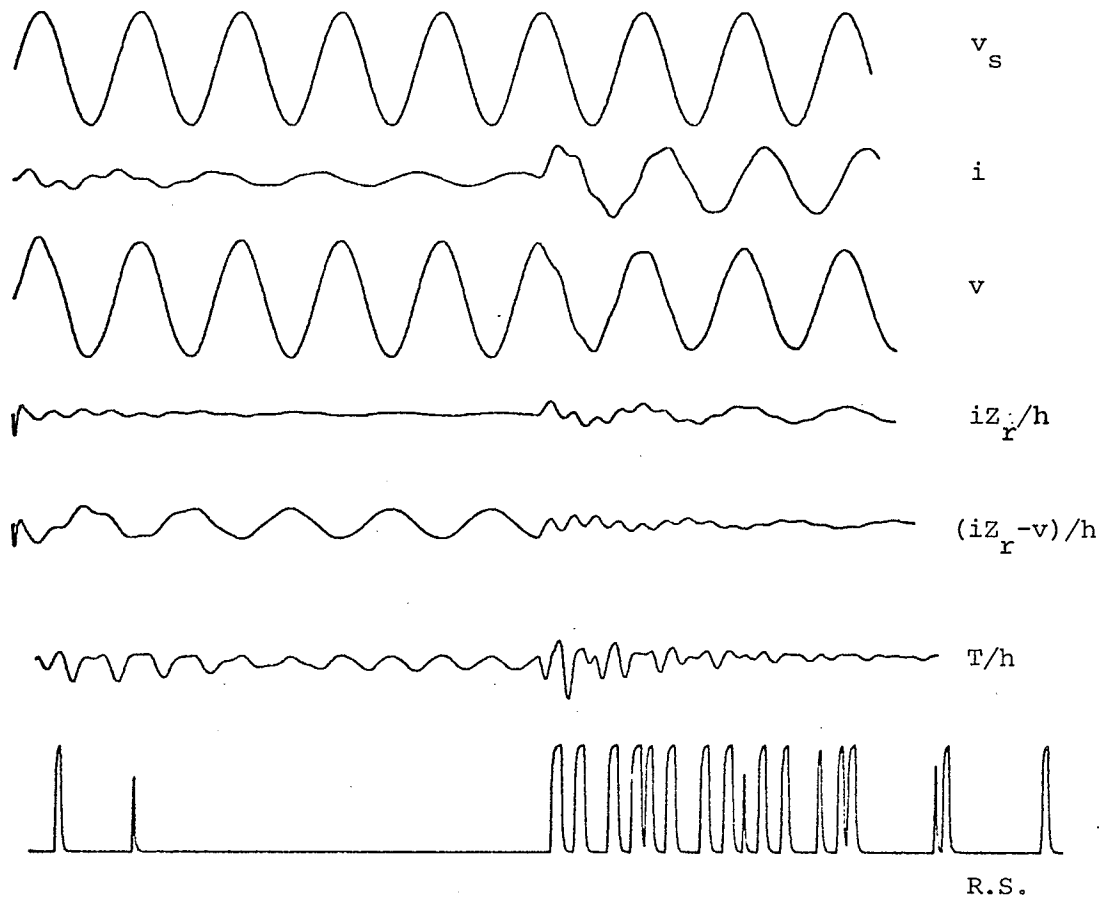


Fig. 5.2.5.4 Line capacitance considered  
 Fault incidence angle =  $90^\circ$   
 $\phi_s = \phi_r$   
 Relay-to-fault impedance = 1.2 line impedance

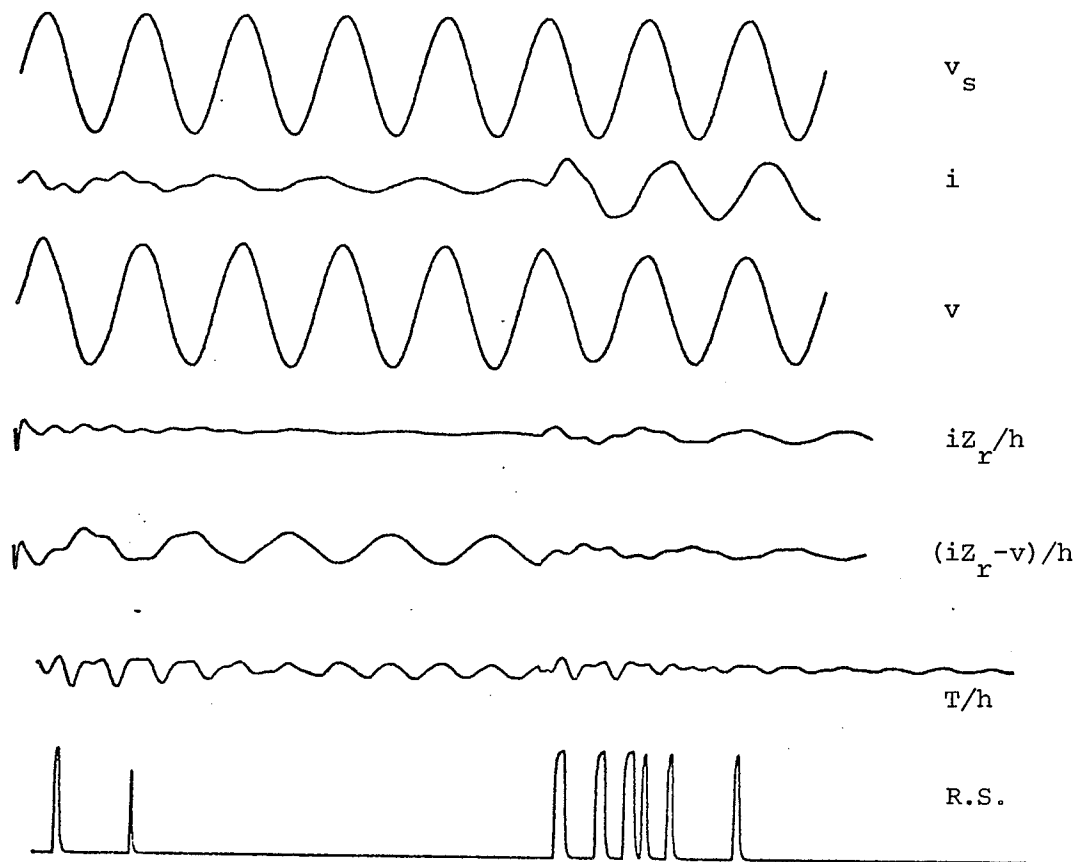


Fig. 5.2.5.5 Line capacitance considered  
Fault incidence angle =  $90^\circ$   
 $\phi_s = \phi_r$   
Relay-to-fault impedance = 1.5 line impedance

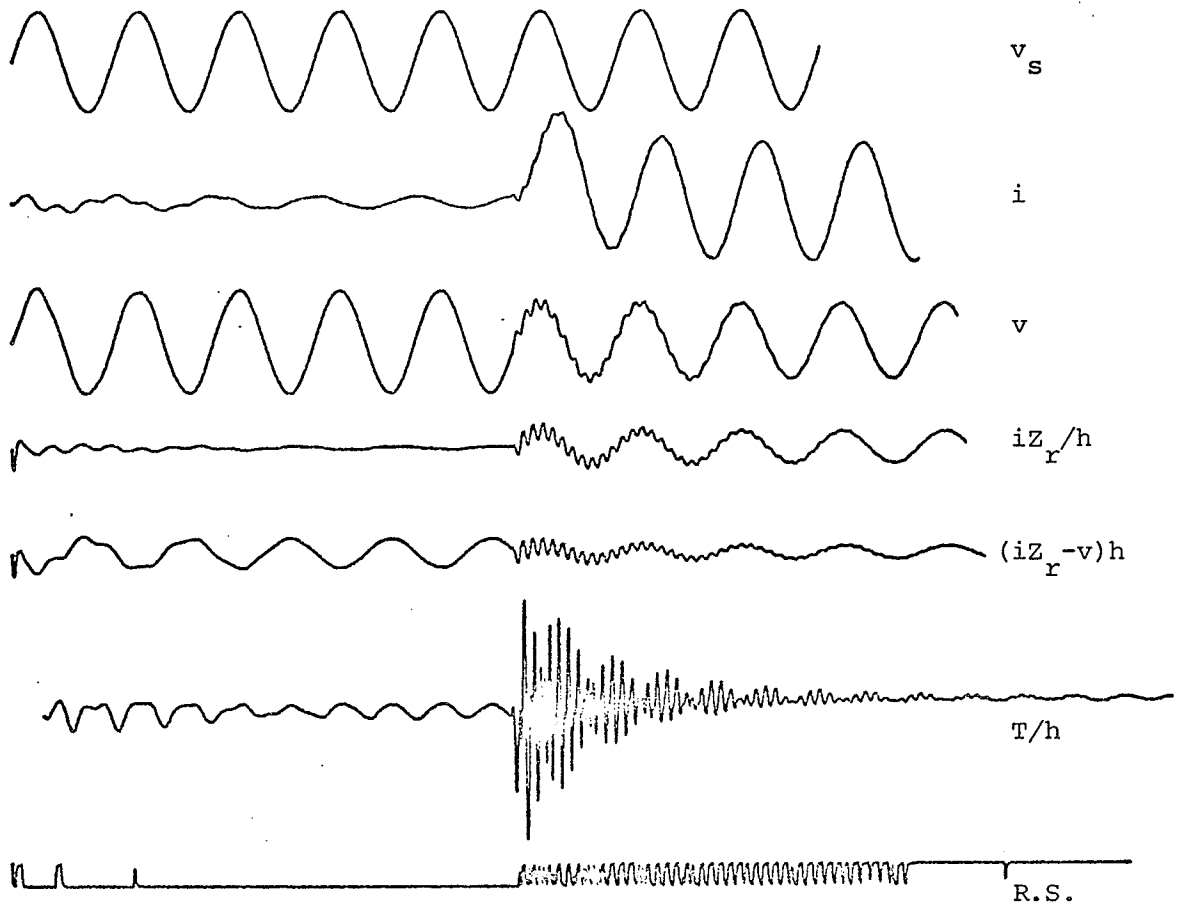


Fig. 5.2.6.1 Line capacitance considered  
 Fault incidence angle =  $0^\circ$   
 $\phi_s = \phi_r$   
 Relay-to-fault impedance = 0.5 line impedance

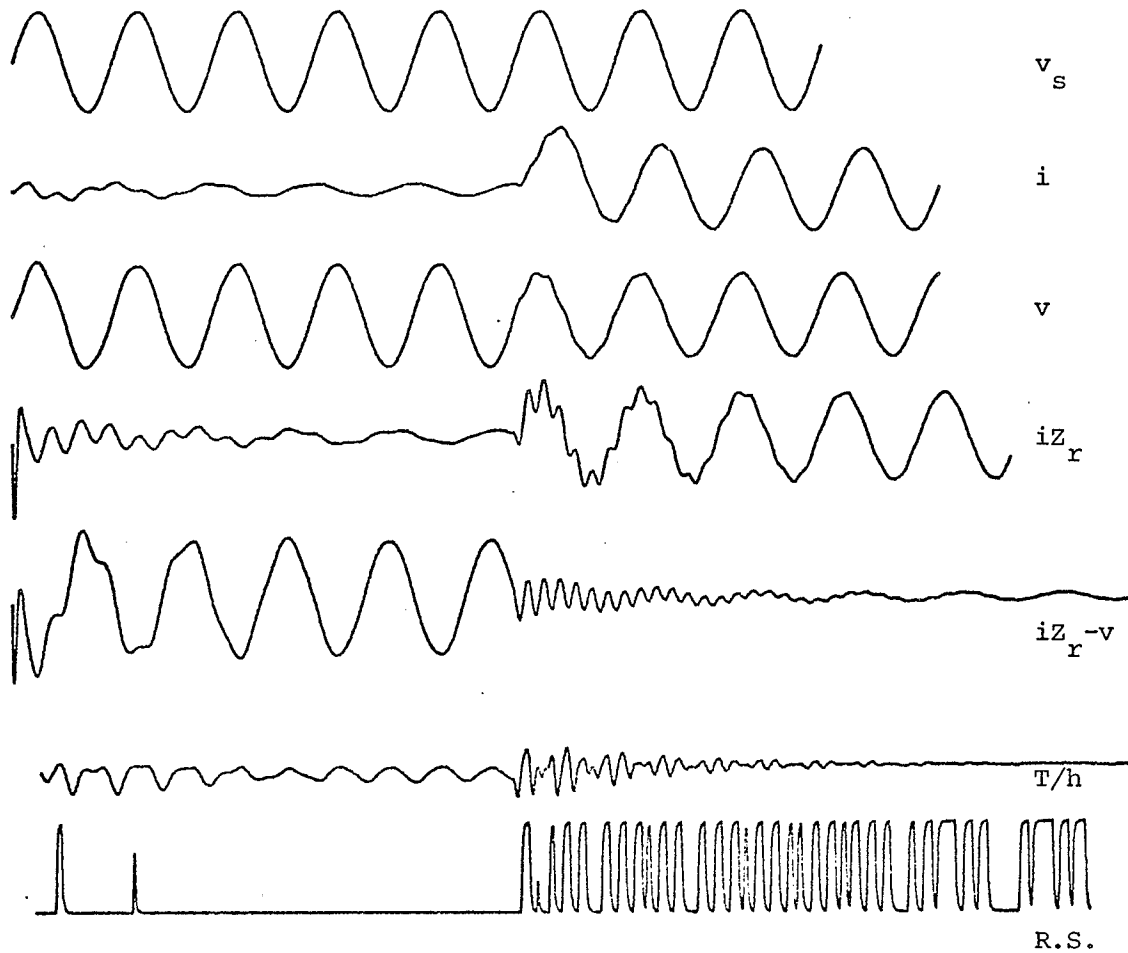


Fig. 5.2.6.2 Line capacitance considered  
 Fault incidence angle =  $0^\circ$   
 $\phi_s = \phi_r$   
 Relay-to-fault impedance = 0.8 line impedance

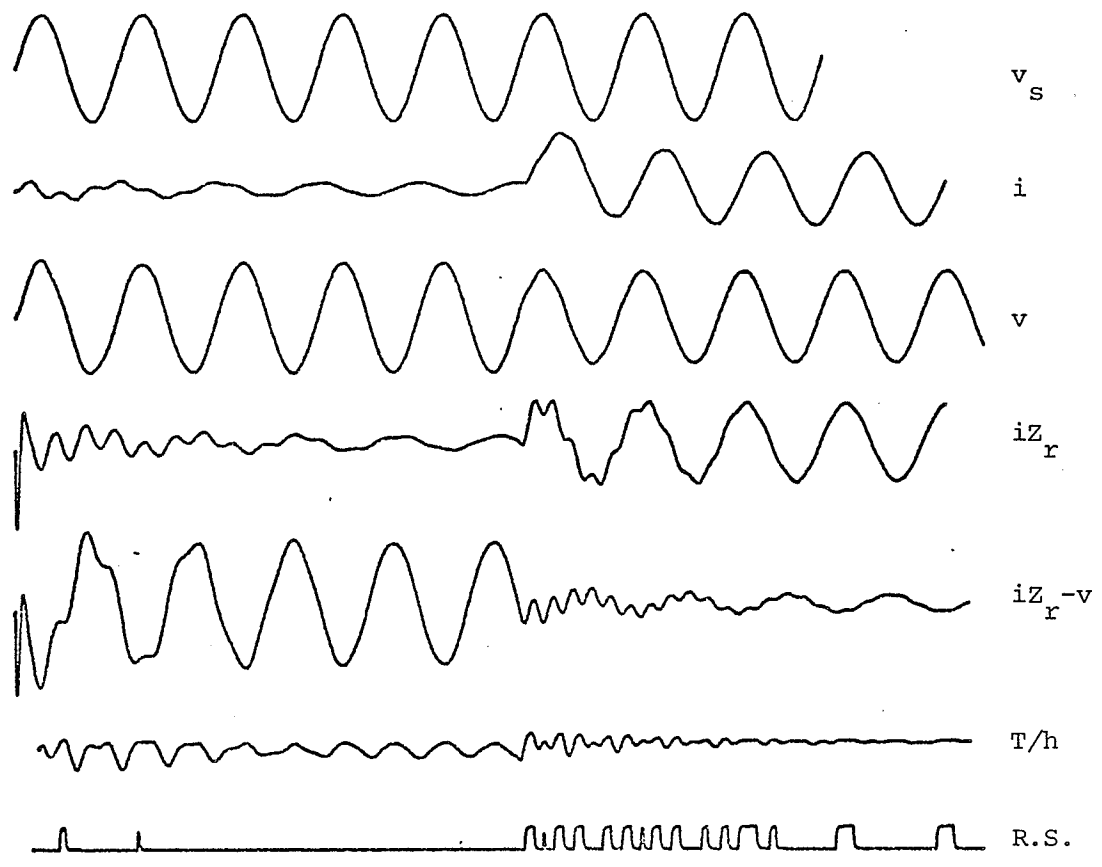


Fig. 5.2.6.3 Line capacitance considered  
Fault incidence angle =  $0^\circ$   
 $\phi_s = \phi_r$   
Relay-to-fault impedance = 1.0 line impedance

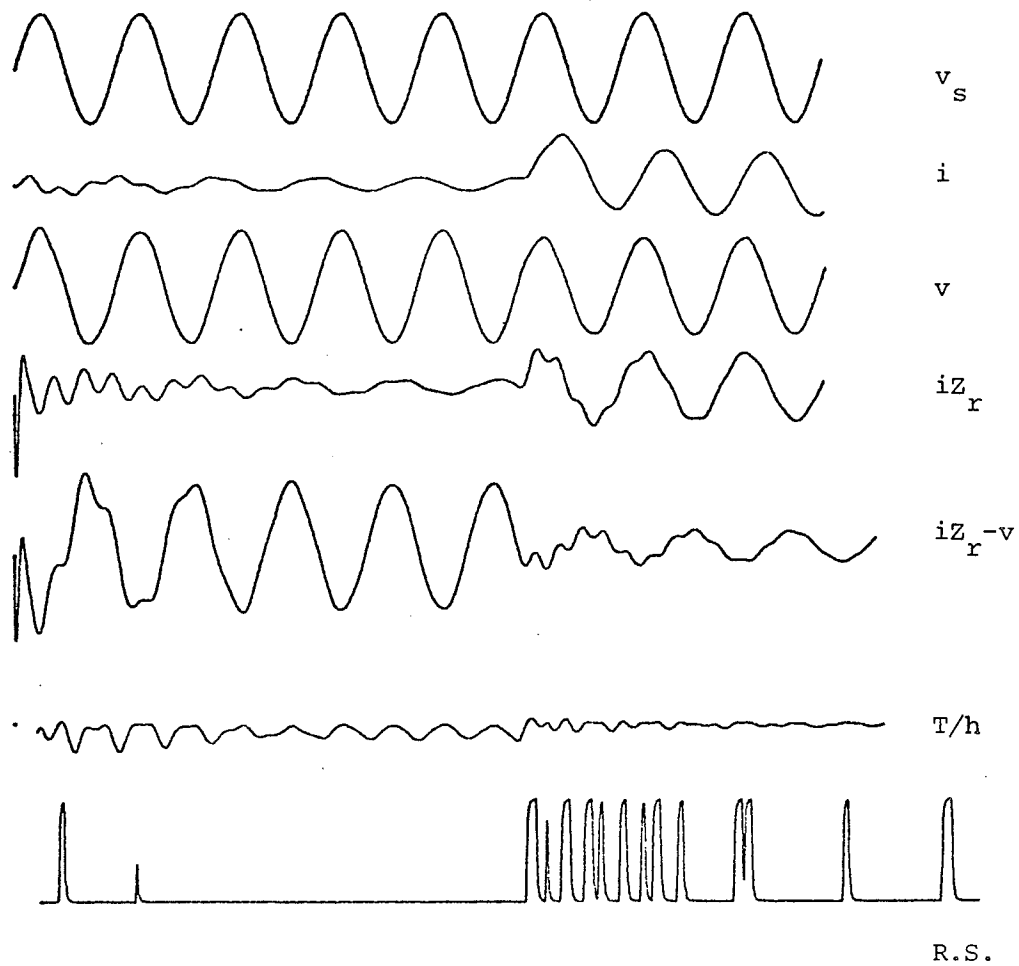


Fig. 5.2.6.4 Line capacitance considered  
 Fault incidence angle =  $0^\circ$   
 $\phi_s = \phi_r$   
 Relay-to-fault impedance = 1.2 line impedance



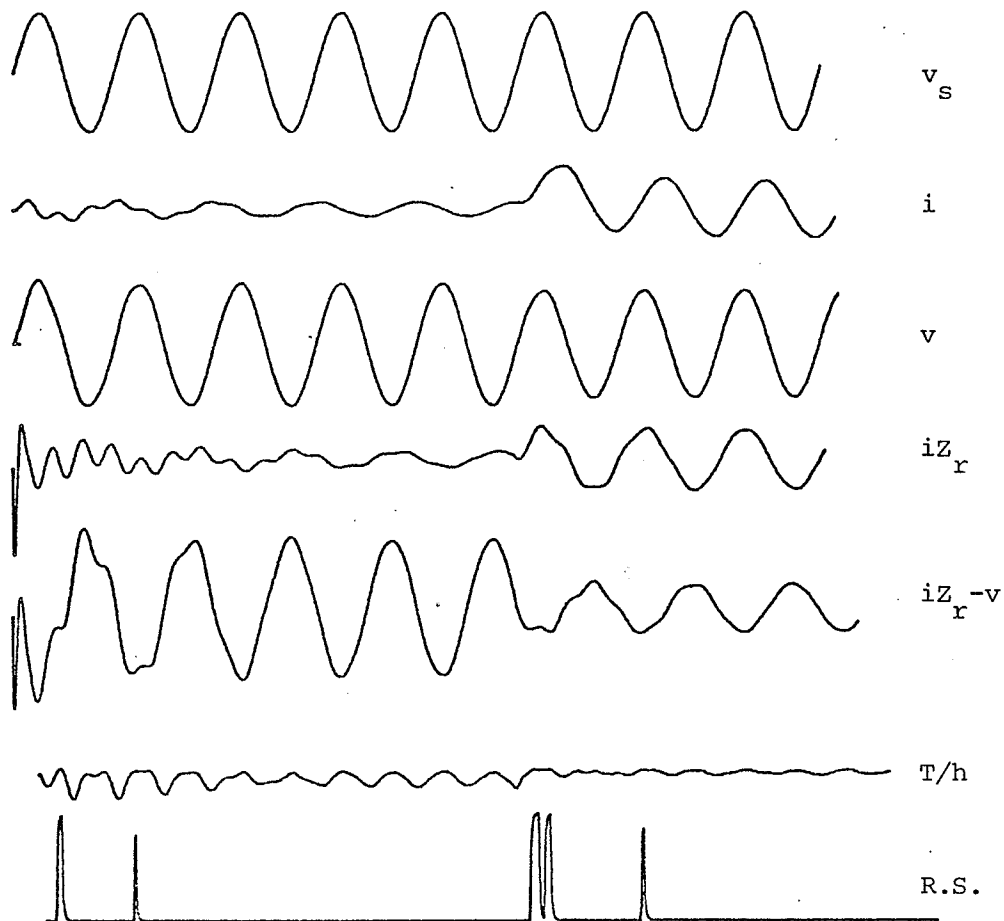


Fig. 5.2.6.5. Line capacitance considered

Fault incidence angle =  $0^\circ$

$$\phi_s = \phi_r$$

Relay-to-fault impedance = 1.5 line impedance

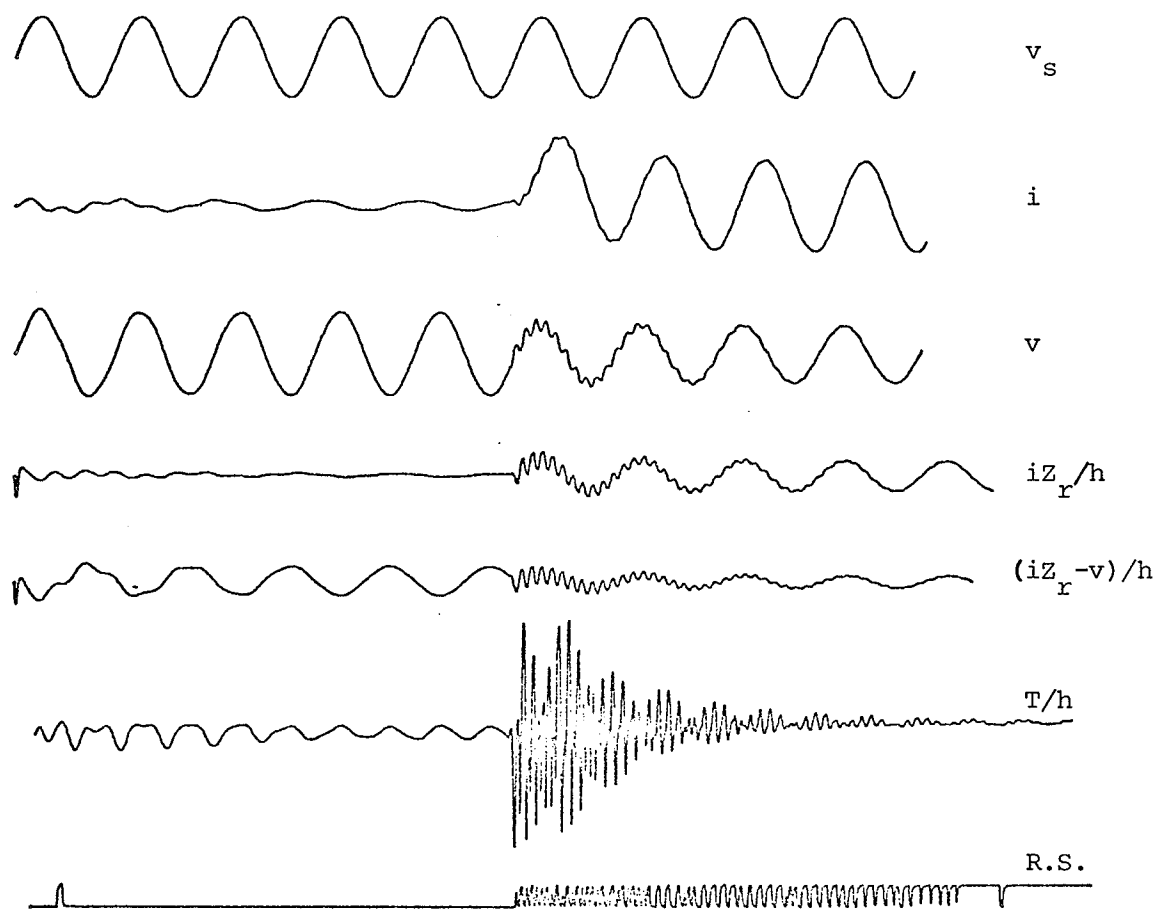


Fig. 5.2.7.1 Line capacitance considered  
 Fault incidence angle =  $0^\circ$   
 $\phi_s \neq \phi_r$   
 Relay-to-fault impedance = 0.5 line impedance

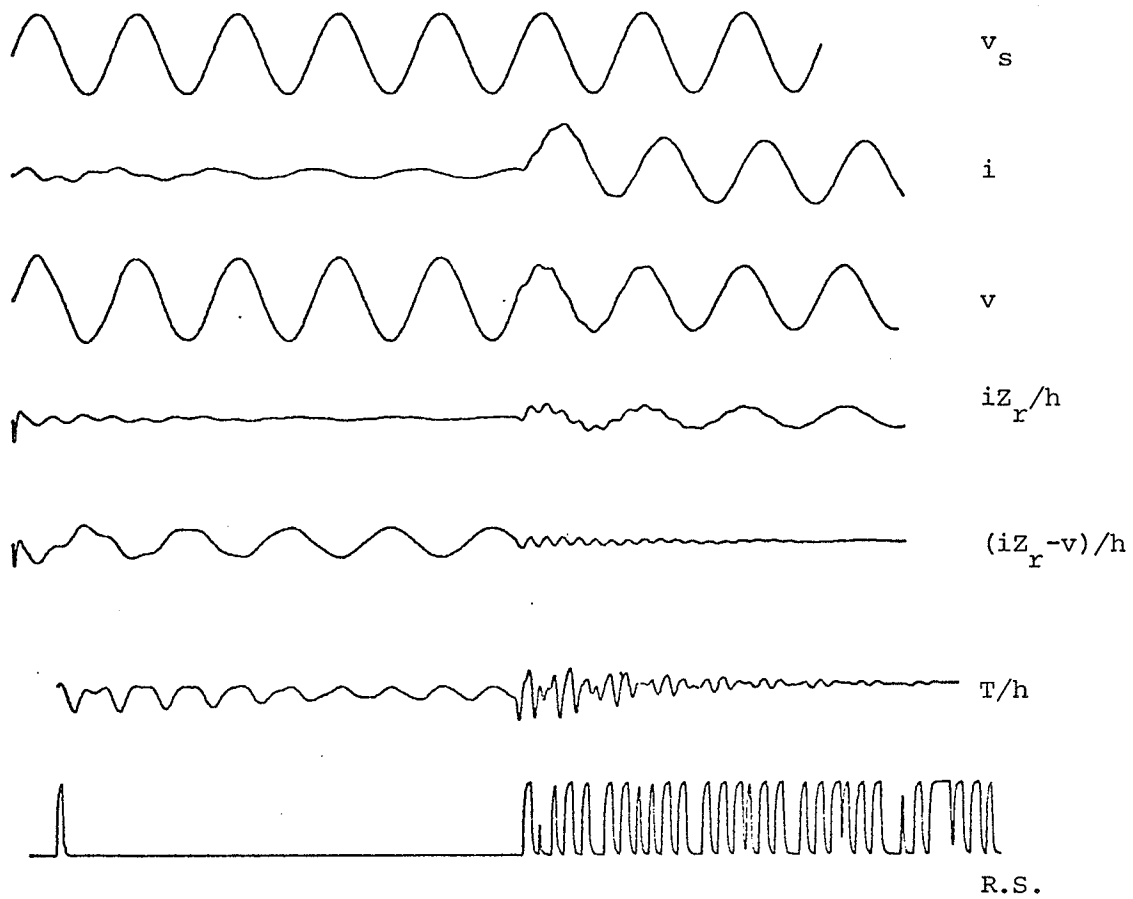


Fig. 5.2.7.2 Line capacitance considered  
 Fault incidence angle =  $0^\circ$   
 $\phi_s \neq \phi_r$   
 Relay-to-fault impedance = 0.8 line impedance

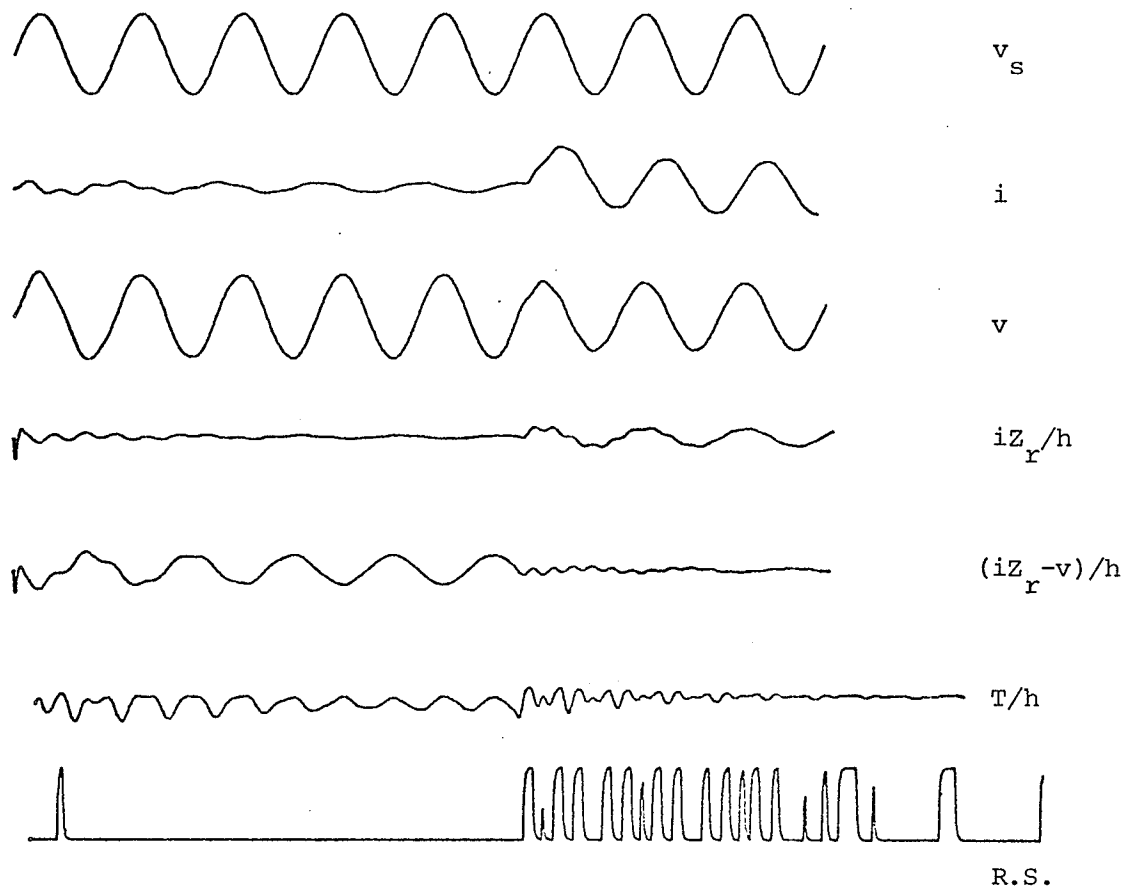


Fig. 5.2.7.3. Line capacitance considered  
 Fault incidence angle =  $0^\circ$   
 $\phi_s \neq \phi_r$   
 Relay-to-fault impedance = 1.0 line impedance

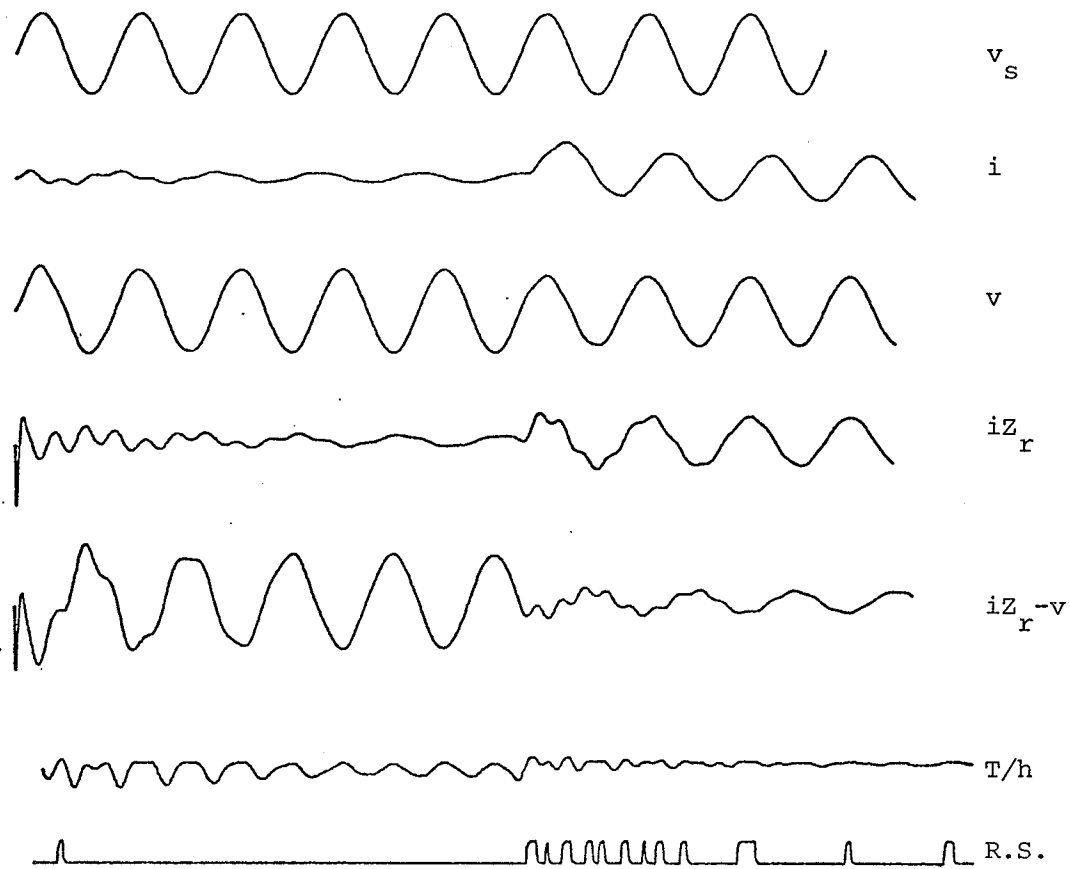


Fig. 5.2.7.4 Line capacitance considered  
 Fault incidence angle =  $0^\circ$   
 $\phi_s \neq \phi_r$   
 Relay-to-fault impedance = 1.2 line impedance

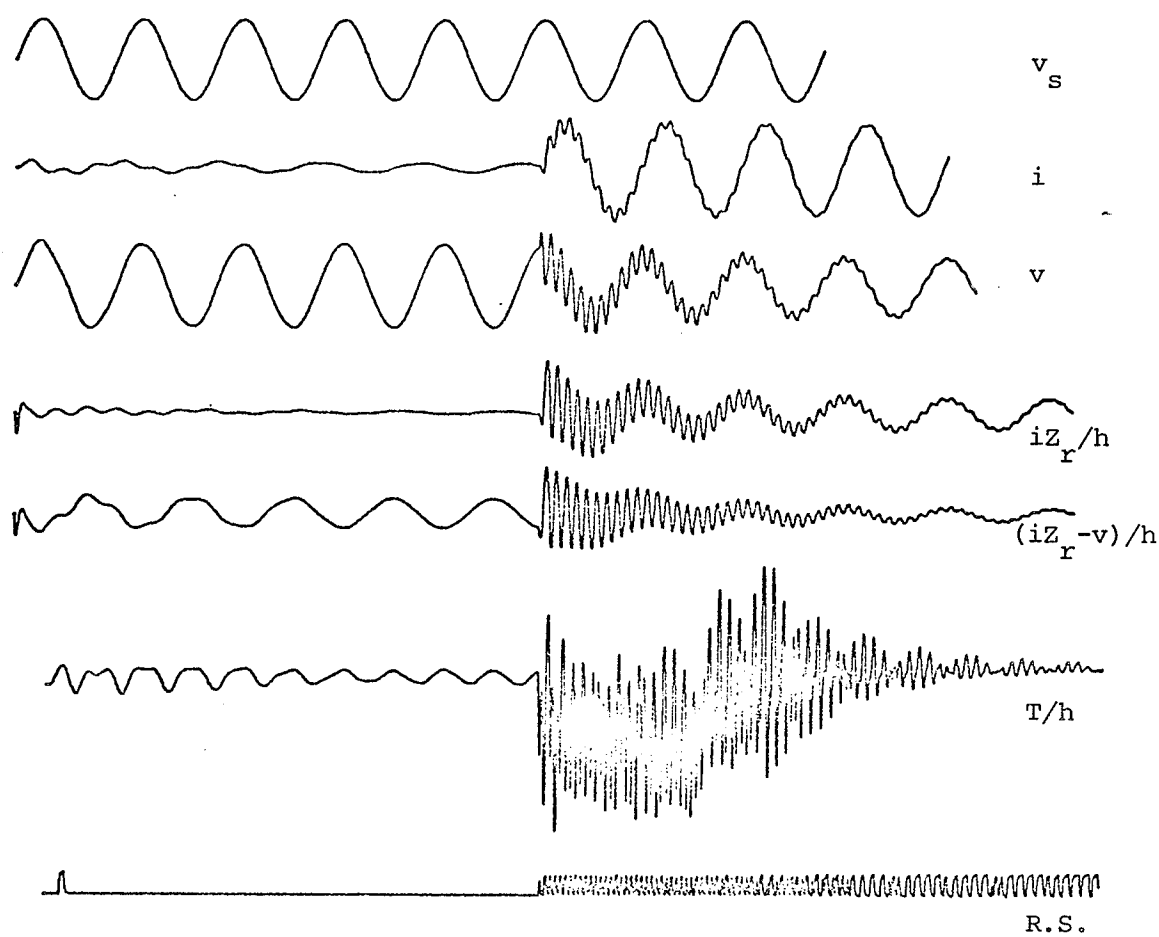


Fig. 5.2.8.1 Line capacitance considered  
 Fault incidence angle =  $90^\circ$   
 $\phi_s \neq \phi_r$   
 Relay-to-fault impedance = 0.5 line impedance

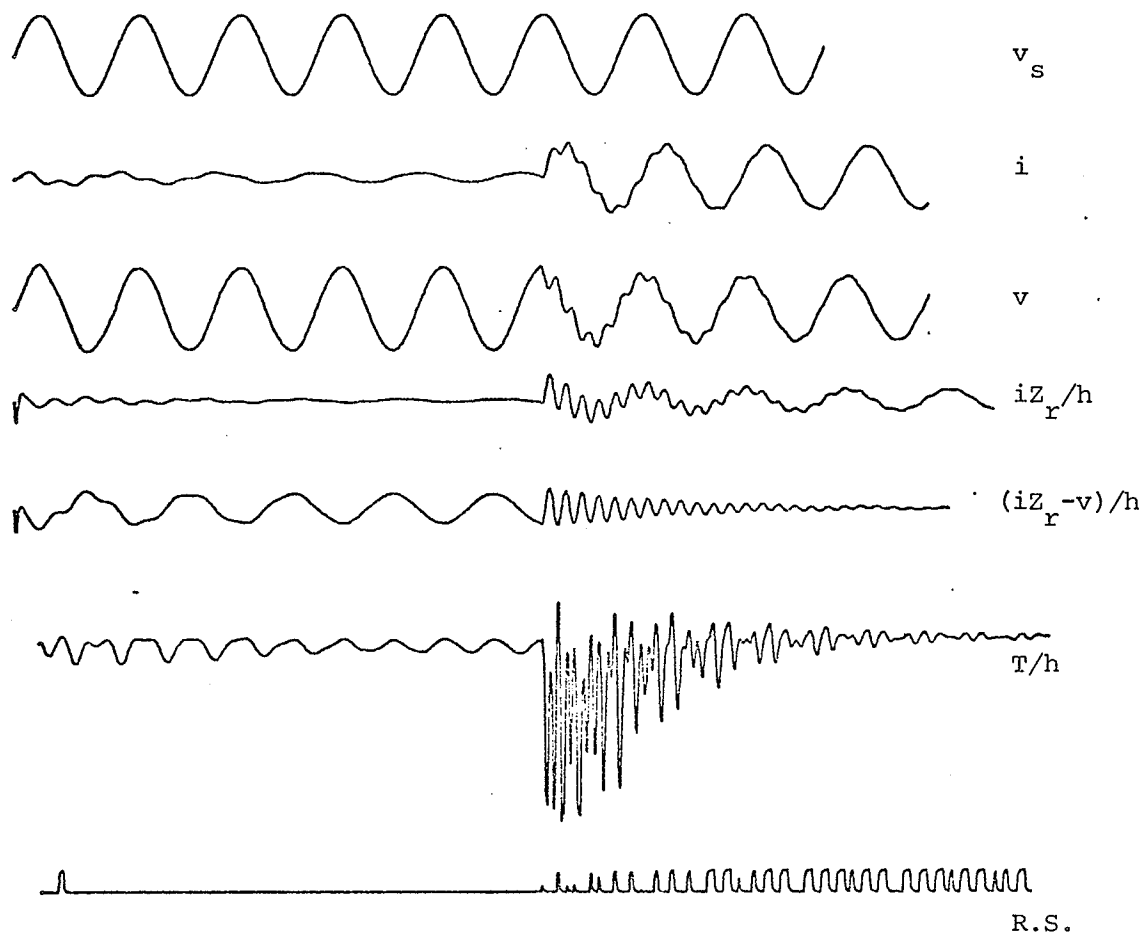


Fig. 5.2.8.2 Line capacitance considered  
 Fault incidence angle =  $90^\circ$   
 $\phi_s \neq \phi_r$   
 Relay-to-fault impedance = 0.8 line impedance

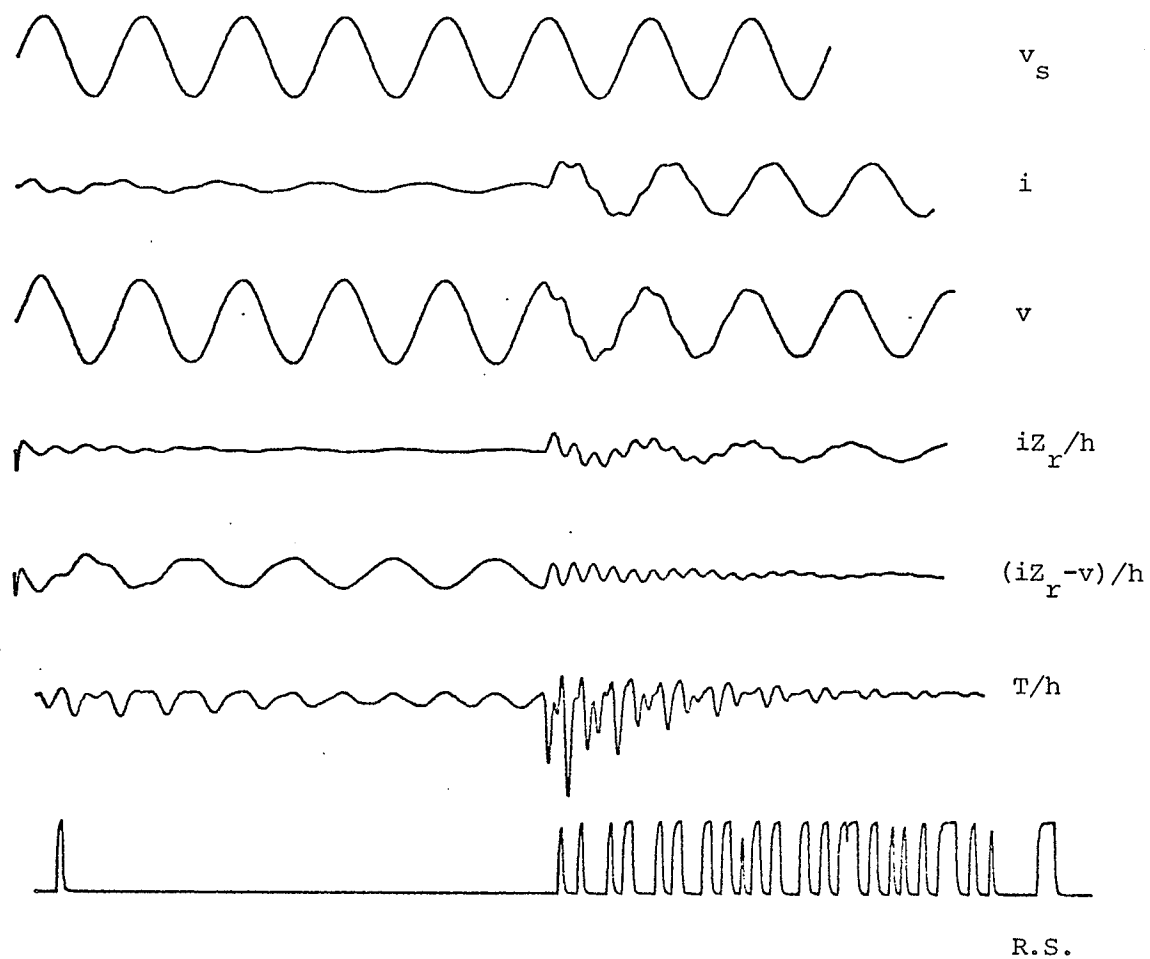


Fig. 5.2.8.3 Line capacitance considered  
 Fault incidence angle =  $90^\circ$   
 $\phi_s \neq \phi_r$   
 Relay-to-fault impedance = 1.0 line impedance



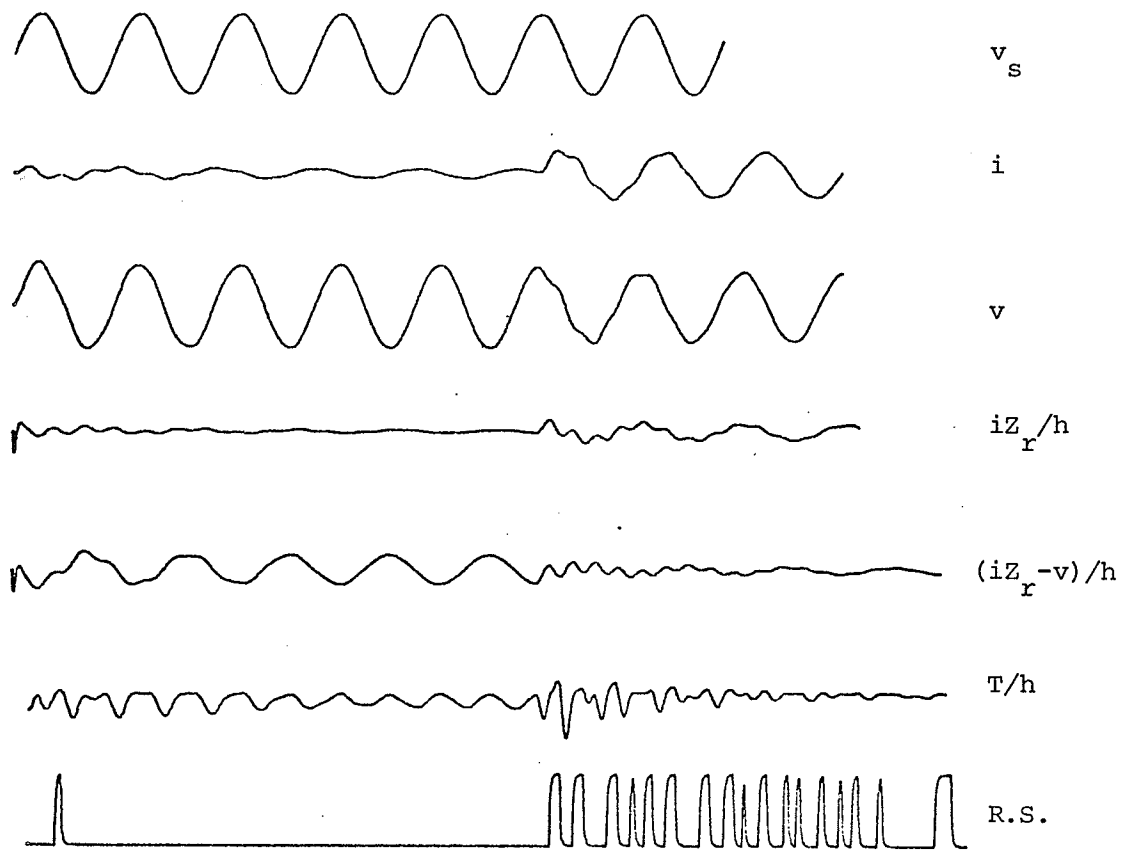


Fig. 5.2.8.4 Line capacitance considered  
 Fault incidence angle =  $90^\circ$   
 $\phi_s \neq \phi_r$   
 Relay-to-fault impedance = 1.2 line impedance

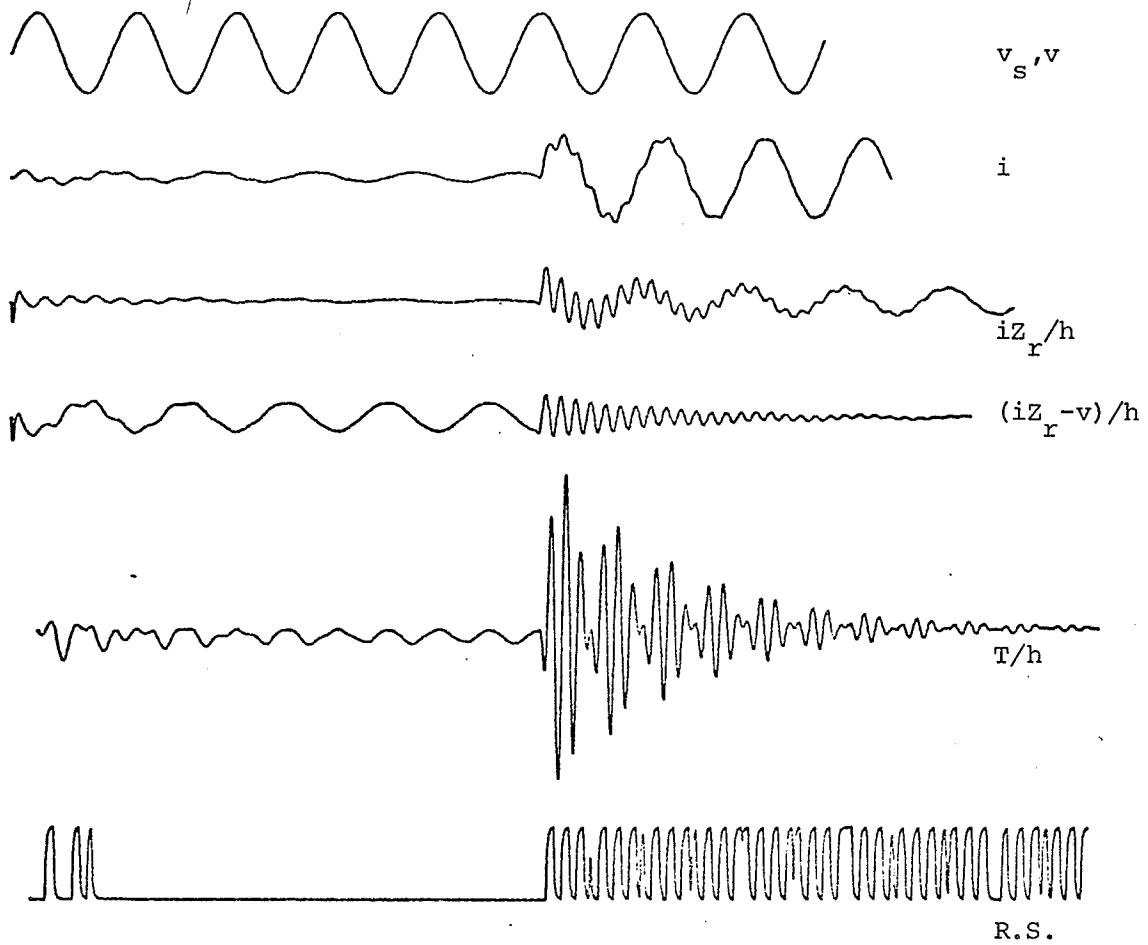


Fig. 5.2.9.1 Line capacitance considered  
 Fault incidence angle =  $90^\circ$   
 $Z_s$  neglected  
 Relay-to-fault impedance = 0.8 line impedance

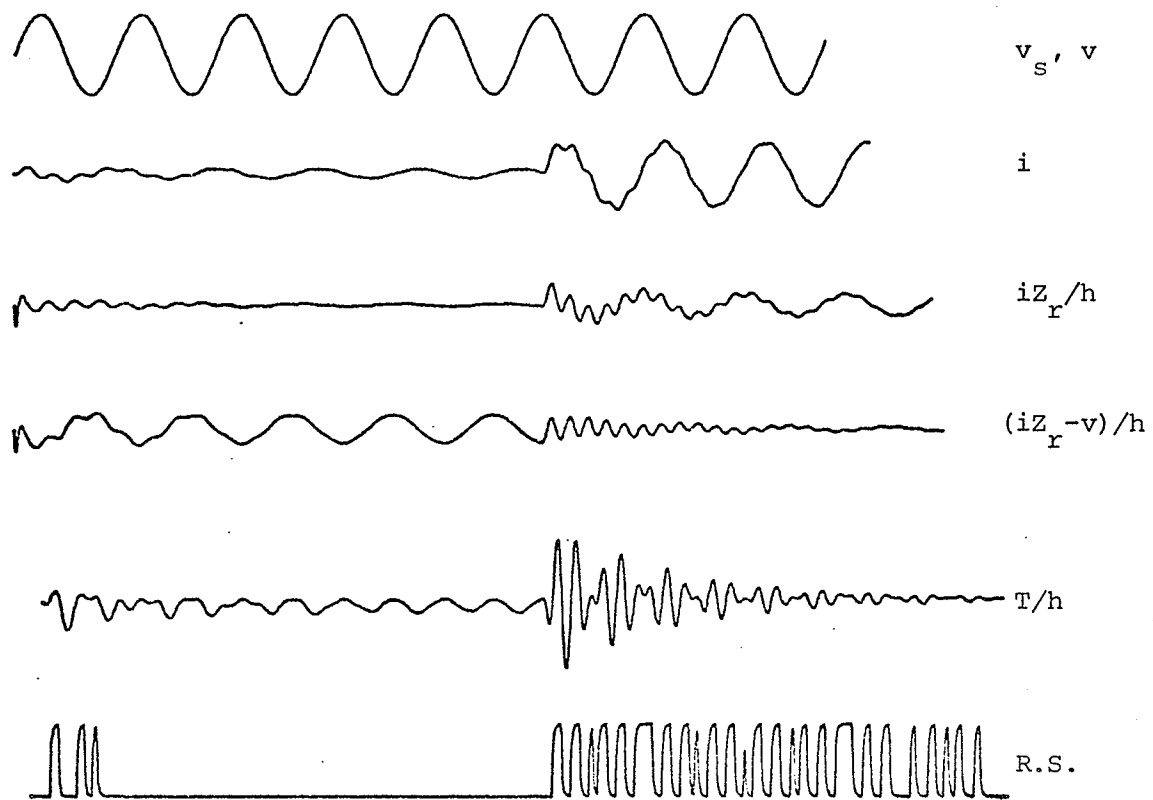


Fig. 5.2.9.2 Line capacitance considered  
 Fault incidence angle =  $90^\circ$   
 $Z_s$  neglected  
 Relay-to-fault impedance = 1.0 line impedance

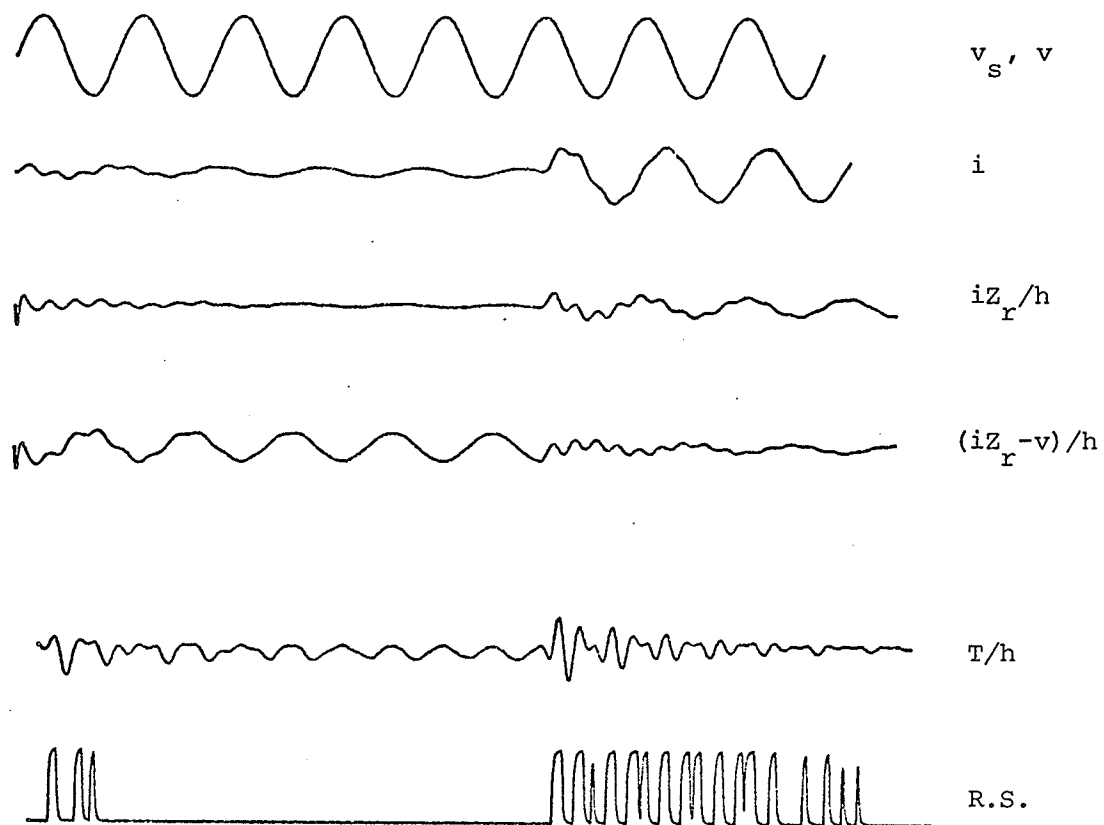


Fig. 5.2.9.3 Line capacitance considered  
 Fault incidence angle =  $90^\circ$   
 $Z_s$  neglected  
 Relay-to-fault impedance = 1.2 line impedance

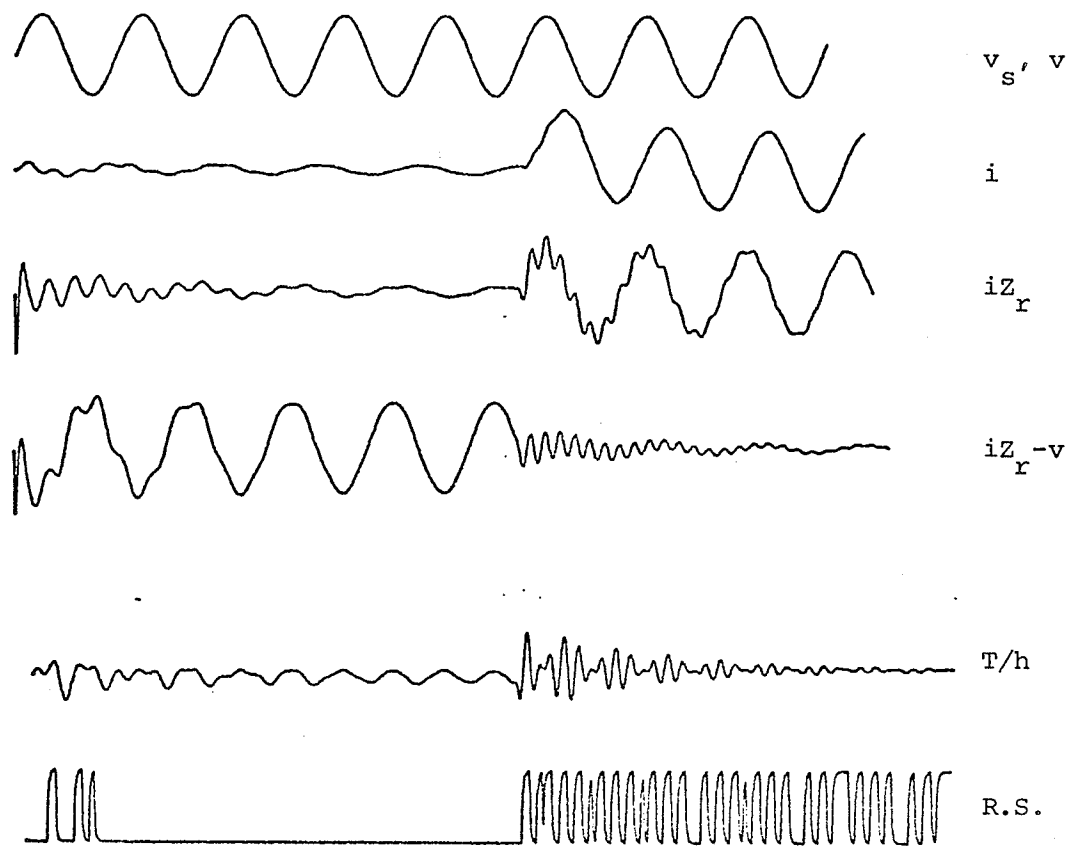


Fig. 5.2.10.1 Line capacitance considered  
 Fault incidence angle =  $0^\circ$   
 $Z_s$  neglected  
 Relay-to-fault impedance = 0.8 line impedance

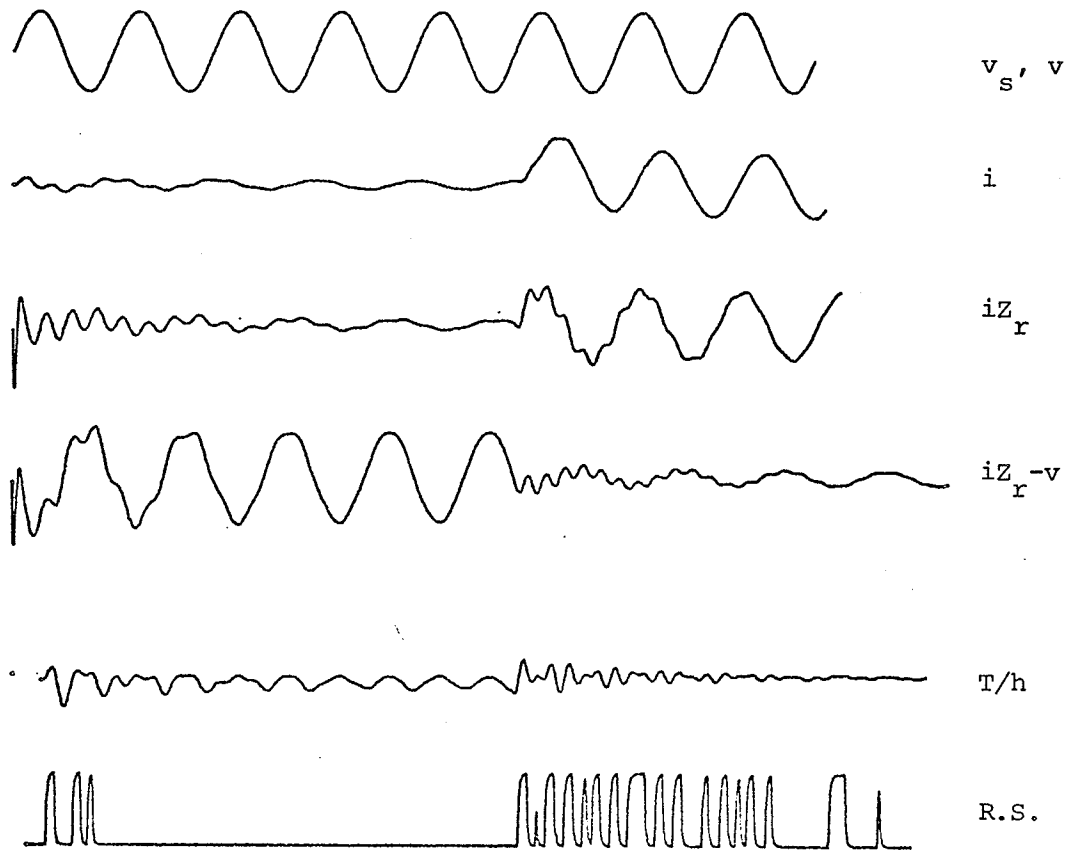


Fig. 5.2.10.2 Line capacitance considered  
 Fault incidence angle =  $0^\circ$   
 $Z_s$  neglected  
 Relay-to-fault impedance = 1.0 line impedance

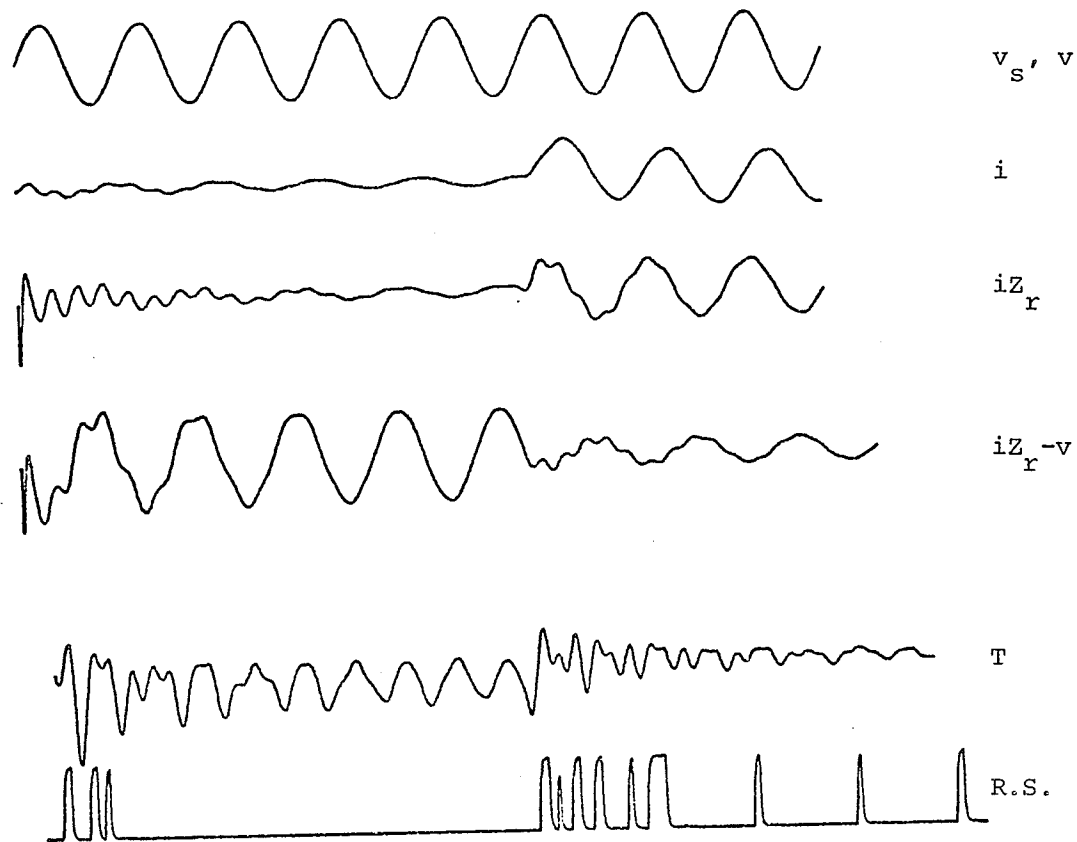


Fig. 5.2.10.3 Line capacitance considered  
Fault incidence angle =  $0^\circ$   
 $Z_s$  neglected  
Relay-to-fault impedance = 1.2 line impedance

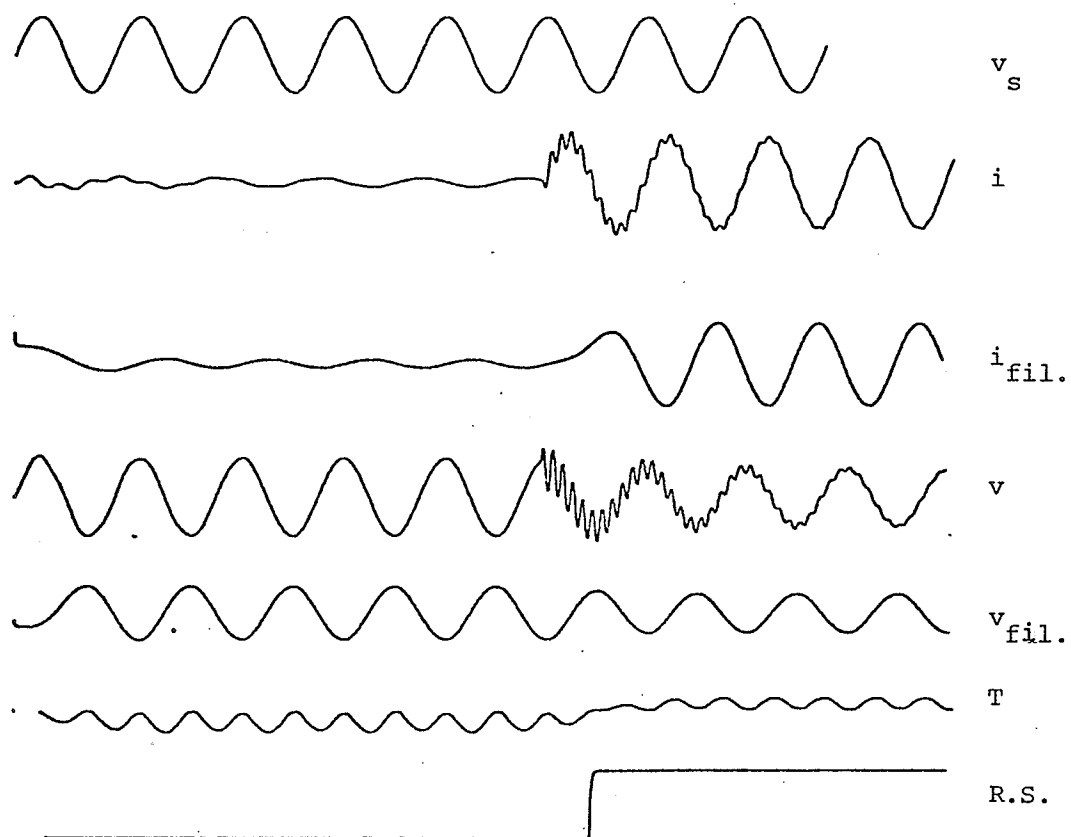


Fig. 5.3.1.1 Line capacitance considered  
 Fault incidence angle =  $90^\circ$   
 $\phi_s = \phi_r$   
 Relaying current and voltage are filtered  
 Relay-to-fault impedance = 0.5 line impedance



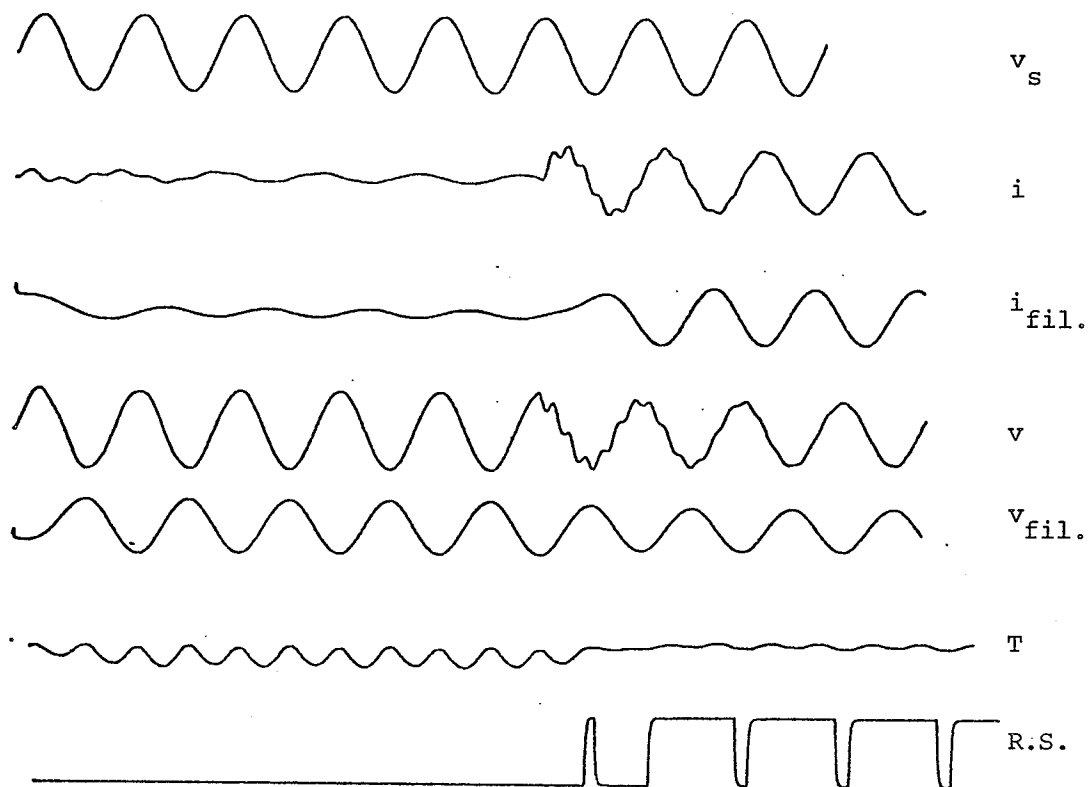


Fig. 5.3.1.2 Line capacitance considered  
 Fault incidence angle =  $90^\circ$   
 $\phi_s = \phi_r$   
 Relaying current and voltage are filtered  
 Relay-to-fault impedance = 0.8 line impedance

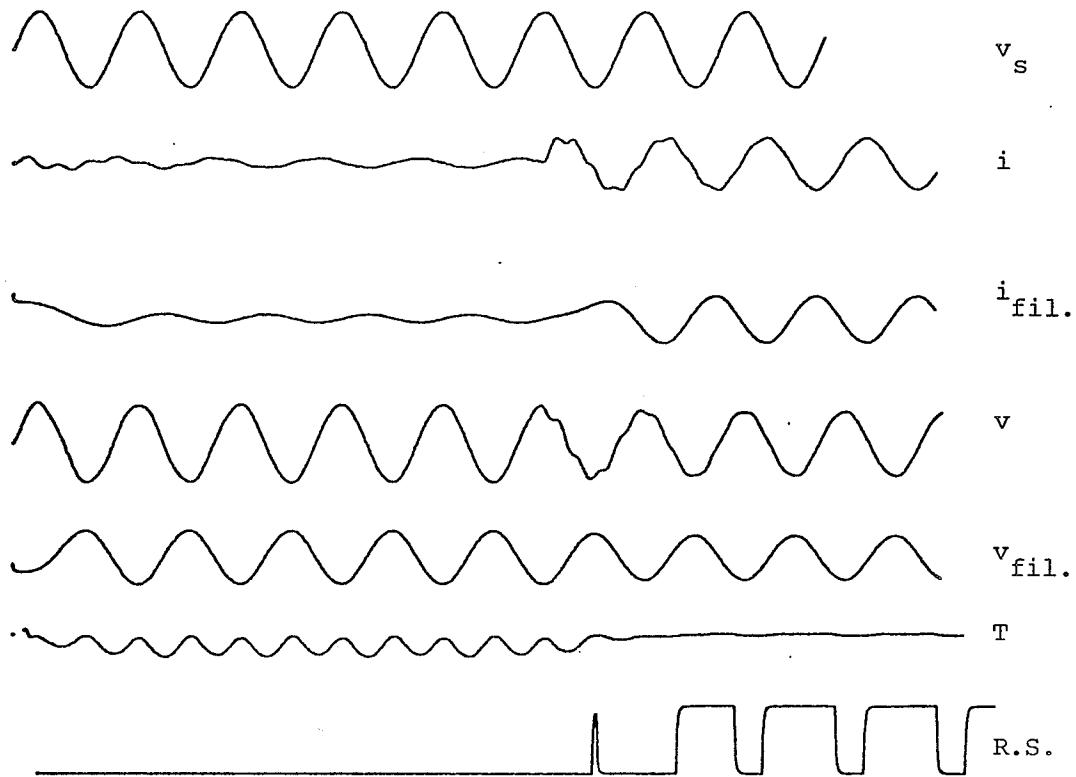


Fig. 5.3.1.3 Line capacitance considered  
 Fault incidence angle =  $90^\circ$   
 $\phi_s = \phi_r$   
 Relaying current and voltage are filtered  
 Relay-to-fault impedance = 1.0 line impedance .

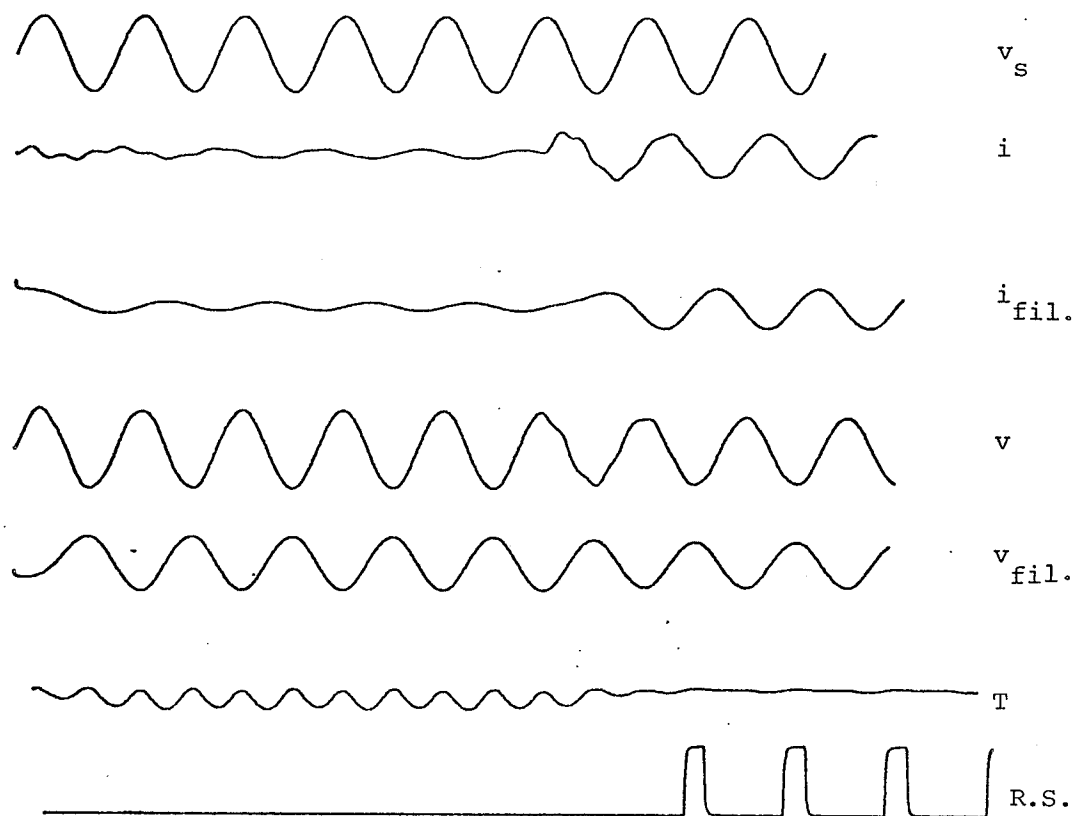


Fig. 5.3.1.4 Line capacitance considered  
Fault incidence angle =  $90^\circ$   
 $\phi_s = \phi_r$   
Relaying current and voltage are filtered  
Relay-to-fault impedance = 1.2 line impedance

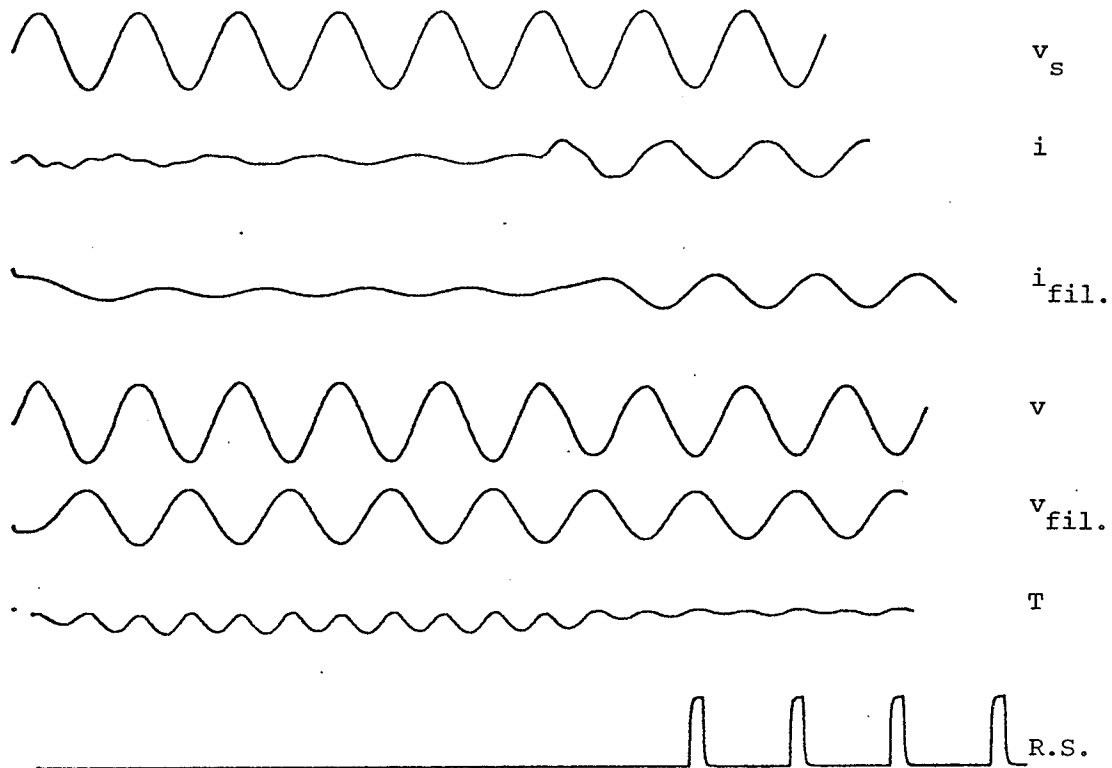


Fig. 5.3.1.5 Line capacitance considered  
 Fault incidence angle =  $90^\circ$   
 $\phi_s = \phi_r$   
 Relaying current and voltage are filtered  
 Relay-to-fault impedance = 1.5 line impedance

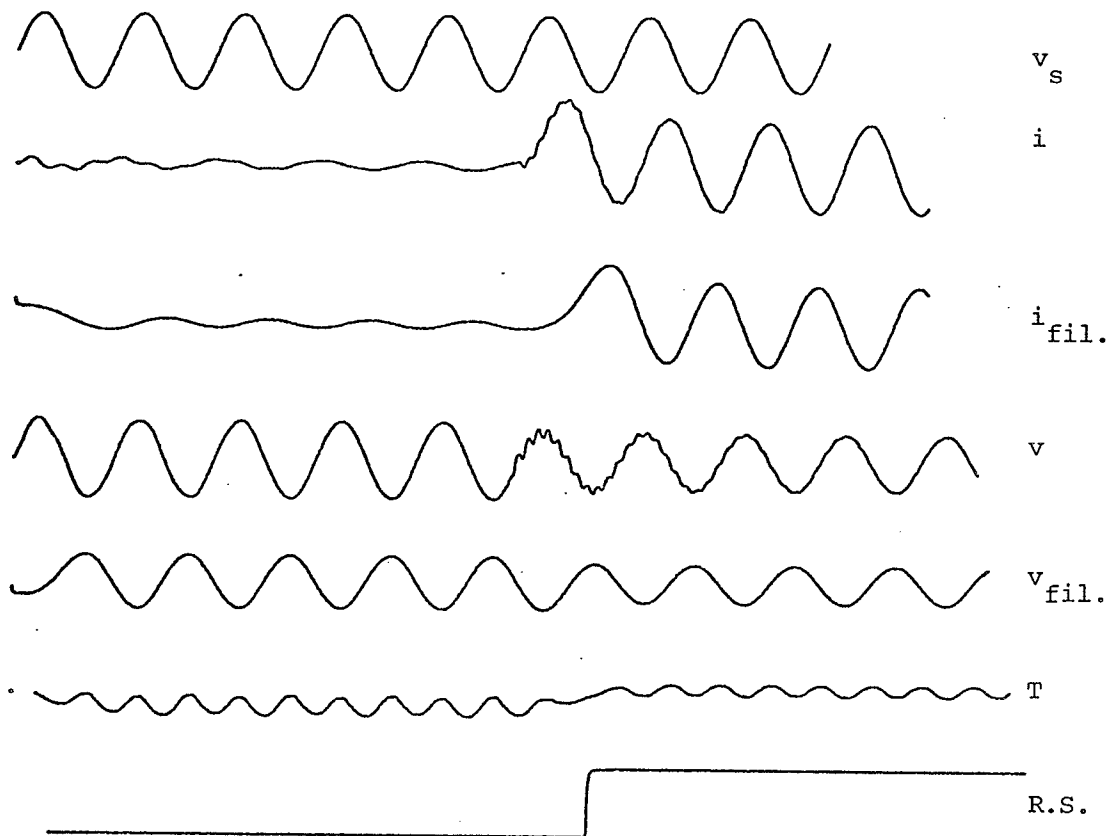


Fig. 5.3.2.1 Line capacitance considered  
 Fault incidence angle =  $0^\circ$   
 $\phi_s = \phi_r$   
 Relaying current and voltage are filtered  
 Relay-to-fault impedance = 0.5 line impedance

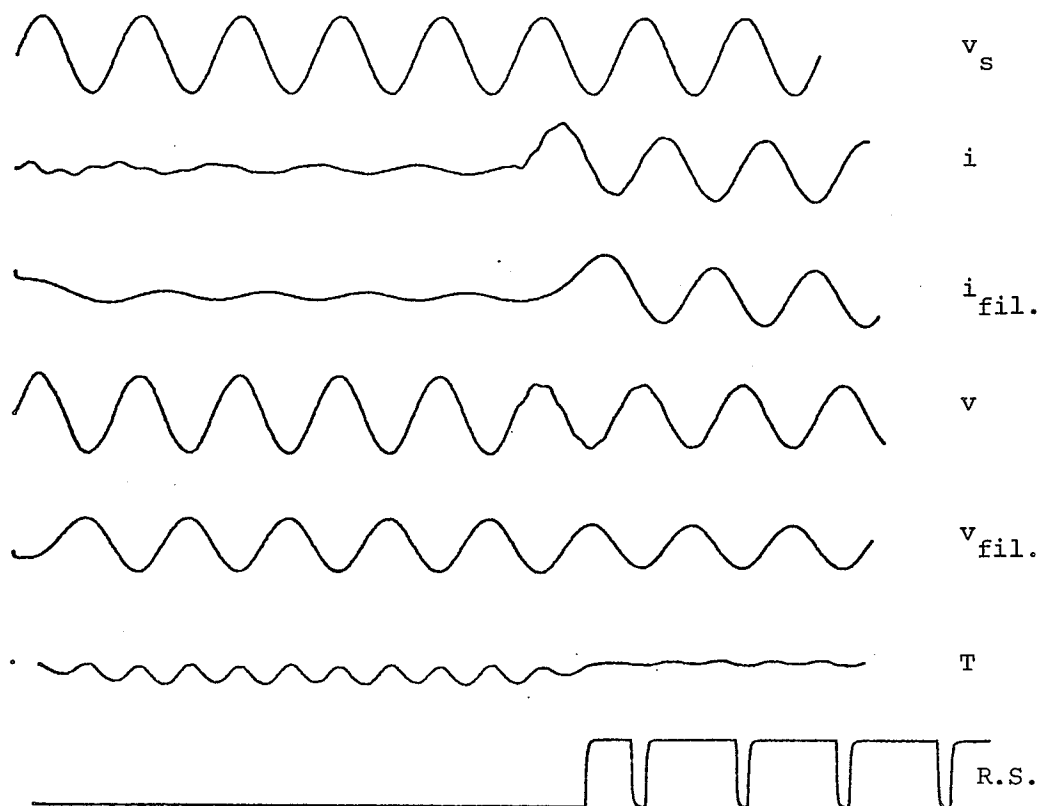


Fig. 5.3.2.2 Line capacitance considered  
 Fault incidence angle =  $0^\circ$   
 $\phi_s = \phi_r$   
 Relaying current and voltage are filtered  
 Relay-to-fault impedance = 0.8 line impedance

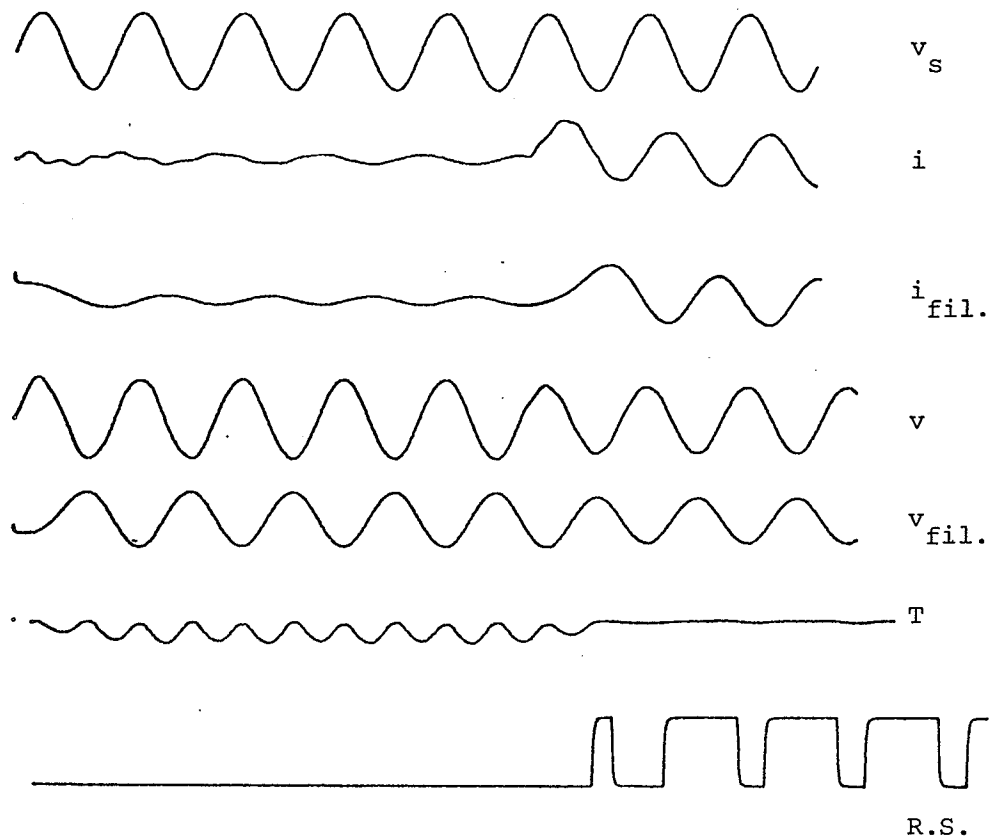


Fig. 5.3.2.3 Line capacitance considered  
 Fault incidence angle =  $0^\circ$   
 $\phi_s = \phi_r$   
 Relaying current and voltage are filtered  
 Relay-to-fault impedance = 1.0 line impedance

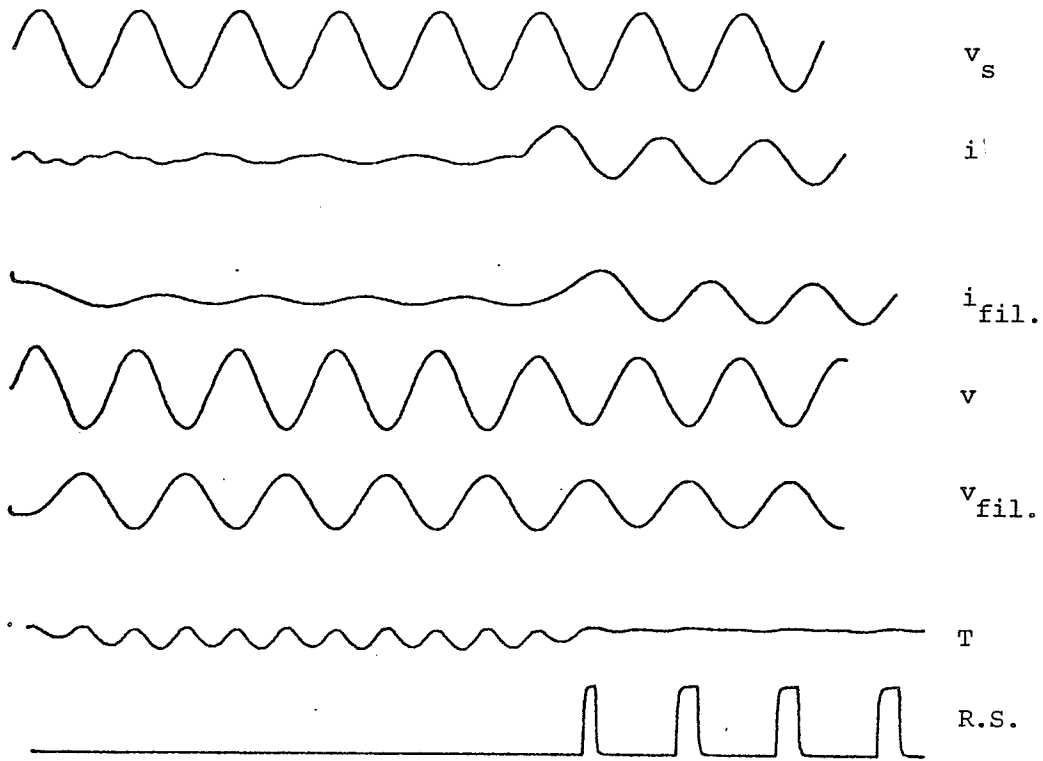


Fig. 5.3.2.4. Line capacitance considered  
 Fault incidence angle =  $0^\circ$   
 $\phi_s = \phi_r$   
 Relaying current and voltage are filtered  
 Relay-to-fault impedance = 1.2 line impedance



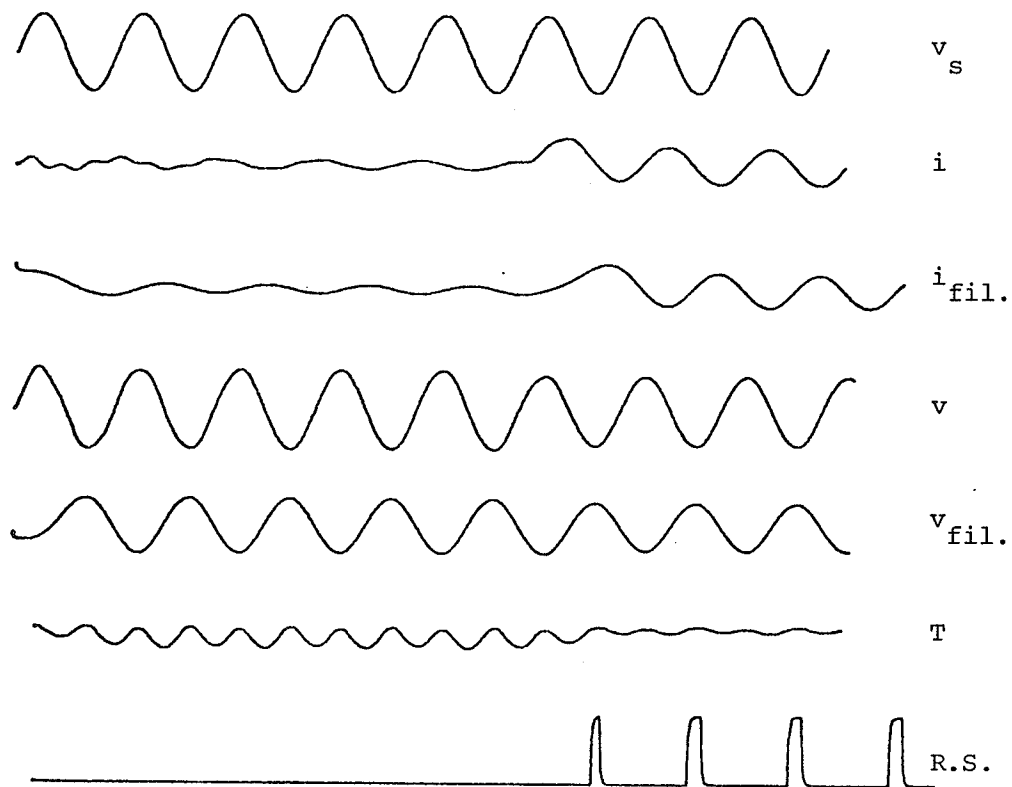


Fig. 5.3.2.5 Line capacitance considered  
 Fault incidence angle =  $0^\circ$   
 $\phi_s = \phi_r$   
 Relaying current and voltage are filtered  
 Relay-to-fault impedance = 1.5 line impedance

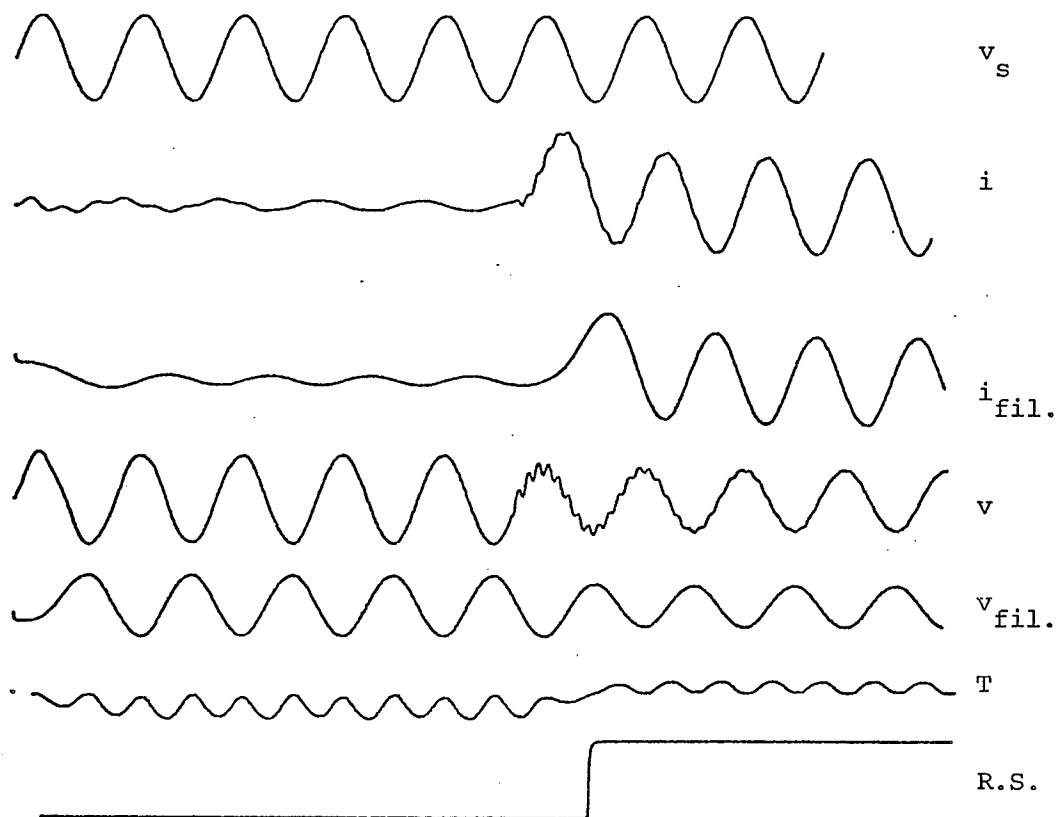


Fig. 5.3.3.1 Line capacitance considered  
Fault incidence angle =  $0^\circ$   
 $\phi_s \neq \phi_r$   
Relaying current and voltage are filtered  
Relay-to-fault impedance = 0.5 line impedance

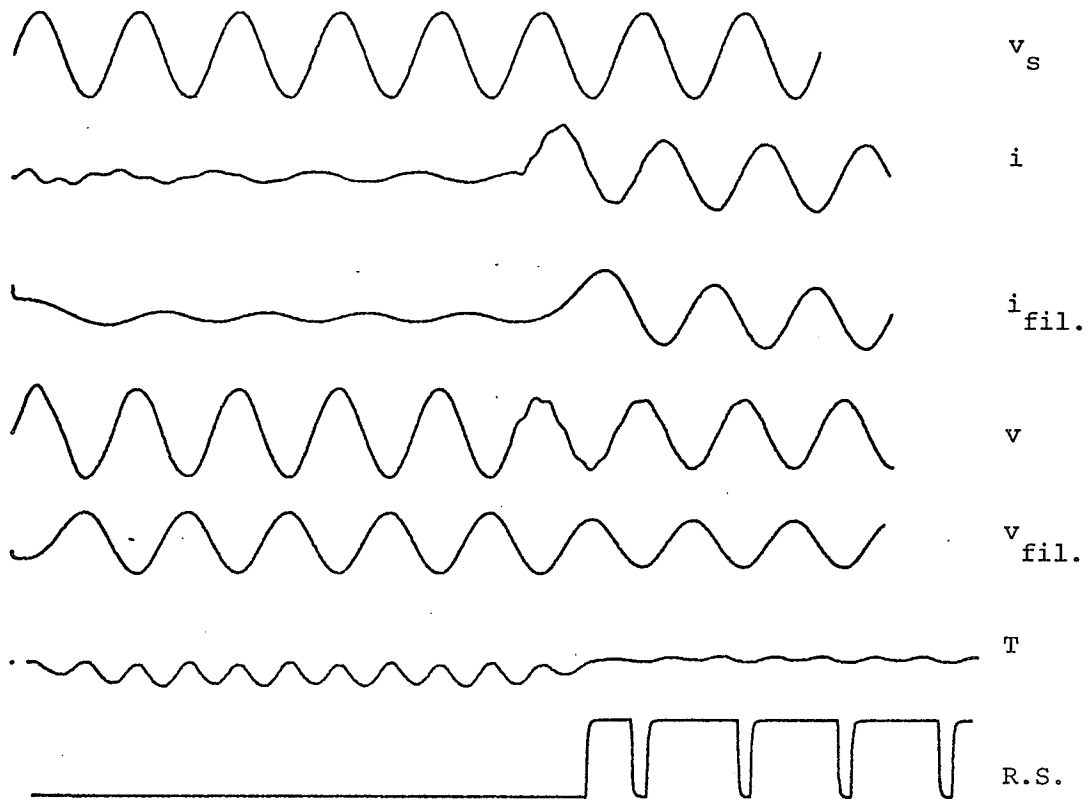


Fig. 5.3.3.2 Line capacitance considered  
 Fault incidence angle =  $0^\circ$   
 $\phi_s \neq \phi_r$   
 Relaying current and voltage are filtered  
 Relay-to-fault impedance = 0.8 line impedance

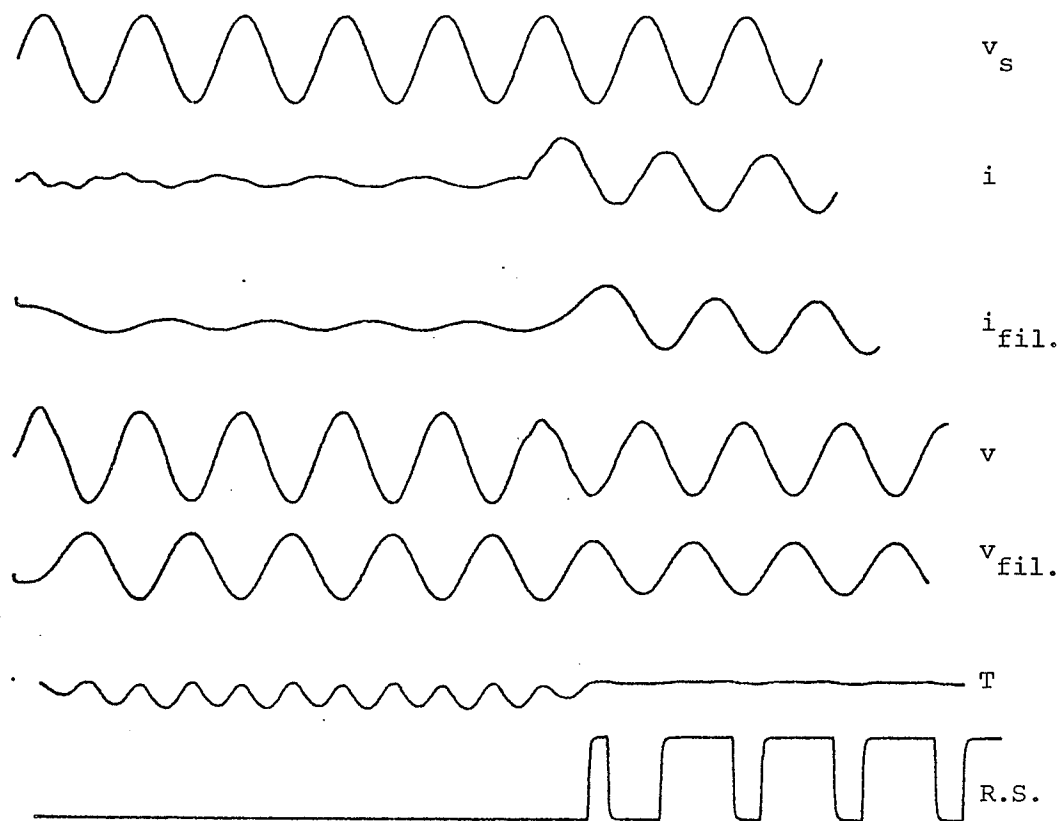


Fig. 5.3.3.3 Line capacitance considered  
 Fault incidence angle =  $0^\circ$   
 $\phi_s \neq \phi_r$   
 Relaying current and voltage are filtered  
 Relay-to-fault impedance = 1.0 line impedance

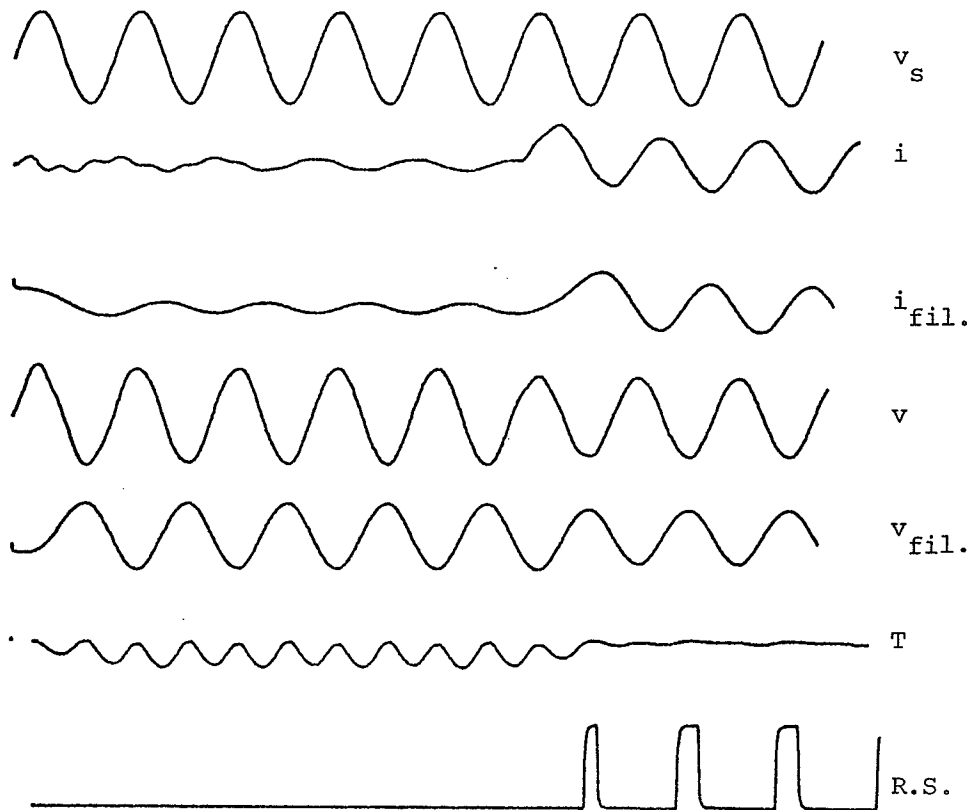


Fig. 5.3.3.4 Line capacitance considered  
 Fault incidence angle =  $0^\circ$   
 $\phi_s \neq \phi_r$   
 Relaying current and voltage are filtered  
 Relay-to-fault impedance = 1.2 line impedance

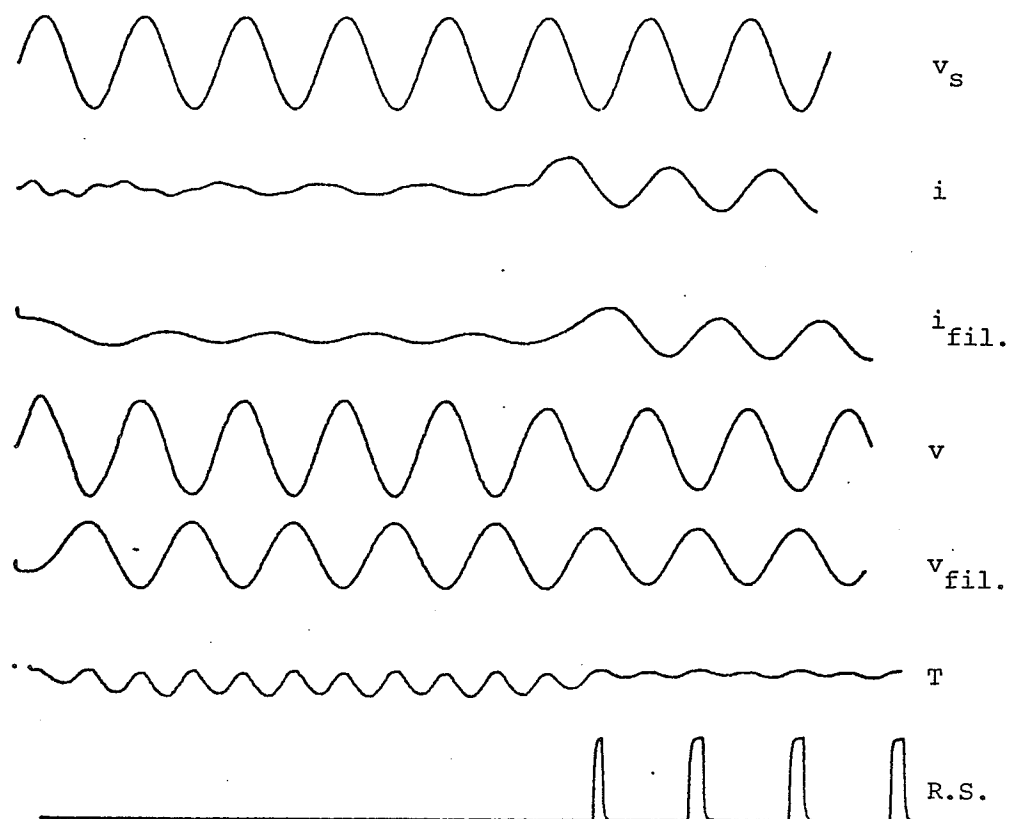


Fig. 5.3.3.5 Line capacitance considered  
 Fault incidence angle =  $0^\circ$   
 $\phi_s \neq \phi_r$   
 Relaying current and voltage are filtered  
 Relay-to-fault impedance = 1.5 line impedance

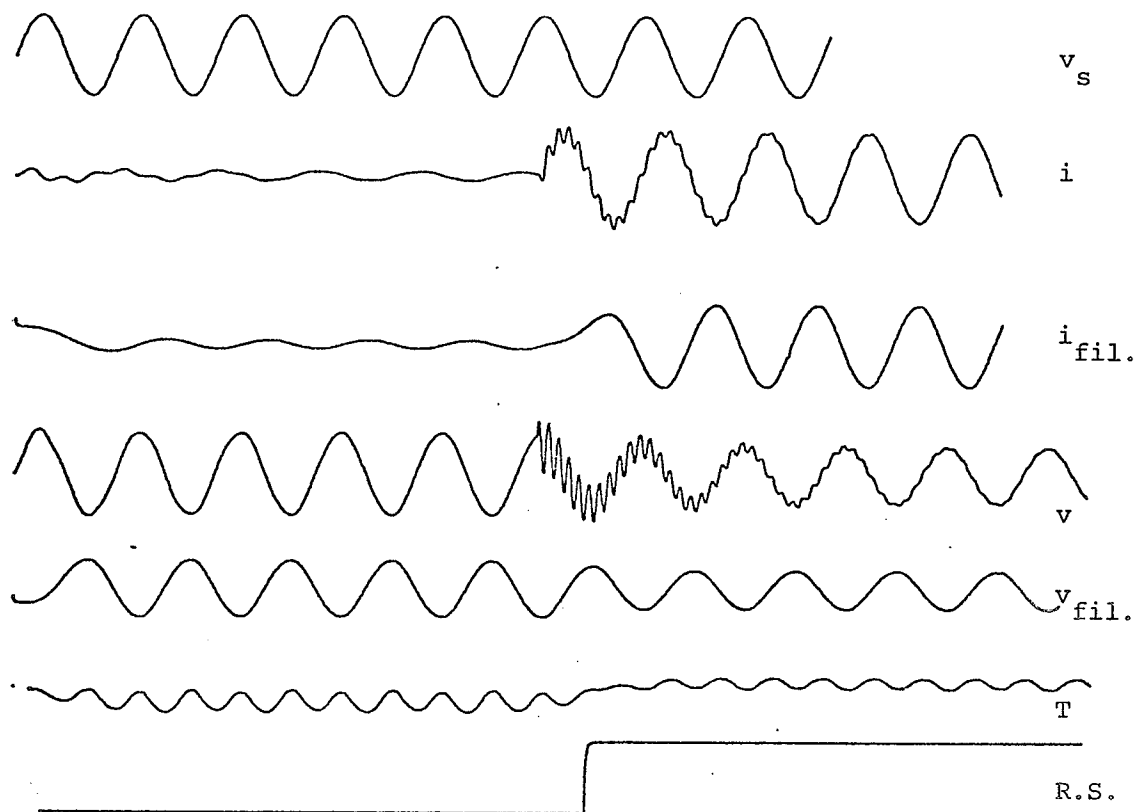


Fig. 5.3.4.1 Line capacitance considered  
 Fault incidence angle =  $90^\circ$   
 $\phi_s \neq \phi_r$   
 Relaying current and voltage are filtered  
 Relay-to-fault impedance = 0.5 line impedance

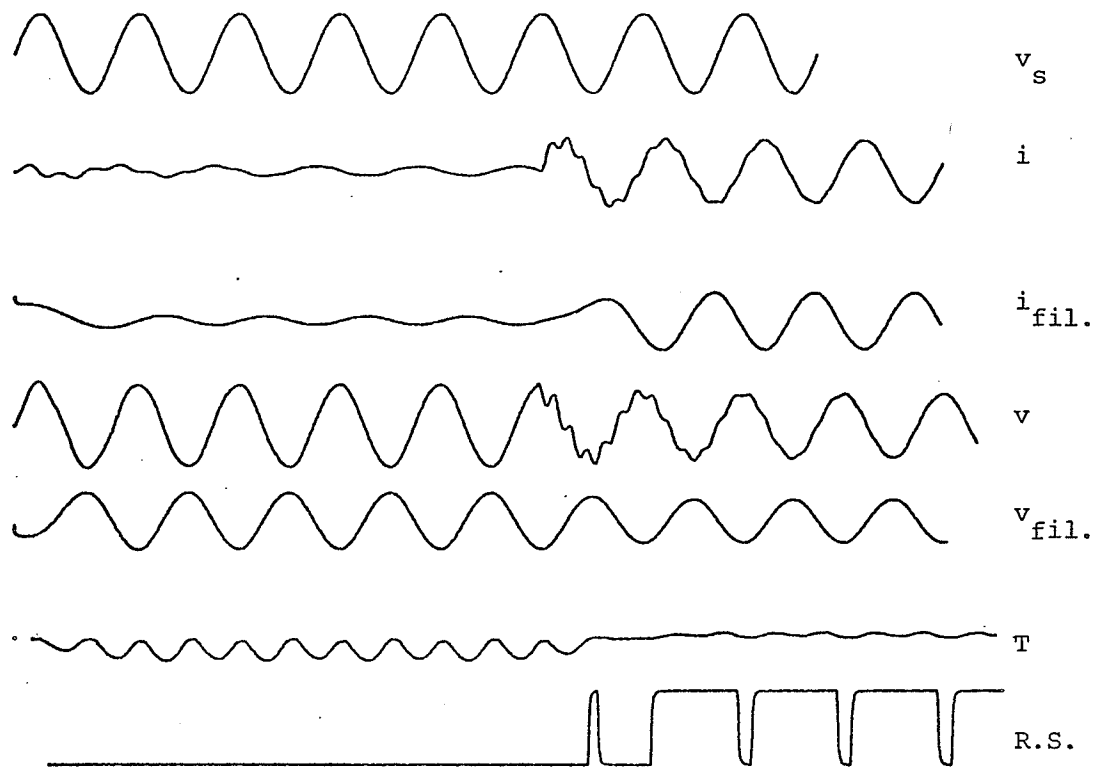


Fig. 5.3.4.2 Line capacitance considered  
 Fault incidence angle =  $90^\circ$   
 $\phi_s \neq \phi_r$   
 Relaying current and voltage are filtered  
 Relay-to-fault impedance = 0.8 line impedance



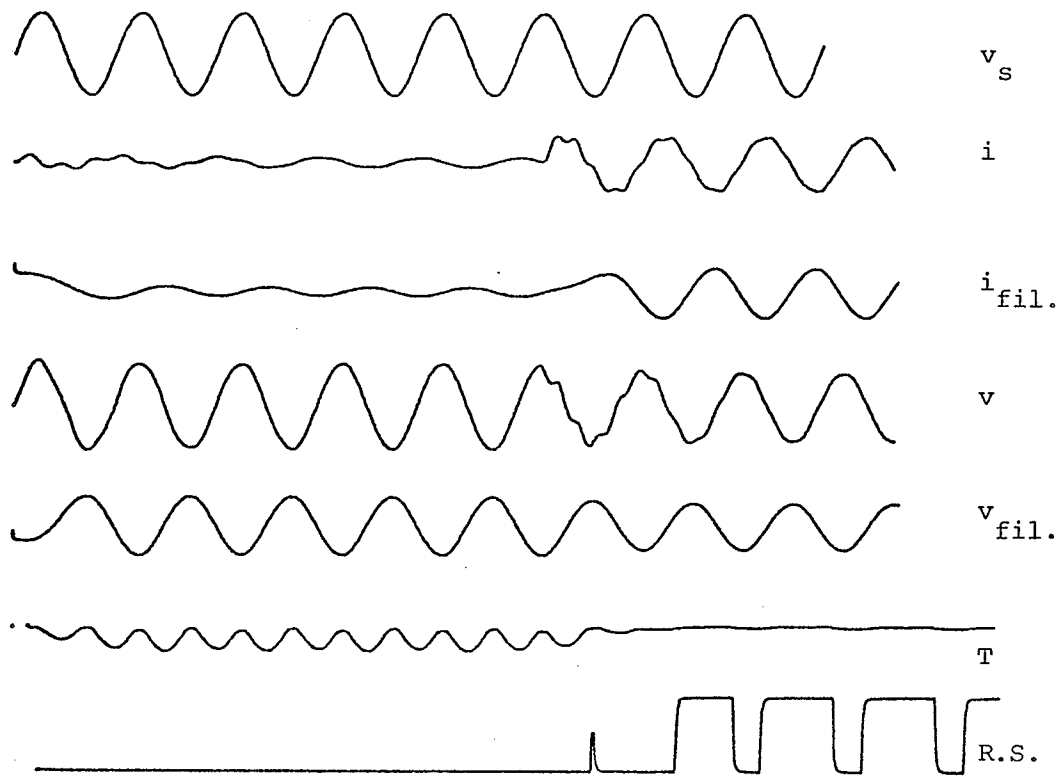


Fig. 5.3.4.3 Line capacitance considered  
 Fault incidence angle =  $90^\circ$   
 $\phi_s \neq \phi_r$   
 Relaying current and voltage are filtered  
 Relay-to-fault impedance = 1.0 line impedance

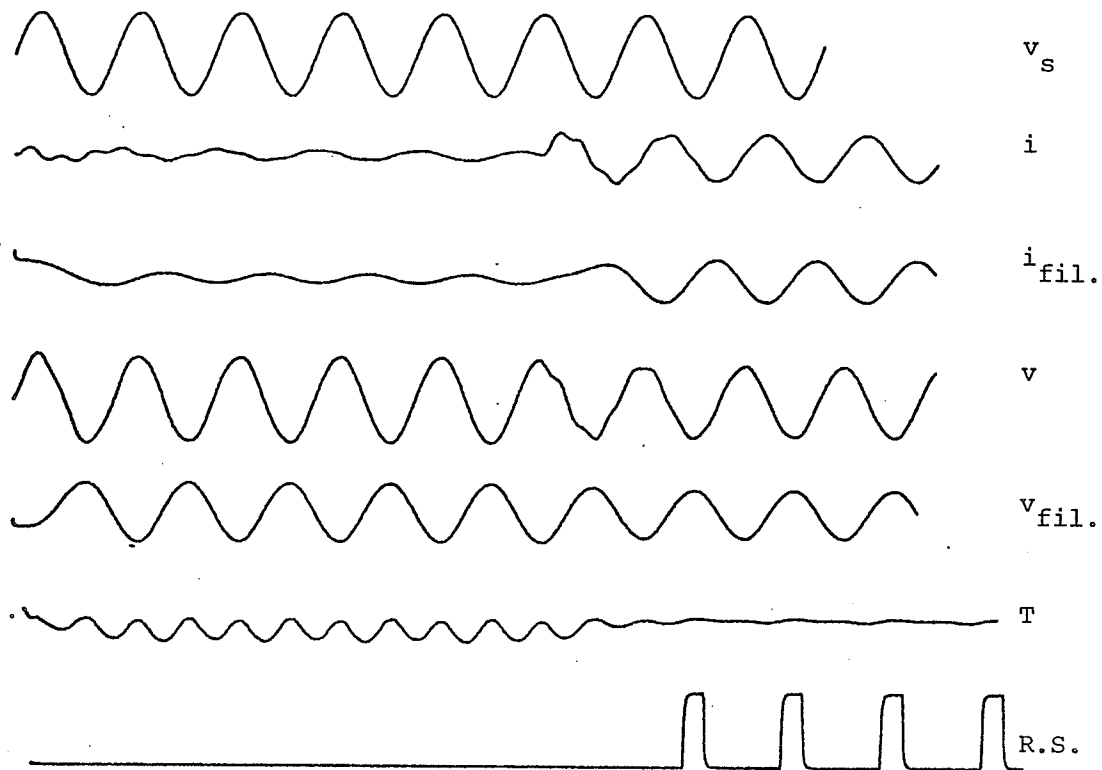


Fig. 5.3.4.4 Line capacitance considered  
 Fault incidence angle =  $90^\circ$   
 $\phi_s \neq \phi_r$   
 Relaying current and voltage are filtered  
 Relay-to-fault impedance = 1.2 line impedance

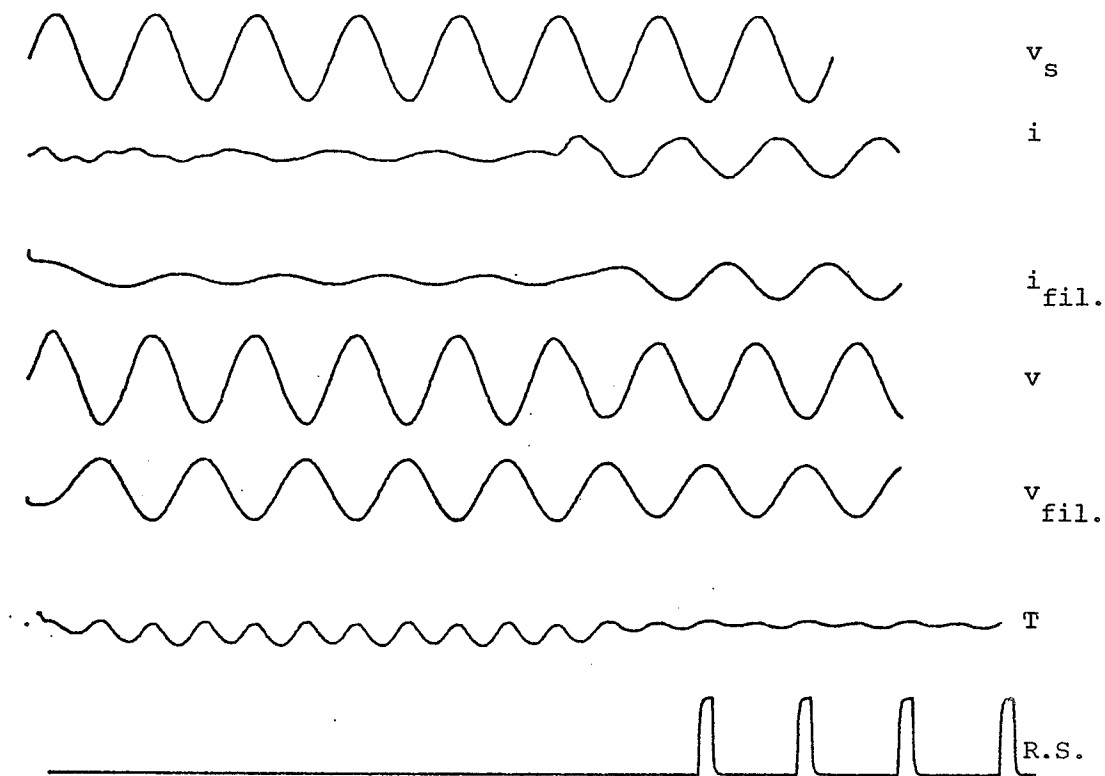


Fig. 5.3.4.5 Line capacitance considered  
 Fault incidence angle =  $90^\circ$   
 $\phi_s \neq \phi_r$   
 Relaying current and voltage are filtered  
 Relay-to-fault impedance = 1.5 line impedance

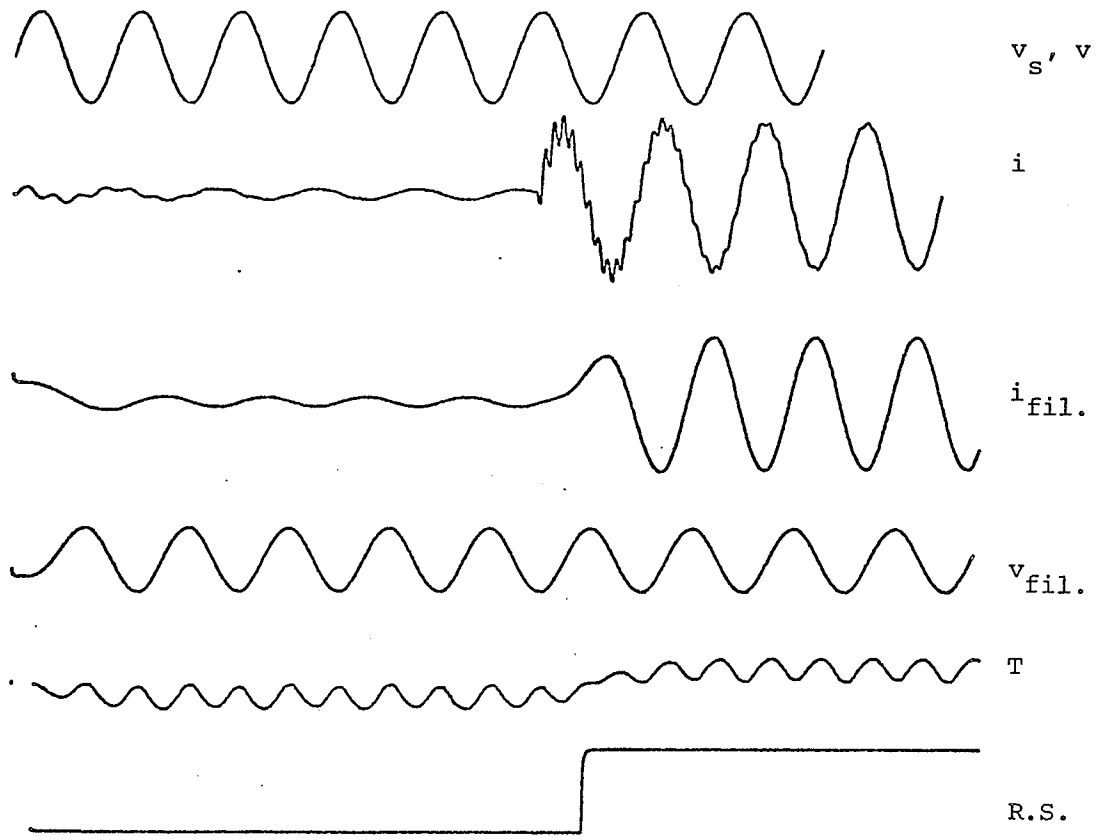


Fig. 5.3.5.1 Line capacitance considered  
 Fault incidence angle =  $90^\circ$   
 $Z_s$  neglected  
 Relaying current and voltage filtered  
 Relay-to-fault impedance = 0.5 line impedance

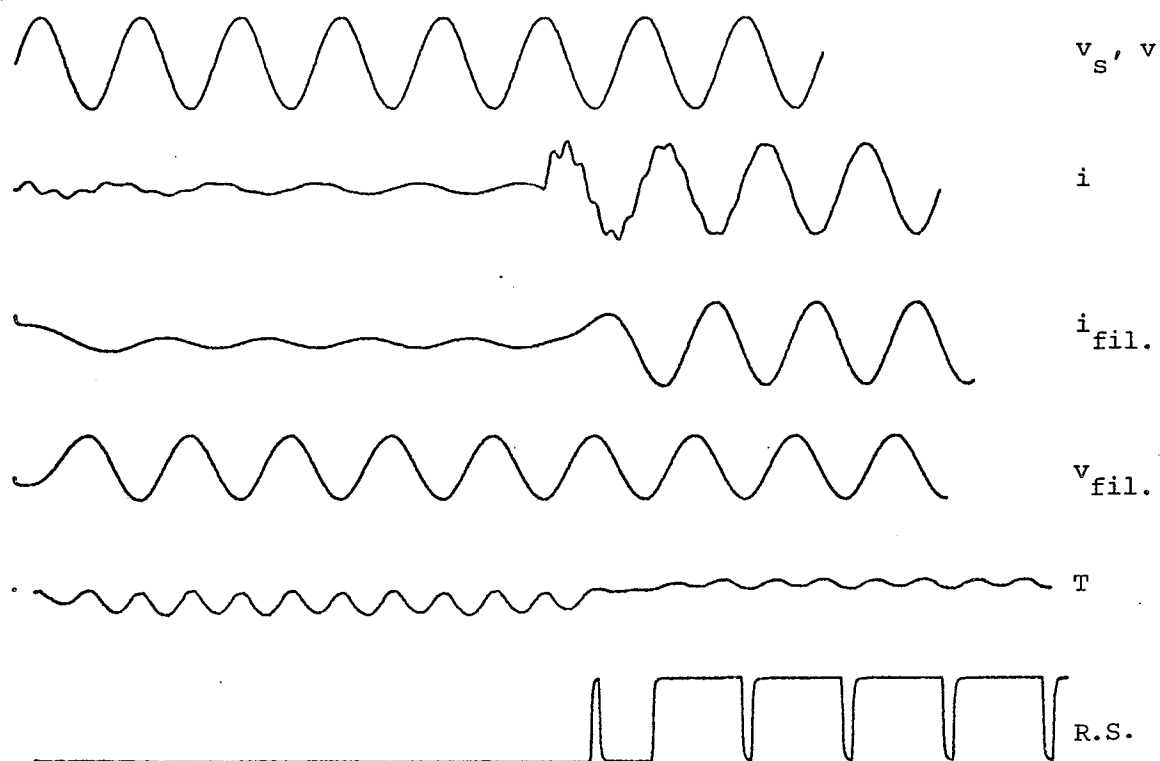


Fig. 5.3.5.2 Line capacitance considered  
Fault incidence angle =  $90^\circ$   
 $Z_s$  neglected  
Relaying current and voltage filtered  
Relay-to-fault impedance = 0.8 line impedance

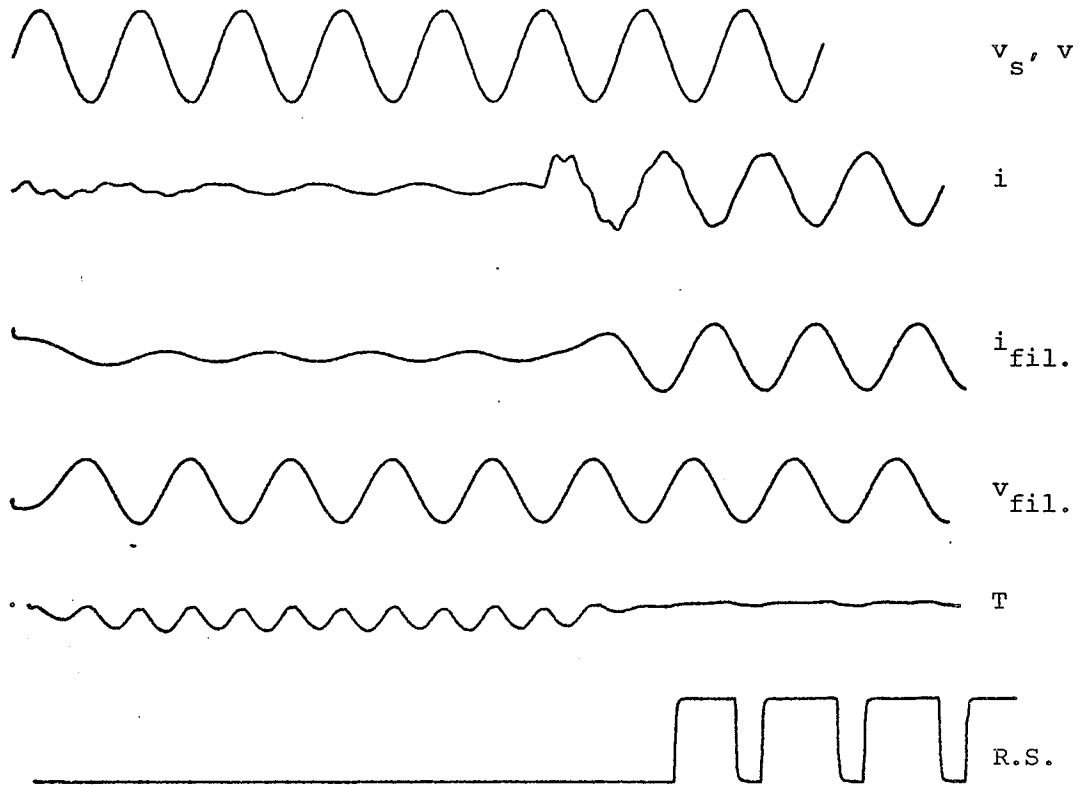


Fig. 5.3.5.3 Line capacitance considered  
 Fault incidence angle =  $90^\circ$   
 $Z_s$  neglected  
 Relaying current and voltage filtered  
 Relay-to-fault impedance = 1.0 line impedance

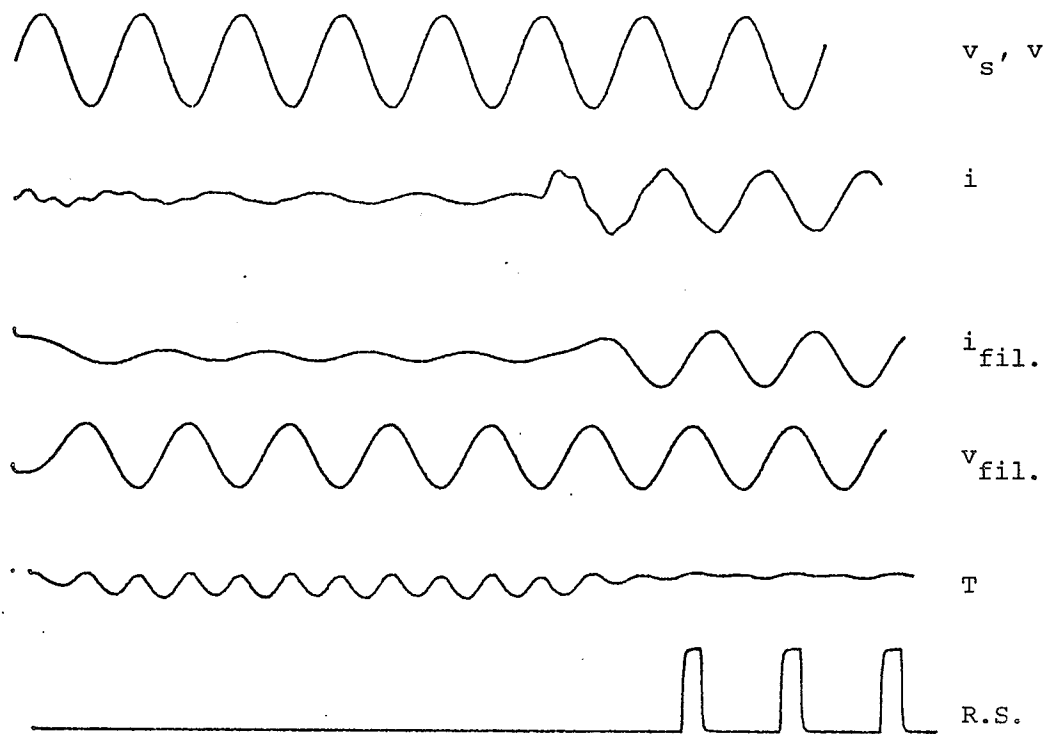


Fig.5.3.5.4 Line capacitance considered  
 Fault incidence angle =  $90^\circ$   
 $Z_s$  neglected  
 Relaying current and voltage filtered  
 Relay-to-fault impedance = 1.2 line impedance

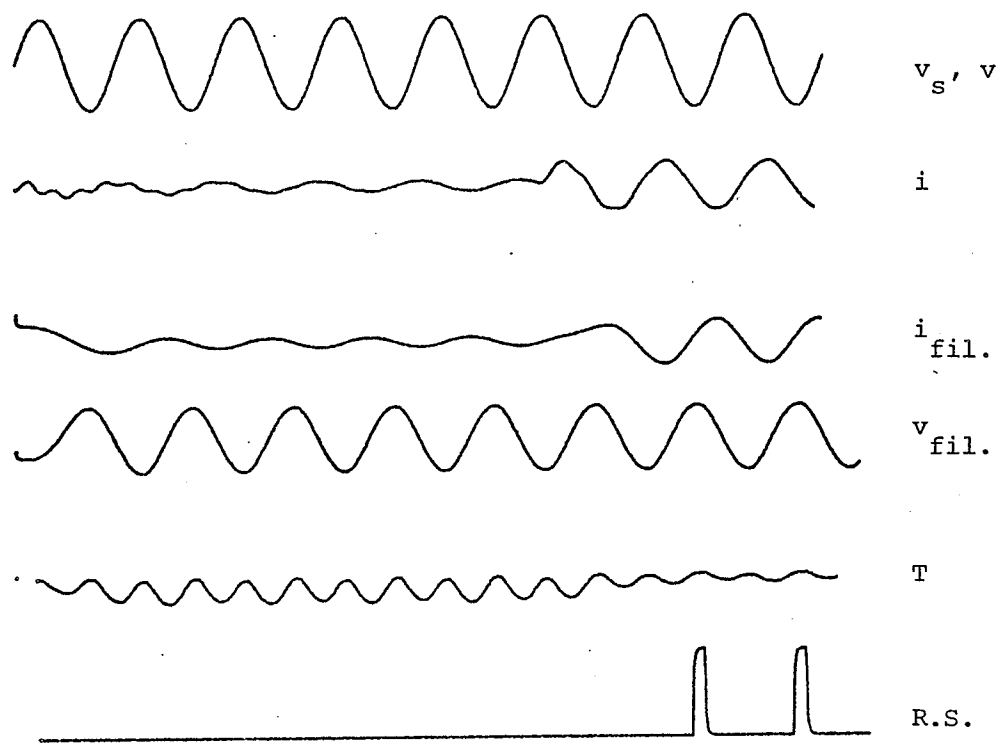


Fig. 5.3.5.5 Line capacitance considered  
Fault incidence angle =  $90^\circ$   
 $Z_s$  neglected  
Relaying current and voltage filtered  
Relay-to-fault impedance = 1.5 line impedance



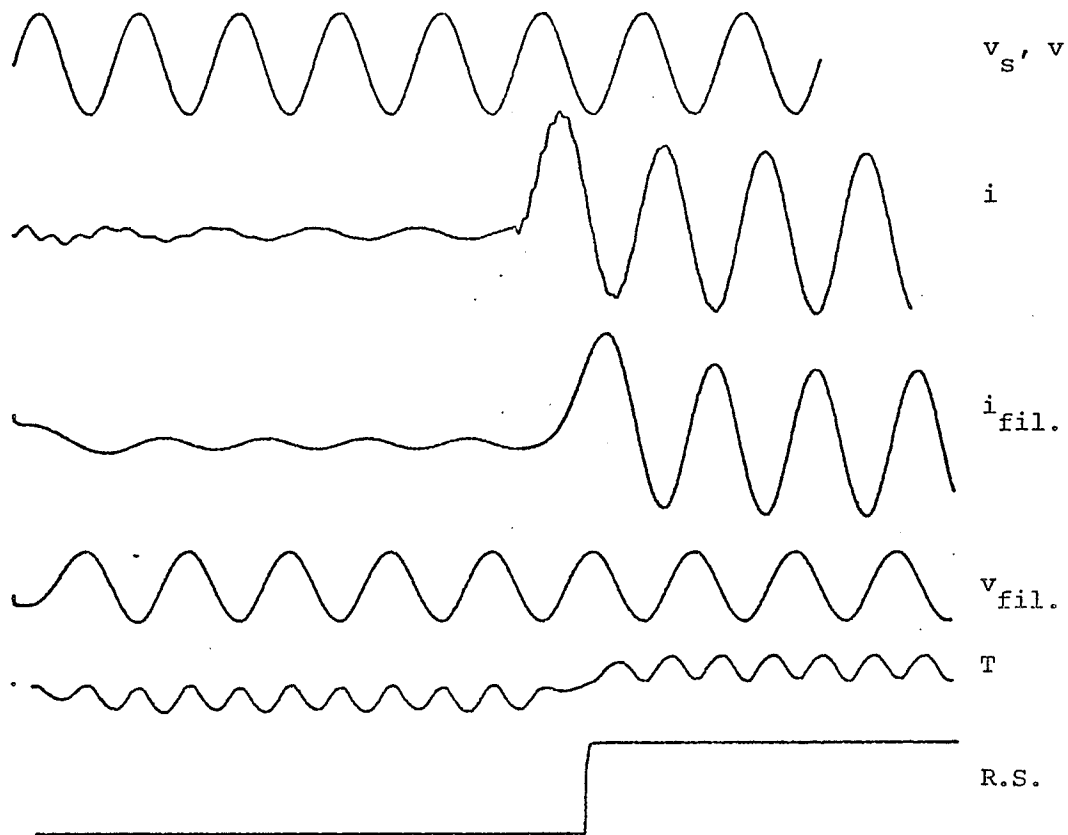


Fig. 5.3.6.1 Line capacitance considered  
 Fault incidence angle =  $0^\circ$   
 $Z_s$  neglected  
 Relaying current and voltage filtered  
 Relay-to-fault impedance = 0.5 line impedance

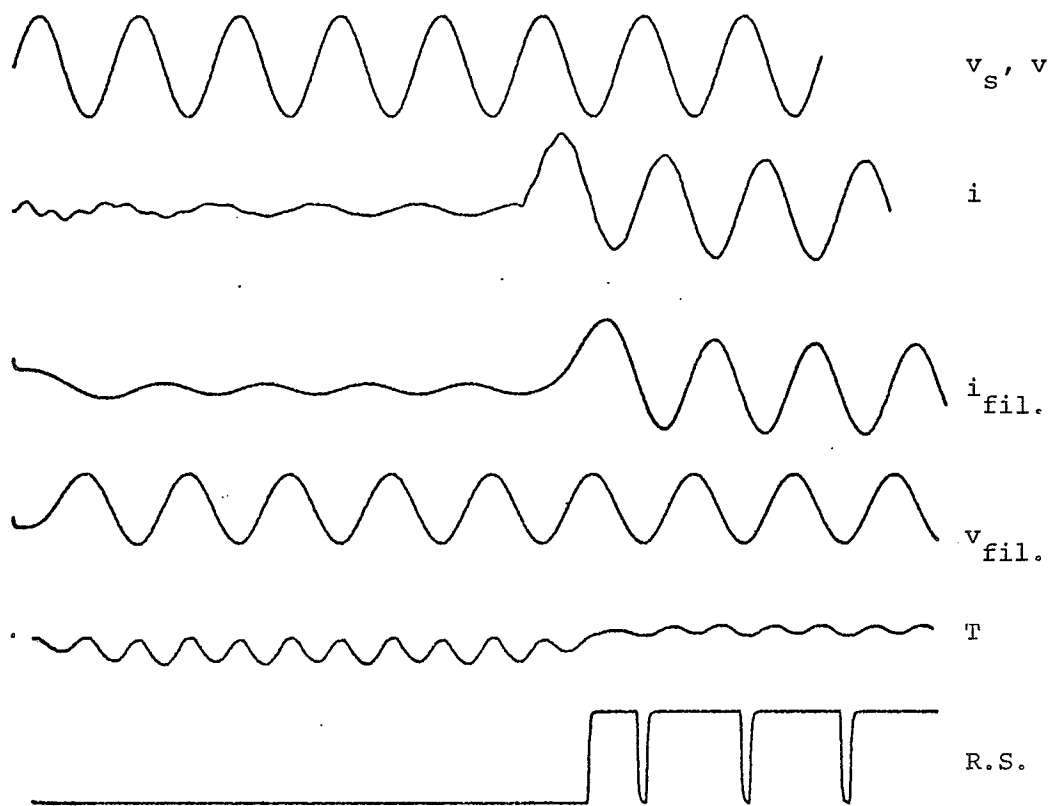


Fig. 5.3.6.2 Line capacitance considered  
 Fault incidence angle =  $0^\circ$   
 $Z_s$  neglected  
 Relaying current and voltage filtered  
 Relay-to-fault impedance = 0.8 line impedance

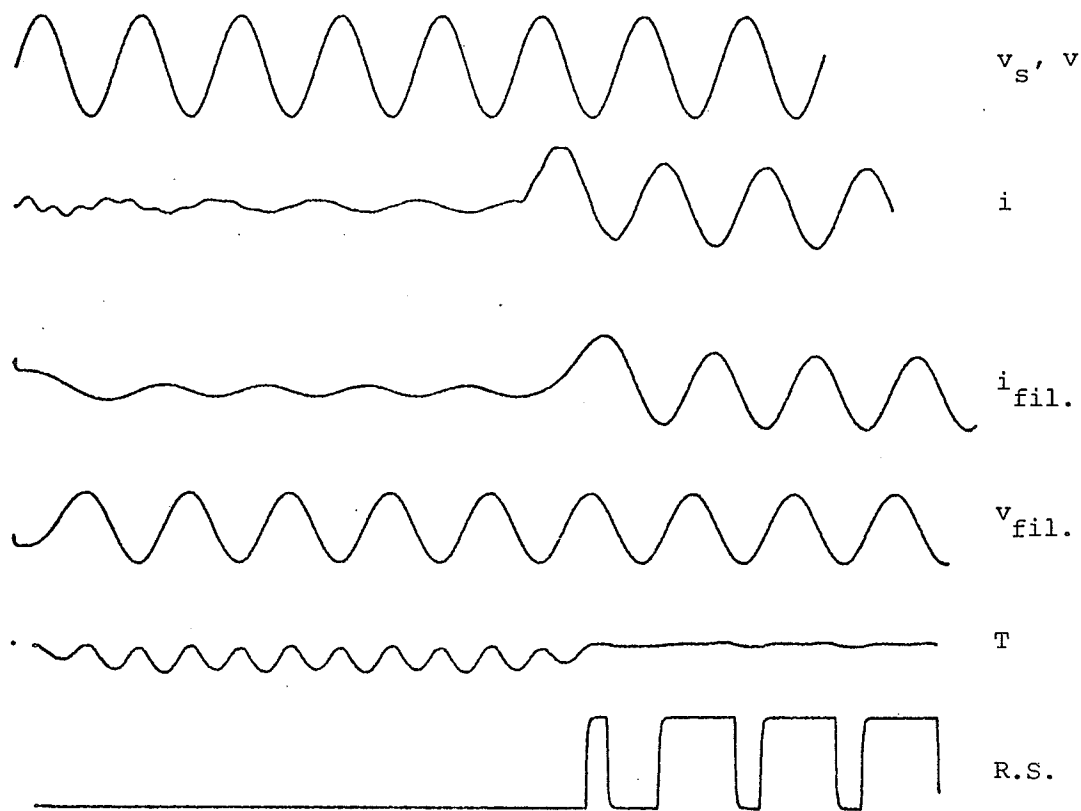


Fig. 5.3.6.3 Line capacitance considered  
 Fault incidence angle =  $0^\circ$   
 $Z_s$  neglected  
 Relaying current and voltage filtered  
 Relay-to-fault impedance = 1.0 line impedance

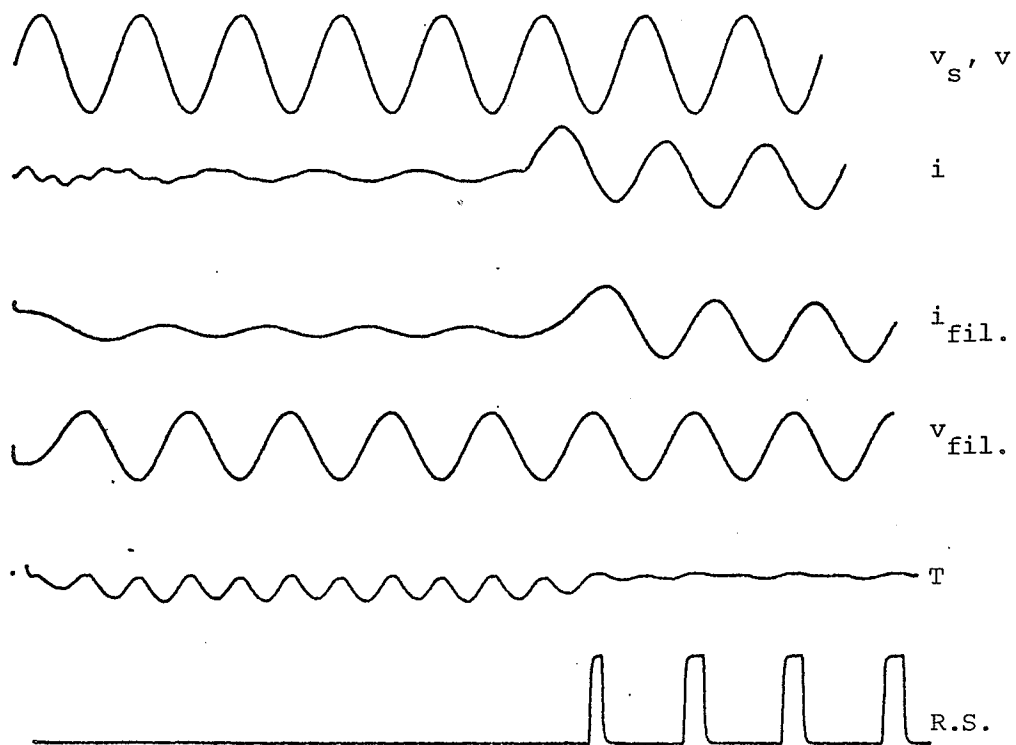


Fig. 5.3.6.4 Line capacitance considered  
 Fault incidence angle =  $0^\circ$   
 $Z_s$  neglected  
 Relaying current and voltage filtered  
 Relay-to-fault impedance = 1.2 line impedance

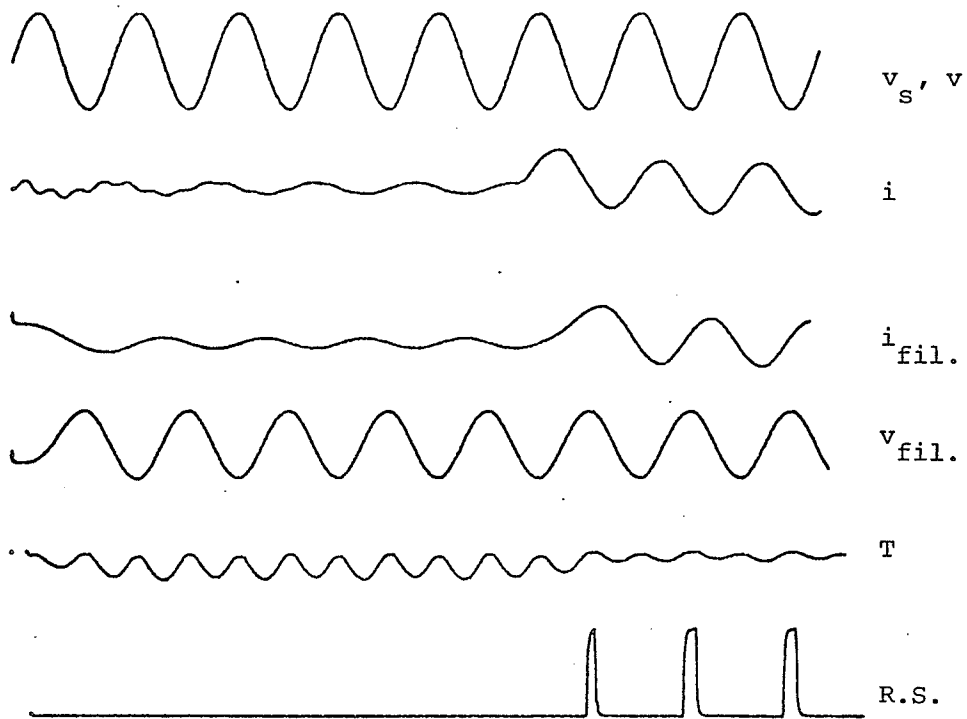


Fig. 5.3.6.5 Line capacitance considered  
Fault incidence angle =  $0^\circ$   
 $Z_s$  neglected  
Relaying current and voltage filtered  
Relay-to-fault impedance = 1.5 line impedance

## CHAPTER 6

### ANALOG REALIZATION OF THE EXPERIMENTAL RELAY USING INTEGRATORS

In Chapter 2, the experimental MHO electronic relay was realized using differentiators and because it is well known that differentiation is a noise amplifying process. It was suggested that integrators be tried in the realization of the relay.

#### 6.1 Theory

If  $S_1$  and  $S_2$  are the input signals to the comparator and if  $S_3$  is  $S_2$  but shifted by  $90^\circ$ , then the quantity

$$T = + S_1 \int S_3 dt - S_3 \int S_1 dt$$

will always have a sign depending on the phase angle between  $S_1$  and  $S_2$ .

Let

$$S_1 = A \sin \omega t$$

$$S_2 = B \sin(\omega t + \psi)$$

hence

$$S_3 = B \cos(\omega t + \psi)$$

$$S_3 \int S_1 = -B \frac{A}{\omega} \cos \omega t \cos(\omega t + \psi) + C_1$$

$$S_1 \int S_3 = \frac{AB}{\omega} \sin \omega t \sin(\omega t + \psi) + C_2$$

(Note: with proper initial conditions  $C_1$  and  $C_2$  can be made zero)

$$\begin{aligned} T &= + S_1 \int S_3 dt - S_3 \int S_1 dt \\ &= \frac{BA}{\omega} (\sin \omega t \sin(\omega t + \psi) + \cos \omega t \cos(\omega t + \psi)) \\ T &= \frac{BA}{\omega} \cos \psi \end{aligned}$$

which is the same result obtained with differentiators. However, it is clear that the result depends essentially on proper conditions for all the integrators.

## 6.2 Analog Computer Simulation

The detailed simulation is given in Fig. 6.1 for the case where the transmission line capacitance is neglected. The initial conditions for all integrators are set to zero, because the values of current and voltage at the fault instant cannot be predicted.

## 6.3 Results

Figures 6.3.1 to 6.3.4 show the relay response for faults outside and within its setting for different fault incidence angles. Note that in all cases the relay trips prior to the fault.

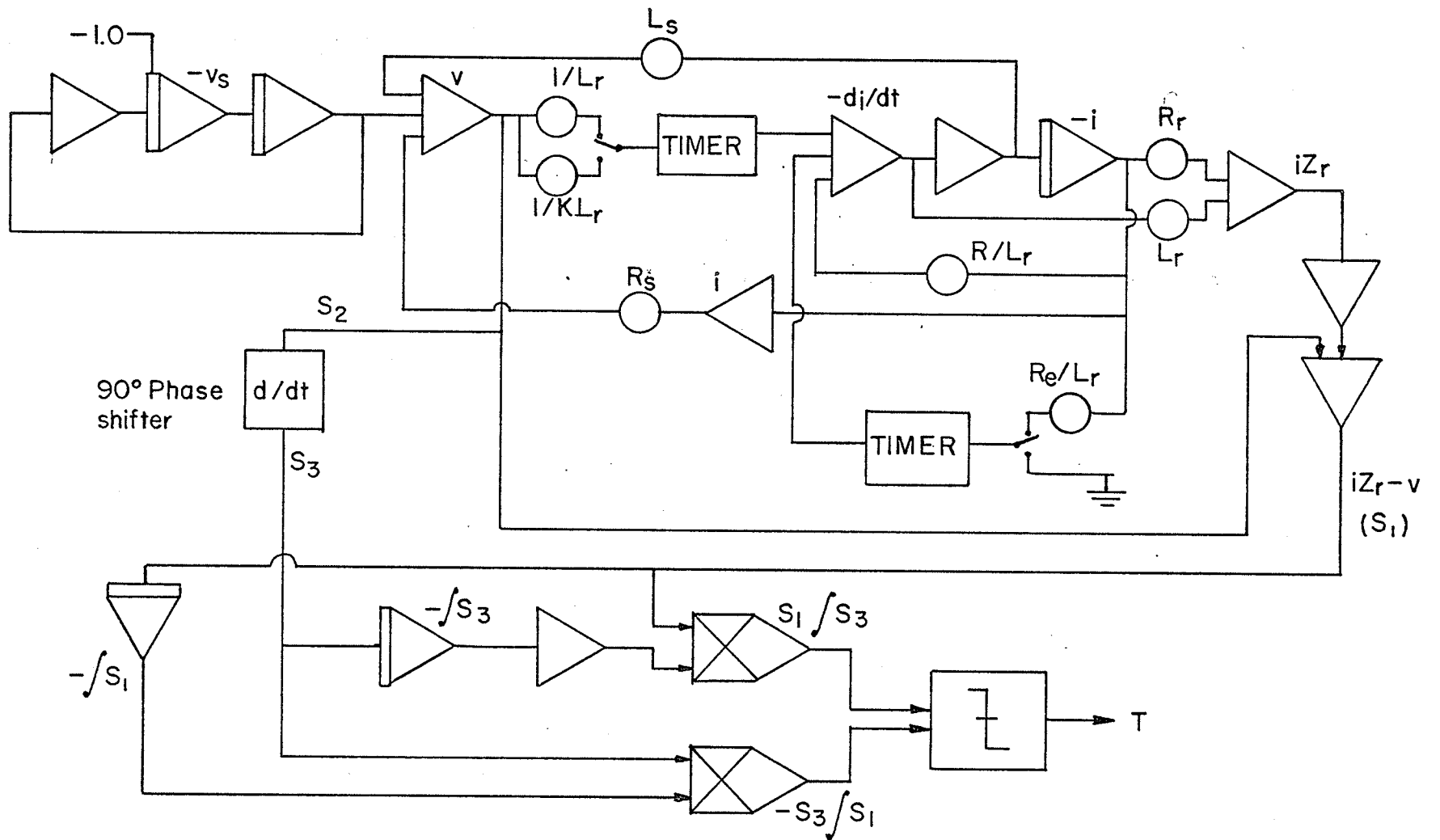


Fig. 6.1 Analog Computer Simulation (With Integrator Realization Relay)



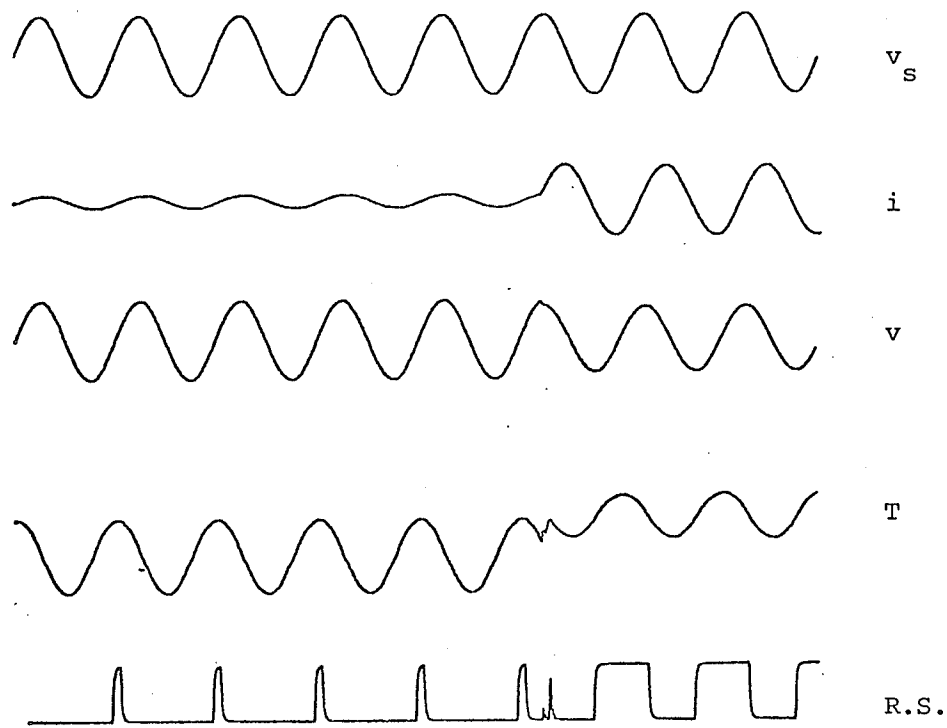


Fig. 6.3.1 Line capacitance neglected  
Fault incidence angle =  $90^\circ$   
 $\phi_s = \phi_r$   
Relay-to-fault impedance = 0.8 line impedance

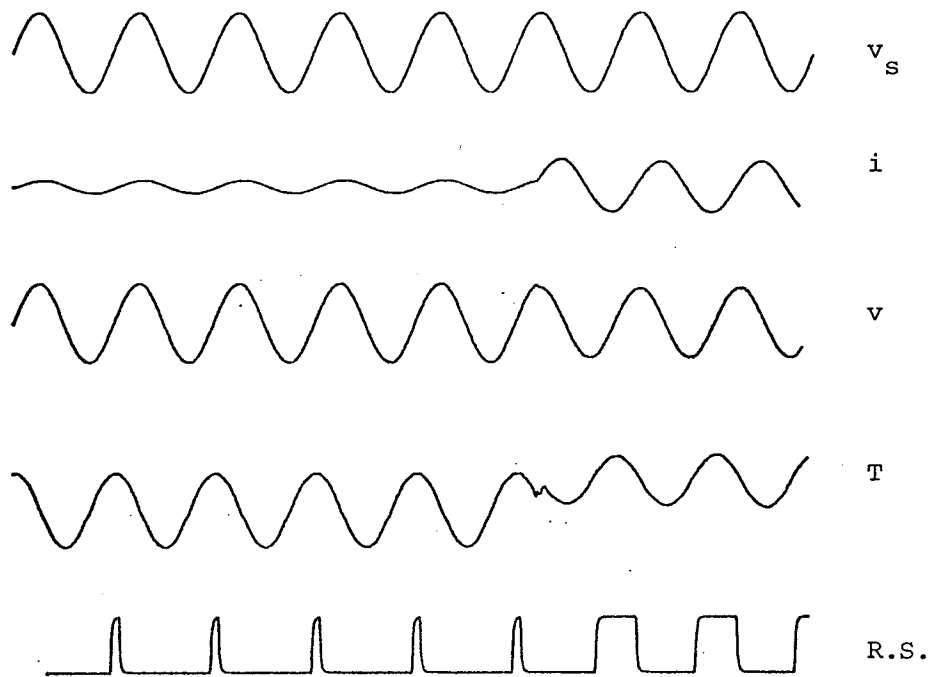


Fig. 6.3.2 Line capacitance neglected  
Fault incidence angle =  $90^\circ$   
 $\phi_s = \phi_r$   
Relay-to-fault impedance = 1.2 line impedance

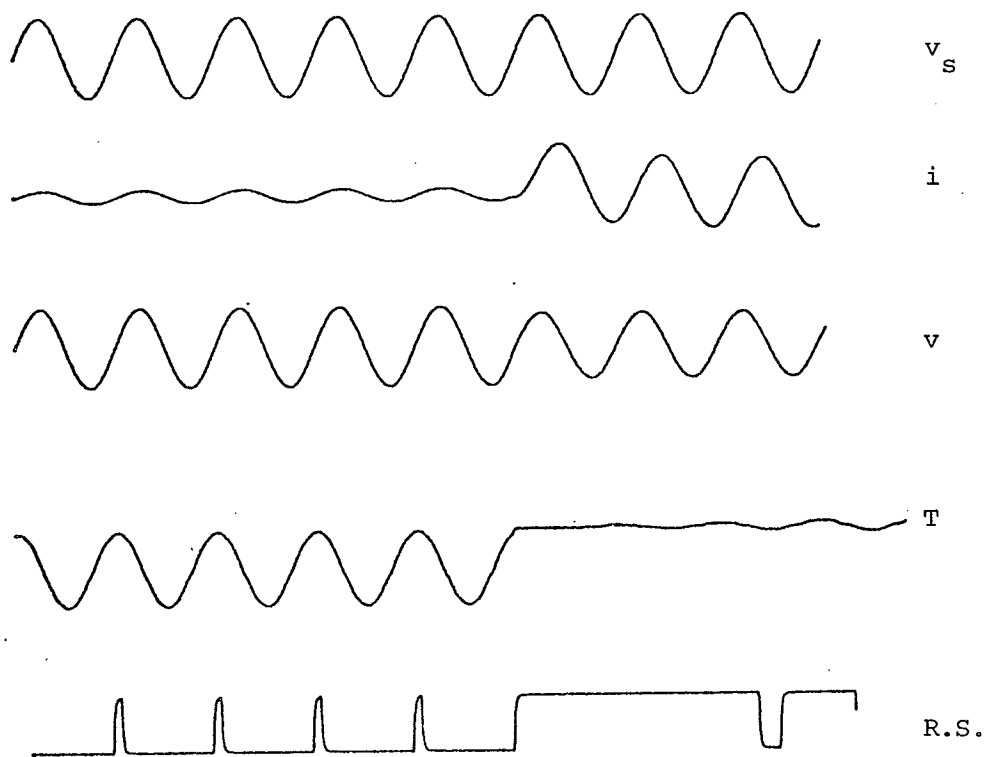


Fig. 6.3.3 Line capacitance neglected  
Fault incidence angle =  $0^\circ$   
 $\phi_s = \phi_r$   
Relay-to-fault impedance = 0.8 line impedance

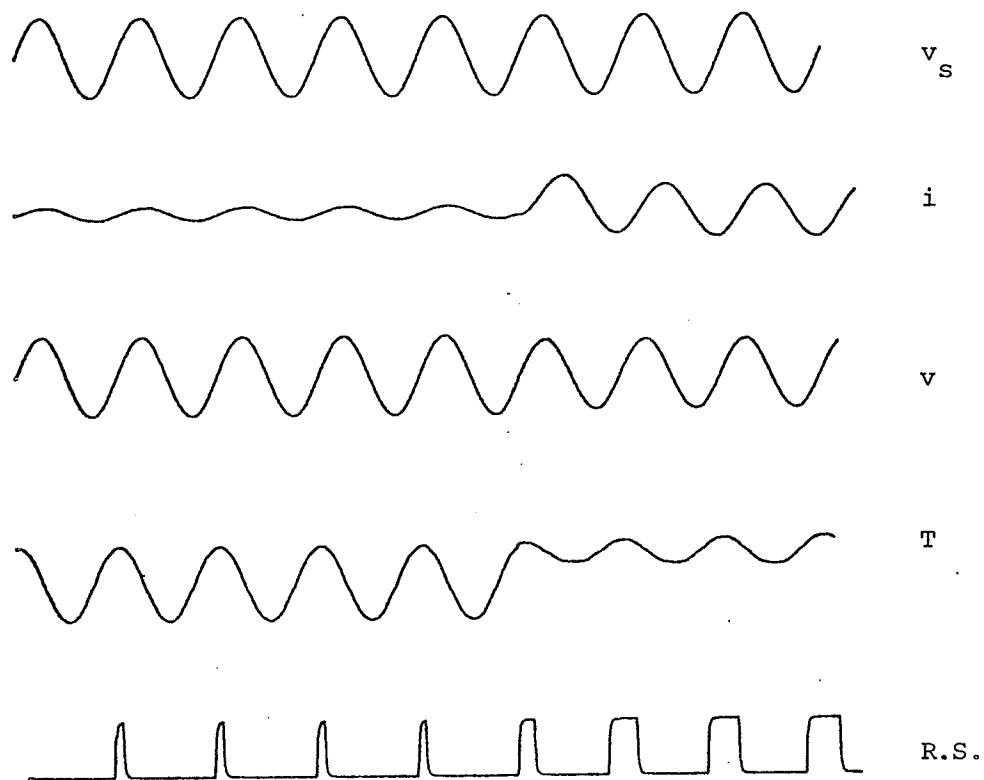


Fig. 6.3.4. Line capacitance neglected  
Fault incidence angle =  $0^\circ$   
 $\phi_s = \phi_r$   
Relay-to-fault impedance = 1.2 impedance

## CHAPTER 7

### CONCLUSIONS

As a result of study and tests of the experimental relay analog computer model, certain conclusions have been reached which may well serve as a summary.

#### 7.1 Shunt Capacitance Neglected

- (1) The experimental relay trips instantaneously for faults within the protected section no matter when the fault occurs at zero or at maximum source voltage.
- (2) Faults outside the protected zone do not cause operation of the relay.
- (3) Angular mismatch between source and line impedance does not have any effect on either the reliability or the security of the relay.

The above results which are mainly due to the use of replica impedance in the current transformer circuit may justify the possibility of using the relay for the protection of short transmission lines, or when the capacitance of the line may be neglected.

## 7.2 Shunt Capacitance Considered

- (1) The relay trips instantaneously for those faults within its setting whatever is the fault incidence angle.
- (2) For faults on an adjacent section, the relay still gives a trip signal to the circuit breaker.
- (3) The magnitude of the source impedance as well as its phase angle do not influence the operation of the relay.
- (4) The use of filters does not help very much, and has the added disadvantage of introducing certain time delay.

From the foregoing points, we conclude that:

- (a) High frequency transients seem to cause great susceptibility of the experimental MHO relay to misoperation.
- (b) For reliable high speed protection, transient wave forms, including both d.c.-offset and high-frequency noise, have to be used in relay design rather than just the steady-state wave forms.

## 7.3 Realization using integrators

- (1) In this case, the relay gives a trip signal

prior to the fault. The reason is probably due to improper initial conditions for the integrators.

- (2) Unless there is a means to fix proper initial conditions at the moment of the fault, it will be difficult to judge the operation of the relay.

#### 7.4 Suggestions for Future Work

Although the experimental relay failed to pass the testing requirement, it might be useful to test the relay with different types of filters, different cut-off frequencies or different filter locations. Tests of analog computer generated fault signals on an actual relay may provide a better insight into the operation of this relay.

In case of integrators-realization model, the use of "wash-out" on integrators might be helpful, and should prevent the trip signal prior to the fault.

## BIBLIOGRAPHY

1. Mathews, P., Nellist. "Transients in distance protection," IEE Proc. Vol. 110, No. 2, Feb. 1963.
2. Zydanowicz, J. "Transients in power network relay protection during faults," Archiwum Elektrotechniki, Vol. 18, No. 1, pp. 69-80, 1969)
3. Evans, R.D., Witzke, R.L. "Practical calculation of electrical transients on power systems," AIEE Trans., Vol. 62, pp. 690-695, 1943.
4. Swift, G.W. "Simulation of fault-generated transmission line transients on an analog computer", To be published.
5. Humpage, W.D., Sabberwal, S.P. "Developments in phase-comparison techniques for distance protection," Proc. IEE, Vol. 112, No. 7, July 1965.
6. Wedepohl, L.M. "Polarized MHO distance relay," Proc. IEE, Vol. 112, No. 3, March 1965.
7. Van C. Warrington, A. R. "Application of the OHM and MHO principles to protective gear relay," AIEE Trans., Vol. 65, p. 378, 1946.
8. MacPherson, R.H., van C. Warrington, A.R., McConnell, A.J. "Electronic protective relays," AIEE Trans., Vol. 167, 1948.
9. Slemon, G.R., Robertson, S.D.T., Ramamoortly, M. "High speed protection of power systems based on improved power systems models," CIGRE 1968, Paper No. 31-09.
10. van C. Warrington, A.R. "Protective relays - their theory and practices," Vol. I, II, 1969.
11. Mason, S.R. The Art and Science of Protective Relaying. Wiley, 1956.
12. Carter, G.W. The Simple Calculation of Electrical Transients. Cambridge University Press, 1944.



13. Mathews, P. Protective Current Transformers and Circuits. Chapmall and Hall, 1955.
14. Johnson, C.L. Analog Computer Techniques. McGraw-Hill, 1963.
15. Bergseth, F.R. "An electronic distance relay using a phase discrimination principle," AIEE Trans., Vol. 73, Part III-B, 1954.
16. Hutchison, R.M. "The MHO distance relay," AIEE Trans., Vol. 65, 1946.
17. Atabekov, G.I. The Relay Protection of High Voltage Network. Pergamon Press, 1962.
18. Greenwood, A. Electrical Transients in Power Systems. Wiley, 1971.
19. Uram, R., Miller, R.W. "Mathematical analysis and solutions of transmission line transient," AIEE Trans., Vol. 83, p. 1116, 1964.
20. Transmission and Distribution Reference Book. Westinghouse.
21. McConnell, A.J., Brandt, D.B. "Fundamentals of static relays," Proceedings of the American Power Conference, 1965, Vol. XXVII, p. 1009.

APPENDIX A

### Current Expression Derivations

In this section, the state variable approach is adopted to derive an expression for the relay current at the moment of the fault if the faulted section is represented by a nominal-T.

The voltage  $v_1(t)$  across the capacitance and the currents  $i_1(t)$  and  $i_2(t)$  through the inductance are chosen to be the state variables, while the voltage source  $v_s(t)$  is the input. Simple applications of the Kirchhoff voltage law and Kirchhoff current law yield the following three equations:

$$\dot{v}_s = v_1 - i_1 \frac{R}{2} - \frac{di_1}{dt} \frac{L}{2}$$

$$\dot{v}_1 = \frac{1}{C}(i_1 - i_2)$$

$$v_1 = i_2 \frac{R}{2} + \frac{di_2}{dt} \frac{L}{2}$$

These equations may be written in the standard state equation form

$$\dot{\mathbf{x}} = \mathbf{A}\mathbf{x} + \mathbf{B}u$$

where

$$\dot{\mathbf{x}} = \begin{bmatrix} \frac{di_1}{dt} \\ \frac{di_2}{dt} \\ \dot{v}_1 \end{bmatrix} \quad u = \hat{V}_s \sin(\omega t + \delta)$$

and

$$A = \begin{bmatrix} -\frac{R}{L} & 0 & -\frac{2}{L} \\ 0 & -\frac{R}{L} & \frac{2}{L} \\ \frac{1}{C} & -\frac{1}{C} & 0 \end{bmatrix} \quad B = \begin{bmatrix} \frac{2}{L} \\ 0 \\ 0 \end{bmatrix}$$

The solution of this equation is given by:

$$x = e^{At} x_0 + \int_0^t e^{A(t-\tau)} B u(\tau) d\tau$$

If  $x_0=0$

$$x = \int_0^t e^{A(t-\tau)} B u(\tau) d\tau$$

and

$$e^{At} = L^{-1} [SI-A]^{-1}$$

$$[SI-A] = \begin{bmatrix} s+\frac{R}{L} & 0 & \frac{2}{L} \\ 0 & s+\frac{R}{L} & -\frac{2}{L} \\ -\frac{1}{C} & \frac{1}{C} & s \end{bmatrix}$$

$$[SI-A]^{-1} = \frac{1}{s + s\frac{R}{L} + \frac{4}{LC}} \begin{bmatrix} s + s\frac{R}{L} + \frac{2}{LC} & \frac{\frac{2}{LC}}{s+\frac{R}{L}} & -\frac{2}{L} \\ \frac{\frac{2}{LC}}{s+\frac{R}{L}} & s + s\frac{R}{L} + \frac{2}{LC} & \frac{2}{L} \\ \frac{1}{C} & -\frac{1}{C} & s + \frac{R}{L} \end{bmatrix}$$

$$e^{At} = \begin{bmatrix} \frac{1}{2} \left[ e^{-\frac{R}{L}t} + e^{-\frac{R}{2L}t} \left( \cos \left( \frac{4}{LC} - \frac{R}{4L} \right)^{\frac{1}{2}} t \right. \right. \\ \left. \left. - \frac{R}{2L} \frac{1}{\left( \frac{4}{LC} - \frac{R}{4L} \right)^{\frac{1}{2}}} \sin \left( \frac{4}{LC} - \frac{R}{4L} \right)^{\frac{1}{2}} t \right) \right] & \dots & \dots \\ \dots & \dots & \dots \\ \dots & \dots & \dots \end{bmatrix}$$

$$B u(\tau) = \begin{bmatrix} \frac{2}{L} \hat{V}_s \sin(\omega\tau + \delta) \\ 0 \\ 0 \end{bmatrix}$$

$$i_1(t) = \int_0^t \frac{2V}{L} \sin(\omega\tau + \delta) \cdot \frac{1}{2} \left( e^{-2a(t-\tau)} + e^{-a(t-\tau)} \left[ \cos b(t-\tau) - \frac{a}{b} \sin b(t-\tau) \right] \right) d\tau$$

where

$$a = \frac{R}{2L} \text{ secs}$$

$$b = \left( \frac{4}{LC} - \frac{R}{4L} \right)^{\frac{1}{2}} \text{ rads/sec}$$

$$i_1(t) = \frac{V}{L} \left[ \cos \delta \left\{ \int_0^t \sin \omega \tau [e^{-2a(t-\tau)} + e^{-a(t-\tau)} (\cos b(t-\tau) - \frac{a}{b} \sin b(t-\tau))] d\tau \right\} \right. \\ \left. + \sin \delta \left\{ \int_0^t \cos \omega \tau [e^{-2a(t-\tau)} + e^{-a(t-\tau)} (\cos b(t-\tau) - \frac{a}{b} \sin b(t-\tau))] d\tau \right\} \right]$$

The above expression when integrated yields the equation for the current in Chapter 3.

APPENDIX B

### Design of Differentiators

Differentiators with cut-off frequencies of ten times the source frequency were designed according to the transfer function:

$$D(s) = \frac{Y(s)}{X(s)} = \frac{s}{1 + \frac{2\xi s}{\omega_n} + \frac{s^2}{\omega_n^2}}$$

where  $X(s)$ ,  $Y(s)$  are the input and output of differentiators, respectively, in the frequency domain.

Taking the inverse Laplace transform, we get:

$$y + \frac{2\xi}{\omega_n} \dot{y} + \frac{\ddot{y}}{\omega_n^2} = \dot{x}$$

$$\int y + \frac{2\xi}{\omega_n} y + \frac{\dot{y}}{\omega_n^2} = x$$

$$\dot{y} = \omega_n^2 x - \omega_n^2 \int t - 2 \xi \omega_n y$$

Figure B-1 gives the amplitude frequency response of the differentiator and the analog computer simulation is shown in Fig. B-2.

If

$$x(t) = \sin t$$



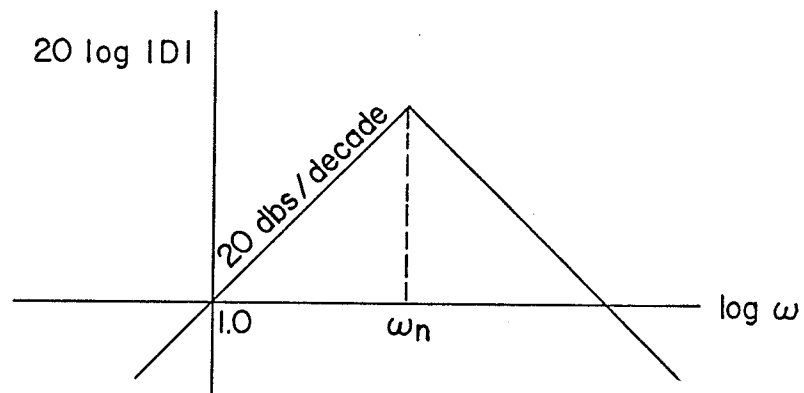


Fig. B-1 Amplitude-frequency response of differentiators

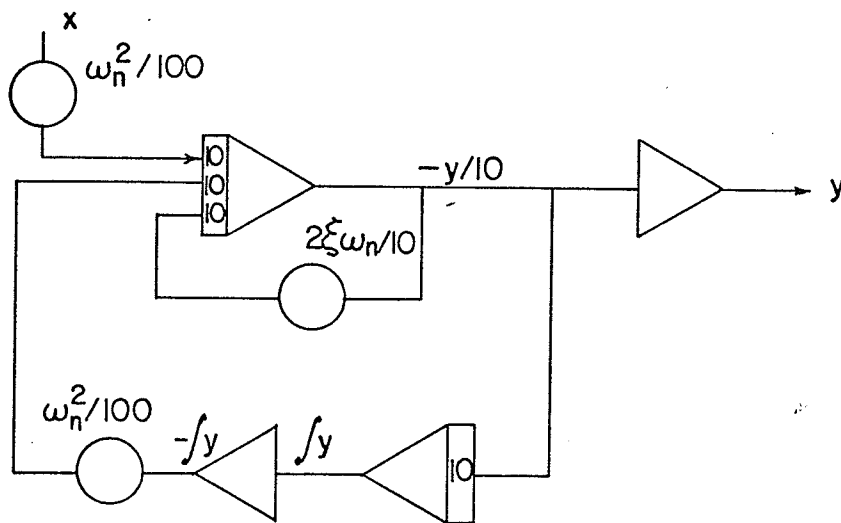


Fig. B-2 Analog computer simulation of differentiators

we get

$$\begin{aligned}
 y(t) = & \frac{1}{1 + \frac{1}{\omega_n^2} + 2\xi\omega_n^2 - \frac{2}{\omega_n}} \left[ \frac{2\xi}{\omega_n} \sin t + \left(1 - \frac{1}{\omega_n}\right) \cos t \right. \\
 & - \frac{\omega_n + 1}{(\omega_n - 4\xi^2)^{\frac{1}{2}}} \sin(\omega_n - 4\xi^2)^{\frac{1}{2}} t e^{-t\xi\omega_n} \\
 & \left. + \left(\frac{1 - \omega_n}{\omega_n}\right) \cos(\omega_n - 4\xi^2)^{\frac{1}{2}} t e^{-t\xi\omega_n} \right]
 \end{aligned}$$

which shows that the output is the derivative of the input in addition to some transients that practically die out after a short time  $T = \frac{1}{\xi\omega_n}$ . The larger the cut-off frequency, the shorter the transient duration.

APPENDIX C

### Filter Description

The transfer function of a Krone-Hite Model 330-A band pass filter is approximately:

$$\frac{\omega^4 T_1^4}{[(1 + 2\zeta\gamma\omega T_1 - \omega^2 T_1^2)^2][(1 + 2\zeta\gamma\omega T_2 - \omega^2 T_2^2)^2]}$$

where the low cut-off frequency is  $\frac{1}{2\pi T_1}$  and the high cut-off frequency is  $\frac{1}{2\pi T_2}$  and the value of  $\gamma$  is fixed at slightly greater than 0.6.

With  $T_1$  very large,  $\frac{1}{T_1}$  shrinks to zero and the transfer function is that of a low pass filter and is given by

$$F(s) = \frac{1}{(1 + 2\gamma s T_2 + T_2^2 s^2)(1 + 2\gamma s T_2 + T_2^2 s^2)}$$

If we let  $F(s) = [G(s)]^2$ , then

$$G(s) = \frac{1}{1 + 2\gamma s T_2 + s^2 T_2^2} = \frac{E_1(s)}{E_2(s)}$$

Figure C-1 shows the analog simulation of  $G(s)$ . Two cascaded circuits will act exactly as a low pass filter. The amplitude-frequency response as well as a complete simulation diagram of the low pass filter for  $\gamma = 0.6$  and

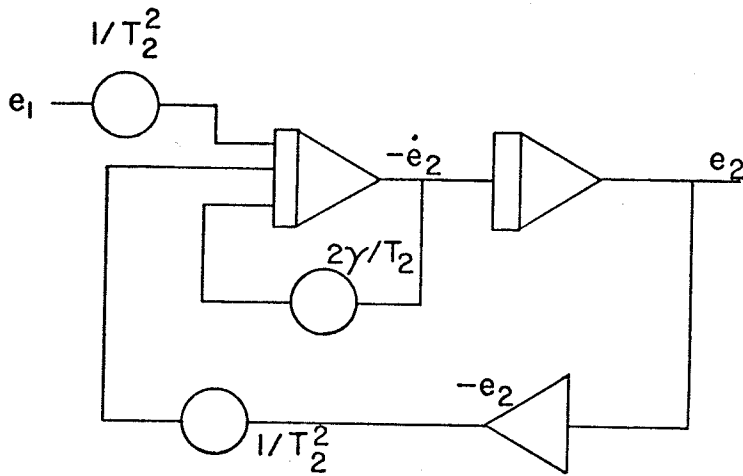
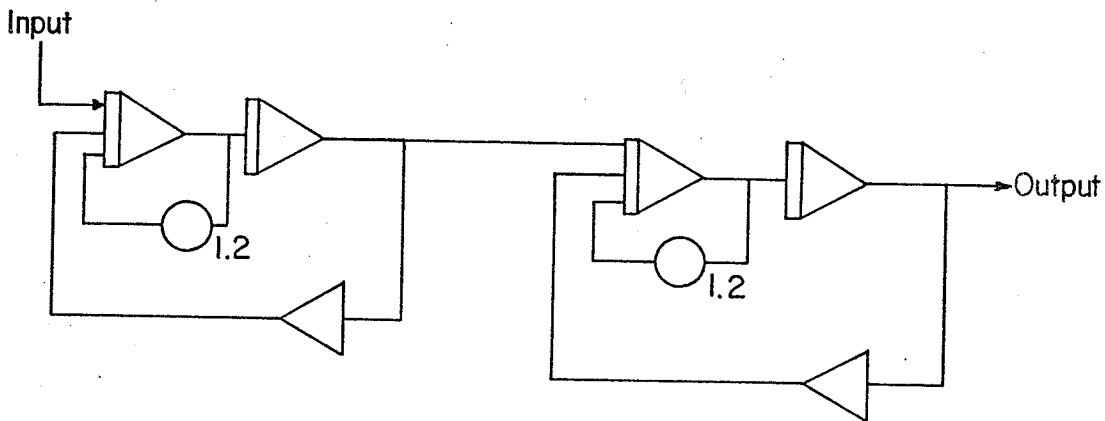
Fig. C-1 Analog simulation for  $G(s)$ 

Fig. C-2 Analog simulation for a low pass filter with (cut off radian frequency = 1.0)

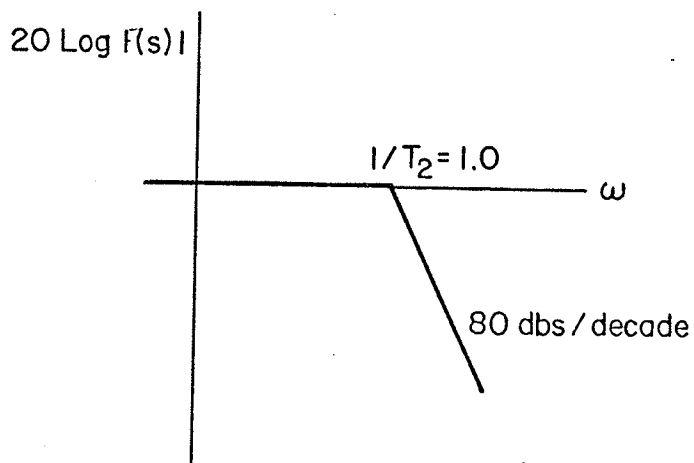


Fig. C-3 Amplitude frequency response for the low pass filter

and  $T_2 = 1.0$  (i.e. cut-off radian frequency 1.0 p.u.) are given in Fig. C-2 and Fig. C-3.